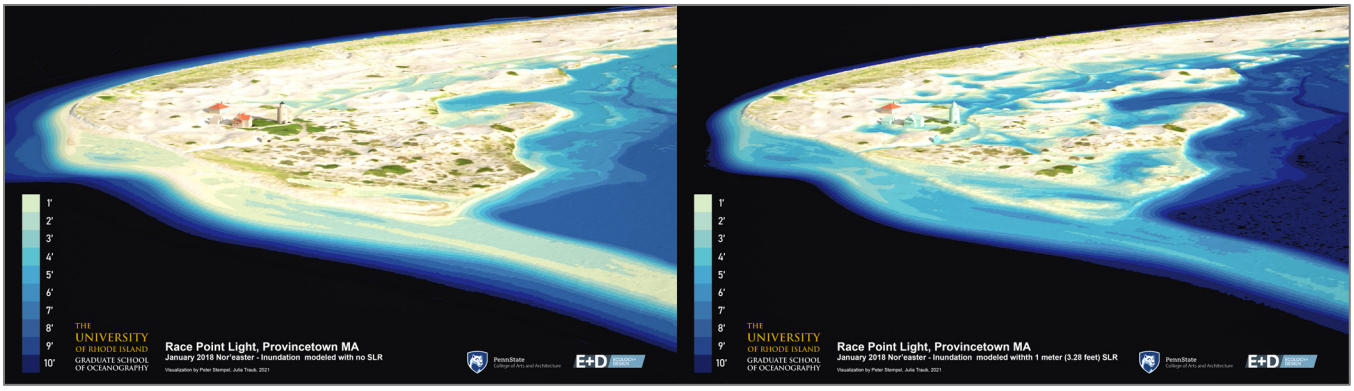
National Park Service
U.S. Department of the Interior

Science Report NPS/SR—2024/133
https://doi.org/10.36967/2304306

The Impact of Sea Level Rise During Nor'easters in New England

Acadia National Park, Boston Harbor Islands, Boston National Historical Park, and Cape Cod National Seashore



Visualization of Race Point Light in Provincetown, MA, depicting the flooding during by the January 2018 nor'easter (left) and with 1m sea level rise (right), generated by the ADCIRC storm surge model.

© PETER STEMPEL / PENN STATE

The impact of sea level rise during nor'easters in New England: Acadia National Park, Boston Harbor Islands, Boston National Historical Park, and Cape Cod National Seashore

Science Report NPS/SR—2024/133

Isaac Ginis[1], Deborah Crowley[1], Peter Stempel[2], Amanda Babson[3]

[1] Graduate School of Oceanography
University of Rhode Island
Narragansett, RI 02882

[2] Stuckeman School of Architecture and Landscape Architecture
Pennsylvania State University
University Park, PA 16802

[3] National Park Service
Interior Region 1, North Atlantic – Appalachian
University of Rhode Island Bay Campus
215 S. Ferry Rd
Narragansett RI 02882

Please cite this publication as:

Ginis, I, D. Crowley, P. Stempel, and A. Babson. 2024. The impact of sea level rise during nor'easters in New England: Acadia National Park, Boston Harbor Islands, Boston National Historical Park, and Cape Cod National Seashore. Science Report NPS/SR—2024/133. National Park Service, Fort Collins, Colorado. https://doi.org/10.36967/2304306

NPS 962/193736, June 2024

The National Park Service Science Report Series disseminates information, analysis, and results of scientific studies and related topics concerning resources and lands managed by the National Park Service. The series supports the advancement of science, informed decisionmaking, and the achievement of the National Park Service mission.

All manuscripts in the series receive the appropriate level of peer review to ensure that the information is scientifically credible and technically accurate.

Views, statements, findings, conclusions, recommendations, and data in this report do not necessarily reflect views and policies of the National Park Service, U.S. Department of the Interior. Mention of trade names or commercial products does not constitute endorsement or recommendation for use by the U.S. Government.

The Department of the Interior protects and manages the nation's natural resources and cultural heritage; provides scientific and other information about those resources; and honors its special responsibilities to American Indians, Alaska Natives, and affiliated Island Communities.

This report is available in digital format from the National Park Service DataStore and the Natural Resource Publications Management website. If you have difficulty accessing information in this publication, particularly if using assistive technology, please email irma@nps.gov.

Contents

Page

Figures v

Tables xiii

Abstract xiv

List of Terms or Acronyms (Optional) xv

Acknowledgments xvii

Executive Summary xviii

Overview xviii

Purpose xviii

Approach & Findings xviii

Introduction 1

Methods 4

Literature Review 4

Observational Data Sources and Analysis 4

Water Level Analysis: Historical MSL 8

Water Level Analysis: SLR, Characterization of Peak Water Levels and Storm Surges 8

ADCIRC-SWAN Modeling Study 9

Model System 9

Model Setup 10

Model Validation 18

Simulations of Nor'easters 18

Analysis of the Role of Waves 18

Analysis of the Effect of Shoreline Configuration on Storm Surge and Peak Water Level 20

3D Visualization 24

Results 25

Contents (continued)

Page

Literature Review of Extratropical Cyclones ("Nor'easters') and Associated Storm Surges in New England 25

Sea Level Rise Literature Review and Data Analysis 26

Results of Historical Water Level Analysis 28

Water Level Analysis: Historical MSL 28

Water Level Analysis: Characterization of Peak Water Levels and Storm Surges 29

Results of Model Validation 37

Tidal Validation 37

Storm Validation 40

Results of Simulations of Nor'easters with Sea level Rise 52

Results of Analysis of Impact of Waves and SLR (CACO East Coast) 68

Results of Analysis of Impact of Shoreline Configuration (Pleasant Bay) 74

Results of 3D Visualizations and Engagement 79

Base Visualizations 80

Engagement 81

Results Summary by Park 83

Conclusions 99

1. What coastal impacts have been observed local to the parks during nor'easters? 99

2. What is the range of SLR expected at the parks from 2020–2100? 99

3. What is the effect of SLR on nor'easter impacts at the parks? 99

4. What is the role of waves in model simulations of storm surge? How does SLR affect the role of waves in model simulated storm surge at the parks? 100

5. What is the effect of shoreline configuration in southeast Cape Cod on the degree of storm surge experienced within coastal embayments behind the barrier beach? 101

6. How can we better communicate the impact of nor'easters, SLR, and the combination of nor'easters with SLR? 101

Literature Cited 102

Figures

Page

Figure 1. Maps of the study areas; all parks within the study area (upper left), National Parks of Boston region (bottom left), Acadia National Park region (upper right), and Cape Cod National Seashore region (bottom right). 2

Figure 2. Map of observation stations from which data were used in *The Impact of Sea Level Rise During Nor'easters in New England* study. 5

Figure 3. Water level data periods of record used for analysis of peak water level and surges at Bar Harbor, Maine, Boston, Massachusetts, and Woods Hole, Massachusetts..... 8

Figure 4. Advanced circulation model (ADCIRC) mesh (entire extent) plot over ESRI ocean basemap imagery with mesh elements colored by elevation (depths are positive). 11

Figure 5. Advanced circulation model (ADCIRC) mesh local to Acadia National Park plot over ESRI satellite imagery with mesh elements colored by elevation (depths are positive)..... 11

Figure 6. Advanced circulation model (ADCIRC) mesh local to the National Parks of Boston plot over ESRI satellite imagery with mesh elements colored by elevation (depths are positive)..... 12

Figure 7. Advanced circulation model (ADCIRC) mesh local to Cape Cod National Seashore plot over ESRI satellite imagery with mesh elements colored by elevation (depths are positive). 13

Figure 8. Snapshot of meteorological forcing during the April 2007 nor'easter from the European Center for Medium Range Forecasts Re-Analysis 5 (ERA-5) data overlaid on satellite imagery. 15

Figure 9. Snapshot of meteorological forcing during the January 2018 nor'easter from the European Center for Medium Range Forecasts Re-Analysis 5 (ERA-5) data overlaid on satellite imagery; top plot shows time series (x-axis is month/day–hour) at the three locations denoted with white circle markers and the bottom plot shows the spatial field of wind speed (color contour) wind direction (vectors) and atmospheric pressure (contour lines with labels of pressure in mbar) at the time identified with the vertical black line in the upper plot. 16

Figure 10. Snapshot of meteorological forcing during the March 2018 nor'easter from the European Center for Medium Range Forecasts Re-Analysis 5 (ERA-5) data overlaid on satellite imagery. 17

Figure 11. Wave analysis study area on the outer east coast of Cape Cod, MA, is depicted by the black box. 19

Figures (continued)

Page

Figure 12. Satellite imagery from the United Stats Geological Survey Land Process Distributed Active Archive Center showing southeastern Cape Cod, MA, for different years showing different shoreline configurations. 21

Figure 13. Delineated mean shoreline for analysis configurations shown over satellite imagery from the United Stats Geological Survey Land Process Distributed Active Archive Center. 23

Figure 14. Mesh resolution shown over satellite imagery from ESRI (left) and modified mesh elevations for configuration 1 (middle-left), 2 (middle-right) and 3 (right) for the Pleasant Bay region located in southeastern Cape Cod.. 23

Figure 15. Projections of sea level rise for the intermediate scenario over time at multiple New England locations relative to 2020 mean sea level. 27

Figure 16. Projections of low, intermediate, and high sea level rise at Boston, MA, relative to 2020 mean sea level along with error bars representing uncertainty. 28

Figure 17. Observed monthly mean sea level at multiple New England locations and their average relative to established mean sea level datum at tide gauges local to the study focus areas. 29

Figure 18. Peak water level (top) and corresponding storm surge (bottom) at Bar Harbor, ME. 31

Figure 19. Water level corresponding to peak surge (top) and peak storm surges (bottom) at Bar Harbor, ME.. 32

Figure 20. Peak water level (top) and corresponding storm surge (bottom) at Boston, MA. 33

Figure 21. Water level corresponding to peak surge (top) and peak storm surges (bottom) at Boston, MA. 34

Figure 22. Peak water level (top) and corresponding storm surge (bottom) at Woods Hole, MA. 35

Figure 23. Water level corresponding to peak surge (top) and peak storm surges (bottom) at Woods Hole, MA. 36

Figure 24. Comparison of astronomical tidal water predictions from National Oceanic and Atmospheric Administration (NOAA) versus simulated advanced circulation model (ADCIRC) at Bar Harbor, ME (top), Boston, MA (middle) and Woods Hole, MA (bottom) for a period prior to the April 2007 nor'easter.. 38

Figures (continued)

Page

Figure 25. Navigation Chart (top), Advanced circulation model (ADCIRC) simulated inundation at high tide (middle), and low tide (bottom) in Boston Harbor, MA, near Logan Airport. 39

Figure 26. Navigation chart (top), advanced circulation model (ADCIRC) predicted inundation at high tide (middle), and low tide (bottom) of Provincetown Harbor, MA, region. 40

Figure 27. Subset of wave, wind and water level observation stations in the New England region used for to validate storm conditions. 42

Figure 28. Comparison of observed vs European Center for Medium Range Forecasts Re-Analysis 5 (ERA-5) wind speed used in advanced circulation-simulating waves in the nearshore (ADCIRC-SWAN) model forcing of the April 2007 nor'easter. 43

Figure 29. Comparison of observed vs European Center for Medium Range Forecasts Re-Analysis 5 (ERA-5) wind speed used in advanced circulation-simulating waves in the nearshore (ADCIRC-SWAN) model forcing of the January 2018 nor'easter. 44

Figure 30. Comparison of observed vs European Center for Medium Range Forecasts Re-Analysis 5 (ERA-5) wind speed used in advanced circulation-simulating waves in the nearshore (ADCIRC-SWAN) model forcing of the March 2018 nor'easter. 45

Figure 31. Comparison of observed versus advanced circulation-simulating waves in the nearshore (ADCIRC-SWAN) model simulated water levels for the April 2007 nor'easter. 46

Figure 32. Comparison of observed versus advanced circulation-simulating waves in the nearshore (ADCIRC-SWAN) model simulated water levels for the January 2018 nor'easter. 47

Figure 33. Comparison of observed versus advanced circulation-simulating waves in the nearshore (ADCIRC-SWAN) model simulated water levels for the March 2018 nor'easter. 48

Figure 34. Comparison of observed versus advanced circulation-simulating waves in the nearshore (ADCIRC-SWAN) model simulated significant wave height for the April 2007 nor'easter. 49

Figure 35. Comparison of observed versus advanced circulation-simulating waves in the nearshore (ADCIRC-SWAN) model simulated significant wave height for the January 2018 nor'easter. 50

Figures (continued)

Page

Figure 36. Comparison of observed versus advanced circulation-simulating waves in the nearshore (ADCIRC-SWAN) model simulated significant wave height for the March 2018 nor'easter. 51

Figure 37. Advanced circulation-simulating waves in the nearshore (ADCIRC-SWAN) results of the April 2007 (left), January 2018 (center), and March 2018 (right) nor'easters at Acadia National Park; peak water levels from the simulation using 2020 MSL (top), change in peak water levels when 1 ft (0.3048m) of SLR is simulated (middle), and change in peak water levels when 1 m of SLR simulated (bottom). 53

Figure 38. Advanced circulation-simulating waves in the nearshore (ADCIRC-SWAN) results of the April 2007 (left), January 2018 (center), and March 2018 (right) nor'easters at Acadia National Park; peak significant wave height (Hs) from the simulation using 2020 mean sea level (top), change in peak Hs when 1 ft (0.3048m) of sea level rise is simulated (middle), and change in peak Hs when 1 m of sea level rise is simulated (bottom)..... 54

Figure 39. Advanced circulation-simulating waves in the nearshore (ADCIRC-SWAN) results of the March 2018 nor'easter at the National Parks of Boston; peak water levels from the simulation using 2020 mean sea level (top), change in peak water levels when 1 ft (0.3048m) of sea level rise is simulated (middle), and change in peak water levels when 1 m of sea level rise simulated (bottom). 55

Figure 40. Advanced circulation-simulating waves in the nearshore (ADCIRC-SWAN) results of the March 2018 nor'easter at the National Parks of Boston; peak significant wave height (Hs) from the simulation using 2020 mean sea level (top), change in peak Hs when 1 ft (0.3048m) of sea level rise is simulated (middle), and change in peak Hs when 1 m of sea level rise is simulated (bottom). 56

Figure 41. Advanced circulation-simulating waves in the nearshore (ADCIRC-SWAN) results of the April 2007 (left), January 2018 (center), and March 2018 (right) nor'easters at Cape Cod National Seashore; peak water levels from the simulation using 2020 mean sea level (top), change in peak water levels when 1 ft (0.3048m) of sea level rise is simulated (middle), and change in peak water levels when 1 m of sea level rise simulated (bottom)..... 57

Figure 42. Advanced circulation-simulating waves in the nearshore (ADCIRC-SWAN) results of the March 2018 nor'easter at Cape Cod National Seashore. 58

Figures (continued)

Page

Figure 43. Maps of the study areas and analysis query points; all parks within the study area (upper left), the National Parks of Boston region showing query points (bottom left), Acadia National Park region showing query points (upper right) and Cape Cod National Seashore region showing query points (bottom right). 60

Figure 44. Water level summary for January 2018 nor'easter at Acadia National Park (left), the National Parks of Boston (middle), and Cape Cod National Seashore (right)..... 61

Figure 45. Significant wave height summary for April 2007 nor'easter (left), January 2018 nor'easter (center) and March 2018 nor'easter (right) at Acadia National Park; top plot shows time series of significant wave height (Hs) from the 2020 mean sea level baseline simulation (top), the middle plot shows the change from baseline from the simulation with 1 ft sea level rise and the bottom plot shows the change from baseline from the simulation with 1 m sea level rise. 62

Figure 46. Inundation over land for January 2018 nor'easter at Acadia National Park; top plot shows inundation for the 2020 mean sea level baseline simulation (top), the middle plot shows the change from baseline from the simulation with 1 ft sea level rise and the bottom plot shows the change from baseline from the simulation with 1 m sea level rise..... 64

Figure 47. Inundation over land for the January 2018 nor'easter at the National Parks of Boston. 65

Figure 48. Inundation over land for the January 2018 nor'easter at Cape Cod National Seashore in the region of Provincetown and Truro. 66

Figure 49. Inundation over land for the January 2018 nor'easter at Cape Cod National Seashore, Eastham region. 67

Figure 50. Comparison of peak water level without sea level rise(left) and with 1 m of sea level rise (right) from simulations of the January 2018 nor'easter along the central east coast of Cape Cod. 69

Figure 51. Comparison of peak water level from simulations of the January 2018 nor'easter with 1m sea level rise with wave coupling (right) and without wave coupling (left) along the central east coast of Cape Cod. 70

Figure 52. The difference in water elevation between the simulations of the January 2018 nor'easter with and without wave coupling along the central east coast of the Cape Cod National Seashore. 71

Figure 53. The peak water elevation and peak significant wave height along the central east coast of the Cape Cod National Seashore (the transect shown in Figure 52) from simulations of the January 2018 nor'easter with and without 1m of sea level rise. 72

Figures (continued)

Page

Figure 54. The difference in peak water elevation in the simulations with and without waves from simulations of the January 2018 nor'easter along a transect in central east Cape Cod (shown in Figure 52) for the cases without and with 1 m of sea level rise. 73

Figure 55. Maximum water elevation for simulation with tides only forcing (no wind) for shoreline configuration 1 (left), 2 (middle) and 3 (right) of the Pleasant Bay region of Cape Cod National Seashore. 74

Figure 56. Water elevation at storm peak from simulation with tides and wind forcing based on the January 2018 nor'easter for shoreline configuration 1 (left), 2 (middle) and 3 (right) of the Pleasant Bay region of Cape Cod National Seashore. 74

Figure 57. Maximum surge for shoreline configuration 1 (left), 2 (middle) and 3 (right) of Pleasant Bay region of Cape Cod National Seashore. 75

Figure 58. Query point locations in the Pleasant Bay region located in southeastern Cape Cod overlaid on maximum water elevation from Configuration 3. 77

Figure 59. Time series of water elevation and storm surge from simulations of the January 2018 nor'easter at query points 5, 6, 15 and 20 all located in the Pleasant Bay region in southeastern Cape Cod from simulations of each of the three shoreline configurations. 78

Figure 60. Maximum water level (top) and maximum surge (bottom) at the 25 query points all located in the Pleasant Bay region in southeastern Cape Cod from simulations of the January 2018 nor'easter for three different shoreline configurations: 79

Figure 61. Overview of existing conditions, Trenton Bridge, left, and Sand Beach, right, Acadia National Park. 80

Figure 62. Existing conditions at Georges Island, Boston Harbor Islands National Recreation Area. 81

Figure 63. Existing conditions at Race Point Light and Herring Cove Beach (showing relocated Herring Cove Bathhouse, Cape Cod National Seashore. 81

Figure 64. Title frame from the interpretation video (top) and a snapshot of video footage from the interpretation video showing URI student Deb Crowley speaking with National Park service project manager Amanda Babson (bottom). 83

Figure 65. Map of bottom elevations at Acadia National Park. 85

Figure 66. High resolution ground elevations relative to mean sea level at Trenton Bridge and Northern Mount Desert Island, Acadia National Park. 86

Figures (continued)

Page

Figure 67. Trenton Bridge illustrating the January 2018 nor'easter under different sea level conditions. 86

Figure 68. Composite visualization showing the extent of surge in relation to mean high water and mean sea level at Sand Beach, Acadia National Park from simulations of the January 2018 nor'easter with and without 1m of sea level rise. 87

Figure 69. Visualization of flood depths from simulations of the March 2018 nor'easter without sea level rise (left,) and with 1m of sea level rise (right) at Georges Island, Boston Harbor Islands National Recreation Area. 89

Figure 70. Map of bottom elevations at the National Parks of Boston, MA. 90

Figure 71. Satellite images of Lovells Island (top left) and Georges Island (bottom left), Boston Harbor Islands National Recreation Area, from the Massachusetts GIS 2021 Aerial Imagery. 91

Figure 72. High resolution bottom elevations relative to mean sea level (elevation positive) in the region of the Charlestown Navy Yard, Boston National Historical Park. 92

Figure 73. Visualization of Charlestown Navy Yard during the March 2018 nor'easter with 1 m sea level rise. 93

Figure 74. Map of bottom elevations in the Cape Cod, MA region. 94

Figure 75. Map of bottom elevations relative to mean sea level (elevation positive) in the Cape Cod, MA region near East Harbor. 95

Figure 76. Visualization of the March 2018 nor'easter at Provincetown–Wood End, MA, showing the Long Point Dike. 96

Figure 77. Visualization of Wellfleet Harbor, MA, during the January 2018 nor'easter including 1 m of sea level rise. 96

Figure 78. Visualization of Eastham, MA, looking from First Encounter Beach across Nauset Marsh towards Coast Guard Beach and Orleans Circle depicting the March 2018 nor'easter with 1 m sea level rise. 97

Figure 79. Visualization of Orleans Circle, MA, January 2018 nor'easter (left) and the January 2018 nor'easter with 1 m sea level rise (right). 97

Figure 80. Herring Cove Beach, Provincetown, MA, shown with January 2018 nor'easter (left), and the January 2018 nor'easter with a 1 m sea level rise (right). 98

Figures (continued)

Page

Figure 81. Race Point Light, Provincetown, MA, shown with January 2018 nor'easter (left), and the January 2018 nor'easter with 1 m sea level rise. 98

Tables

Page

Table 1. Summary of nor'easters modeled in The Impact of Sea Level Rise During Nor'easters in New England study. 4

Table 2. Summary of the observation stations used in *The Impact of Sea Level Rise During Nor'easters in New England* study. 6

Table 3. Summary of advanced circulation model (ADCIRC) nodal attributes. 13

Table 4. Summary of Manning's n used for each modeling event. 14

Table 5. Summary of shoreline configurations assessed at Pleasant Bay, MA. 22

Table 6. Summary of three-dimensional visualizations developed for *The Impact of Sea Level Rise During Nor'easters in New England* study. 24

Table 7. Summary of offsets of mean sea level for historic and future events assumed for the New England region. 29

Table 8. Summary of simulations for analysis of nor'easters with sea level rise. 52

Table 9. Summary of peak water levels at the query points across the different park regions in Region 1. 84

Abstract

This study examines the potential impact of sea level rise (SLR) caused by climate change on the effects of extratropical cyclones, also known as nor'easters, in four New England coastal parks: Acadia National Park (ACAD), Boston Harbor Islands National Recreation Area (BOHA), Boston National Historical Park (BOST) and Cape Cod National Seashore (CACO). A multi-method approach is employed, including a literature review, observational data analysis, coupled hydrodynamic-wave numerical modeling, 3D visualizations, and communication of findings. The literature review examines previous studies of nor'easters and associated storm surges in New England and SLR projections across the study domain due to climate change. The observational data analysis evaluates the characteristics of nor'easters and their effects, providing a basis for validating the model. Numerical modeling is performed using the Advanced Circulation (ADCIRC) model, coupled with the Simulating Waves in the Nearshore (SWAN) model to simulate storm surges and waves. The model was validated against available observations and demonstrated its ability to simulate water levels, inland inundation, and wave heights in the study area with high accuracy. The validated model was used to simulate three powerful nor'easters (April 2007, January 2018, and March 2018) and each storm was simulated for three sea levels, (1) a baseline mean sea level representative of the year 2020, as well as with a (2) 1 ft of SLR and (3) 1 m of SLR. Analysis of the model output was used to assess the vulnerability of the parks to nor'easters by examining peak impacts in the park areas. Additional simulations were conducted to evaluate the role of waves in predicting peak water levels and the impact of inlet configurations on storm surges within coastal embayments behind the barrier beach systems in the southern Cape Cod region. The project developed maps, three-dimensional visualizations, and an interpretive film to assist the parks in planning for resource management, maintenance, emergency management, visitor access, safety, education, and outreach. These tools provide a better understanding of the potential impacts of nor'easters and SLR and enable the parks to better prepare for future storms.

List of Terms or Acronyms (Optional)

ACAD: Acadia National Park

ADCIRC: Advanced Circulation Model

AGL: Above ground level

BOHA: Boston Harbor Island National Recreational Area

BOST: Boston National Historical Park

CACO: Cape Cod National Seashore

ECMWF: European Centre for Medium Range Weather Forecasts

ERA5: ECMWF Re: Analysis (fifth generation)

HSOFS: Hurricane Surge on: demand Forecast System

Hs: Significant wave height, which is the top 1/3 of waves within a given time interval

IPCC: Intergovernmental Panel on Climate Change

K1: Lunar diurnal constituent

K2: Lunisolar semi: diurnal constituent

MHHW: Mean higher high water

MHW: Mean high water

MLLW: Mean lower low water

MLW: Mean low water

MSL: Mean sea level

M2: Principal lunar semidiurnal constituent

N2: Larger lunar elliptic semidiurnal constituent

NAVD88: North American Vertical Datum of 1988

NWS: National Weather Service

NDBC: National Data Buoy Center

NOAA: National Oceanic and Atmospheric Administration

O1: Lunar diurnal constituent

P1: Solar diurnal constituent

Q1: Larger lunar elliptic diurnal constituent

SLR: Sea Level Rise

S2: Principal solar semidiurnal constituent

SSP: Shared socioeconomic pathway

SWAN: Simulating Waves in the Nearshore Model

Acknowledgments

This project was funded by the NPS Servidewide Combined Call. Thanks are extended to Catherine Schmitt, Rebecca Cole-Will, Abe Miller-Rushing, Marc Albert, Mark Adams, Sophia Fox, Geoff Sanders, Dave Ullman, Mansur Ali Jisan and Louis Borrelli. This report was much improved thanks to the peer review input from John Cannon, Rebecca Cole-Will, Geoffrey Sanders, Peter Sharpe, and Ksienya Taylor.

Executive Summary

Overview

In this report, we investigate how sea level rise (SLR) caused by climate change will impact the effects of extratropical cyclones (also known as northeasters or nor'easters) at four New England coastal parks: Acadia National Park (ACAD), Boston Harbor Islands National Recreation Area (BOHA), Boston National Historical Park (BOST) and Cape Cod National Seashore (CACO). Our analysis, based on numerical model simulations, assesses the exposure of the parks to nor'easters by examining peak water levels, inundation, and waves in the park areas. We have developed maps and three-dimensional visualizations to assist the parks in planning for resource management, maintenance, emergency management, visitor access and safety, education, and outreach. These tools provide a better understanding of the potential impacts of nor'easters and SLR and enable the parks to better prepare for future storms.

Purpose

This project aims to (1) comprehensively investigate the hazards posed by nor'easters in four New England coastal parks (CACO, BOHA, BOST, and ACAD) using advanced coastal ocean circulation/storm surge and wave model conditions; (2) develop projections of the potential impacts of nor'easters under higher sea level; (3) incorporate improved storm vulnerability information into park planning and decision-making processes through collaboration with park managers; and (4) communicate the findings of the research to park visitors, students, scientists, and other interested stakeholders.

Approach & Findings

This study employs a multi-method approach, including a literature review, observational data analysis, coupled hydrodynamic-wave numerical modeling, 3D visualizations, and communication of findings. The literature review examines previous studies of nor'easters and associate storm surges in New England and SLR projections across the study domain due to climate change. The observational data analysis evaluates the characteristics of nor'easters and their effects in the study area and provides a basis for validating the model simulations. The coupled hydrodynamic-wave numerical modeling is used to simulate storm surges and coastal impacts during nor'easters, with and without SLR. The 3D- visualizations are employed to better represent the model results and more effectively communicate the impacts of storms and SLR at sites of interest within the parks.

National Oceanic and Atmospheric Administration (NOAA) tide gauge measurements at Bar Harbor, ME, Boston, MA, and Woods Hole, MA, were used to analyze historic peak water levels and storm surges. The results indicate that nor'easters are the leading cause of large surges and high-water levels in the study area north of Woods Hole, emphasizing the importance of studying these storms in the region, relative to hurricanes which are more important further south. Notably, the January 2018 nor'easter resulted in one of the most significant water levels across all parks, with the Boston tide gauge measuring the highest water level ever recorded. Given its impact, we selected the January 2018 nor'easter as one of the high-impact storms in our study. In addition, we simulated the effects of two other significant nor'easters: the April 2007 and March 2018 nor'easters.

To simulate storm surges, we utilized the Advanced Circulation (ADCIRC) model, coupled with the Simulating Waves in the Nearshore (SWAN) model. Our computational mesh was derived from NOAA's Hurricane Surge and On-Demand Forecasting System (HSOFS), but we refined it to ensure accurate representation of the coastline, topography, and bathymetry in the study area. We validated the model against available observations and demonstrated that it successfully simulated the spatial variability and magnitudes of tides, as well as the extent of inundation during high and low tides.

We simulated each storm event as it occurred for model validation, with a baseline mean sea level (MSL) reflecting 2020 and with 1ft and 1m of SLR. The addition of SLR changes the peak water levels experienced during the storms. The amount that the peak water level changes is not equal to the applied SLR increment due to nonlinear effects. The deviation from the applied SLR varies in space and time. However, the overall deviation increases with increasing SLR. The trends of the change in peak water level were consistent across all parks.

The increased peak water levels from SLR can induce more overland inundation. Shorelines with low grades are more susceptible to inundation over land as opposed to high grade or steep shorelines. The shoreline at each park is variable. Generally speaking, a lot of the ACAD shoreline is high grade, a lot of the CACO shoreline is low grade, BOHA has a mix and employs armoring around much of the shoreline, and the shoreline at BOST is manmade bulkheads. BOHA has some low-lying areas that may be vulnerable, and the modeling showed that they are spatially limited and SLR will mostly deepen areas rather than cause widespread changes to the inundation footprint, while SLR may change the flooding footprint at CACO more dramatically.

The addition of SLR changes the nearshore wave environment, allowing for larger waves and a greater inland extent of waves on shores with gradually decreasing bathymetry (increasing topography), most notable at the east coast of CACO and northeast coasts of some BOHA islands. At ACAD, where there is a steep change in bottom grade, the higher water level from SLR will alter where the waves interact with the coast vertically on steep, bluffed shorelines.

The southeast Cape Cod region has a dynamic barrier beach system, and this part of the shoreline has experienced various morphological configurations over time. The number, width, and depth of inlet openings, as well as the bathymetry within the embayments behind the barrier, affect the tide range and the amount of storm surge that occurs within the embayments. To investigate this, we simulated multiple configurations of the shoreline during the January 2018 nor’easter. The results show that larger opening widths to the Atlantic Ocean (adjacent body of water to the east) increase the storm surge within the coastal embayments, while the presence of a hydraulic connection with Nantucket Sound (adjacent water body to the southwest) decreases the peak storm surge. The differences in peak surge vary by up to 0.24m, which is between 20-30% of the total surge. Additionally, there is a shift in the timing of the peak surge, with the peak occurring approximately one hour later in Pleasant Bay when the connection to Nantucket Sound exists.

We have developed a range of communication tools to effectively convey the impact of nor’easters and SLR, including maps, diagrams, visualizations, web stories, and films. The associated lessons learned about best practices for coastal climate communication will be published separately (Schmitt,

C., in review). Our work demonstrates the effectiveness of a combination of modalities when communicating with stakeholders. Each product serves as a "boundary object," providing a shared reference point that facilitates interactions between the project team experts, national park managers, and other stakeholders at the National Park Service. Our film, in particular, has been highly effective, as the personal narratives of individuals make the project work tangible and relatable to a broader audience. Our use of exhibits and visual aids aligns with best practices for climate communication. By engaging scientists and audiences in conversation, we believe that science can have its greatest impact.

Introduction

Coastal communities and critical habitats are facing increased risk due to sea-level rise (SLR). Adapting to SLR and extreme weather conditions in our changing climate is a growing concern. In New England, eastern facing coastlines are particularly vulnerable to extratropical storm events with strong winds and heavy precipitation (known as northeasters, or colloquially referred to as nor'easters) followed by hurricanes. Despite being the most common coast-shaping (i.e., morphodynamic changes such as erosion or overwash) storms in the region, nor'easters are often overlooked as a major contributor of coastal flooding. This is because they occur most frequently during the cold season, from November to March, when attention is typically focused on the amount of ice and snow, and wind associated with these storms. Historic data indicate that most coastal flooding events in New England are caused by nor'easters, rather than tropical cyclones. Although tropical cyclones typically bring stronger winds and higher surges, nor'easters are usually larger in size, move slower, and remain in the region for longer periods of time. A strong nor'easter can cause high coastal inundation levels and as much, if not more, damage than a tropical cyclone. Therefore, it is critical that we understand the severity and geographic variability of storm surges caused by nor'easters to properly assess future risk, aid in preparedness, and ultimately reduce the severe impacts from coastal flooding.

Future projections on the intensity, size, and storm track positions of extratropical cyclones due to changing synoptic atmospheric patterns in the future climate are currently inconclusive. However, it is well established that these storms will have a more severe impact due to rising sea levels. Several previous studies included the effect of SLR in projecting future coastal flooding caused by severe storm events. The North Atlantic Coast Comprehensive Study by the U.S. Army Corps of Engineers (Cialone et al. 2015) evaluated the potential effect of SLR in calculating the future return periods of severe coastal flooding caused by tropical and extratropical cyclone events. Other studies, such as Tebaldi et al. (2012) and Douglas et al. (2017) incorporated SLR to project frequency and severity of future coastal flood events. However, these studies did not consider the combined factors of storm surge, astronomical tide, and SLR in determining the total water elevations and coastal inundation during extratropical cyclones in the study area. This information gap is likely to result in under-informed and ineffective adaptation measures. This project investigates how the impacts of nor'easters will change with sea level rise (SLR) from a changing climate at four New England coastal parks, Acadia National Park (ACAD), Boston Harbor Islands National Recreation Area (BOHA), Boston National Historical Park (BOST) and Cape Cod National Seashore (CACO). Through numerical model simulations, we analyze vulnerability to nor'easters, looking at peak water levels, inundation, and waves in the park areas. We then develop maps and three-dimensional visualizations that will help parks better plan for resource management, maintenance, and visitor access and safety as well as patron education and outreach. Maps of the study area are presented in Figure 1.

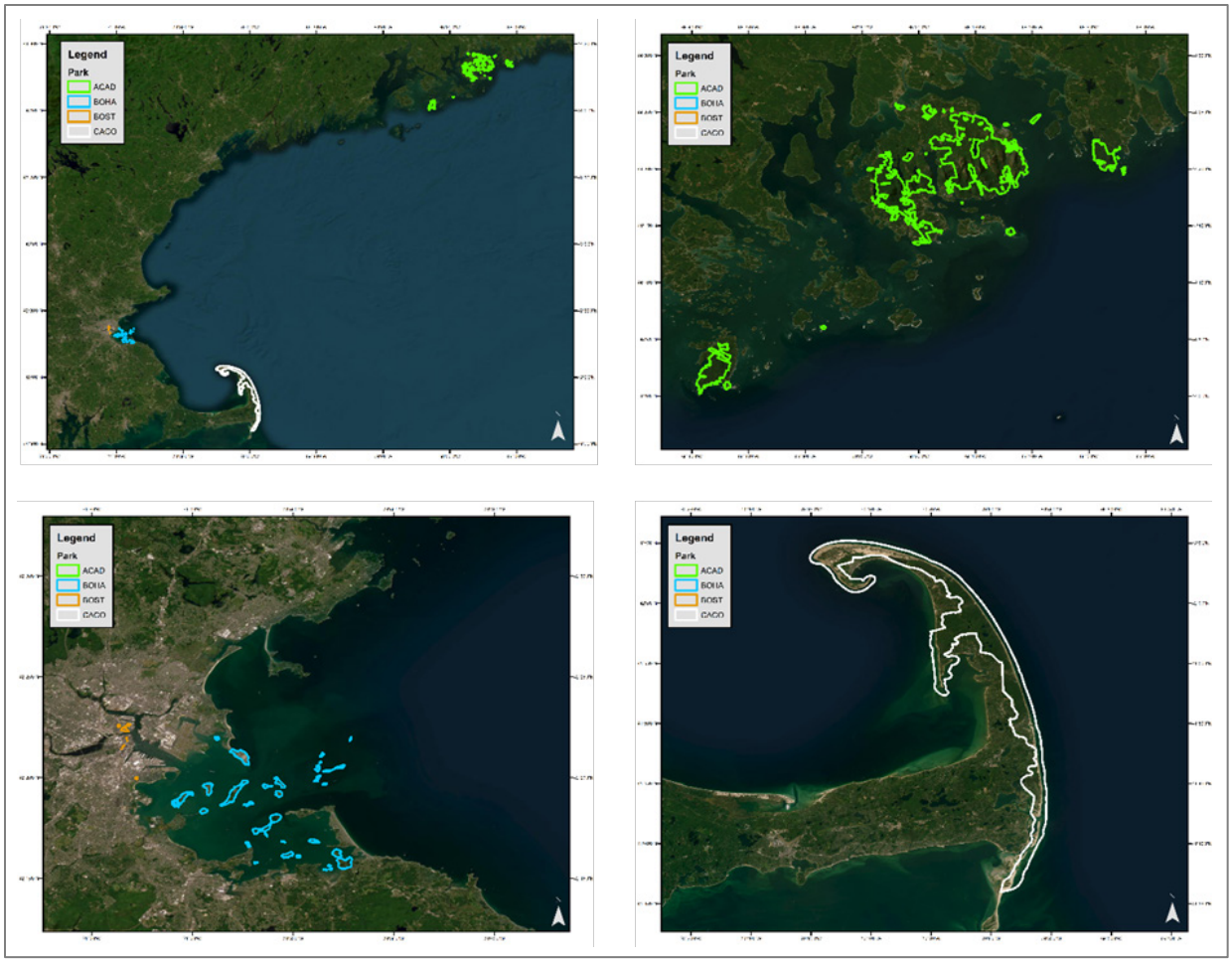


Figure 1. Maps of the study areas; all parks within the study area (upper left), National Parks of Boston region (bottom left), Acadia National Park region (upper right), and Cape Cod National Seashore region (bottom right).

The objectives of this project are to:

- Comprehensively investigate the hazards from nor'easters in the focus parks (CACO, BOHA, BOST and ACAD) using the most advanced coastal ocean circulation/storm surge and wave models. Develop information that provides (1) a spatially explicit analysis of historical nor'easter characteristics (frequency, intensity, inundation) and impacts; (2) detailed high-resolution computer simulations of coastal flooding induced by selected high impact storms; and (3) projections of changes in potential impacts of nor'easters due to storms arriving at higher sea level and potential changes in storm characteristics.
- Incorporate improved storm vulnerability information into planning processes and decision making by working with park managers.
- Communicate role of nor'easters, changes in storms, and other research insights to park visitors, students, and local communities.

The questions that this study investigates are:

1) What coastal impacts have been observed local to the parks during nor'easters?
2) What is the range of SLR expected at the parks from 2020-2100?
3) What is the effect of SLR on nor'easter impacts at the three parks?
4) What is the role of waves in model simulations of storm surge? How does SLR affect the role of waves in storm surge simulations at the parks?
5) What is the effect of shoreline configuration in southeast Cape Cod on the degree of storm surge experienced within coastal embayments behind the barrier beach?
6) How can we better communicate the impact of nor'easters, SLR, and the combination of nor'easters with SLR?

Methods

This study includes a literature review, observational data analysis, coupled hydrodynamic-wave numerical modeling, 3D visualizations of modeling results, and communication of study findings. The literature review was performed to investigate the expected magnitude of SLR across the study domain due to climate change. Observational data analysis was used to inform on the characteristics of the study area and to provide a basis for validating the model simulations. The modeling was used to simulate the coastal impacts during nor'easters with and without SLR and investigate different questions relative to the simulated storm surge. The 3D visualizations were performed to provide products that capture the findings of the modeling that can be used to communicate the impacts of nor'easters and SLR at different sites across the park.

Three separate nor'easters were modeled in this study, chosen because they were identified as high impact events by National Park Service (NPS) affiliates or based on observations and reports of impacts. We note that these storms had larger impacts to the Massachusetts parks than ACAD, but there wasn't a similar historical storm identified for ACAD with sufficient data. The three events that were modeled and the dates of the events are summarized in chronological order in Table 1.

Table 1. Summary of nor'easters modeled in The Impact of Sea Level Rise During Nor'easters in New England study.

ID	Event	Event Dates
1	April 2007 Nor'easter	April 14–17, 2007
2	January 2018 Nor'easter	January 2–6, 2018
3	March 2018 Nor'easter	March 1–3, 2018

Literature Review

We conducted a thorough review of literature and data related to sea level rise, nor'easters, and how these storms may be impacted by climate change. We also analyzed observational data to determine the MSL in the region relative to tidal and elevation datums. This information was necessary to use the appropriate MSL in our modeling efforts. Details on this analysis are provided in the *Water Level Analysis* sub-section of the *Observational Data Sources Analysis* section.

Observational Data Sources and Analysis

Observations of wind, waves, water levels, and flooding are essential for different aspects of the study. Wind observations are available over water at NOAA National Ocean Service (NOS) stations, National Data Buoy Center (NDBC) Buoys, and over land at airports from the National Weather Service (NWS). Wind data are available at varying heights above the ground or water surface. To compare with meteorological model outputs that provide wind data at 10 meters (m) height, all observed wind speeds were converted to a standard height of 10 m assuming a logarithmic wind profile (Shearman & Zelenko, 1989). Water level observations are available at NOAA NOS stations or USGS stations local to the study area. Wave observations are obtained from NDBC stations. Figure 2 shows the locations of observation stations used in this study, all stations with available data

in the overall domain were queried. Details of each station, including an inventory of the different types of observations available for the three simulated events (ID 1, 2, or 3 per Table 1) are presented in Table 2. Note some NDBC buoys are owned, operated, and maintained by third parties, including (1) Northeast Regional Association of Coastal Ocean Observing Systems; (2) University of New Hampshire Scripps Institute of Oceanography (3) Woods Hole Group– Scripps Institute of Oceanography; and (4) Scripps Institute of Oceanography; see the footnotes in Table 2 for details.

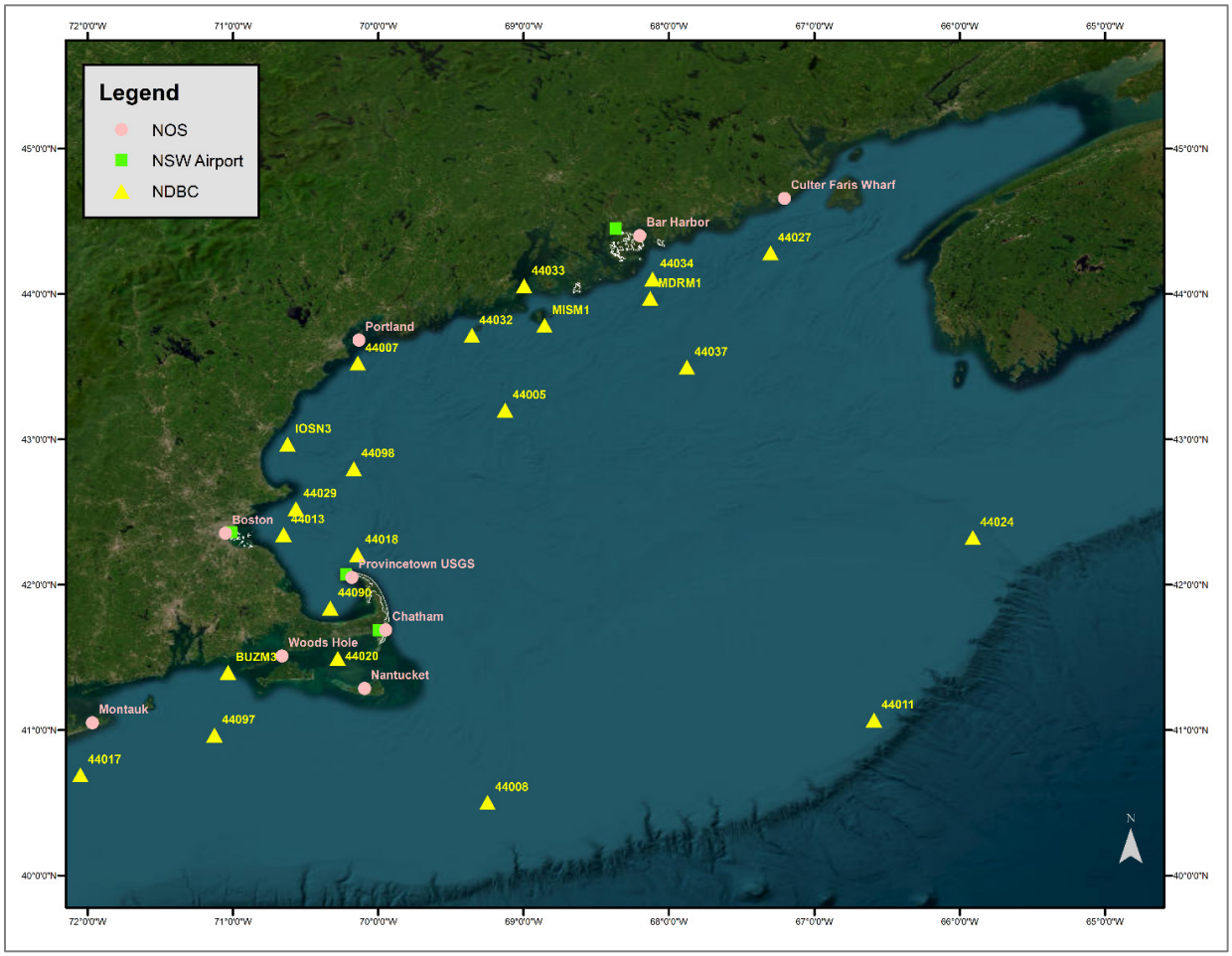


Figure 2. Map of observation stations from which data were used in *The Impact of Sea Level Rise During Nor'easters in New England* study.

Table 2. Summary of the observation stations used in *The Impact of Sea Level Rise During Nor'easters in New England* study. The summary of nor'easters modeled are listed in Table 1.

Station ID	Station Name	Wind	Wave	WSE	Latitude	Longitude
NWS-KBHB	Bar Harbor APT-ME	1,2,3	–	–	44.450	-68.367
NWS-KBOS	Logan APT Boston-MA	1,2,3	–	–	42.361	-71.010
NWS-KPVC	Provincetown Muni APT-MA	1,2,3	–	–	42.072	-70.221
NWS-KCQX	Chatham Municipal APT-MA	1,2,3	–	–	41.688	-69.993
NDBC 44027	Jonesport Maine-ME	–	2,3	–	44.283	-67.300
NDBC 44034[1]	Eastern Maine Shelf-ME	1,3	1,3	–	44.103	-68.112
NDBC 44033[1]	Penobscot Bay-ME	1,2,3	1,2,3	–	44.055	-68.996
NDBC 44032[1]	Buoy E01-Central Maine Shelf	1,2,3	1,2,3	–	43.715	-69.355
NDBC MDRM1	Mt. Desert Rock-ME	1,2,3	–	–	43.969	-68.128
NDBC MISM1	Matinicus Rock-ME	1,2,3	–	–	43.784	-68.855
NDBC 44007	12NM SE of Portland-ME	1,2	1,2,3	–	43.525	-70.140
NDBC 44037	Jordan Basin-ME	1,2,3	1,2,3	–	43.497	-67.876
NDBC 44005	GOM-NH	–	3	–	43.201	-69.127
NDBC IOSN1	Isle of Shoals-ME	1,2,3	–	–	42.967	-70.623
NDBC 44098[2]	Jeffreys Ledge-NH	–	1,2	–	42.798	-70.168
NDBC 44029[1]	Mass Bay-MA	1,2,3	1,2,3	–	42.523	-70.566
NDBC 44013	Boston-MA	1,2,3	1,2,3	–	42.346	-70.651
NDBC 44024[1]	Northeast Channel N01	3	3	–	42.325	-65.909
NDBC 44018	Cape Cod Provincetown-MA	–	3	–	42.206	-70.143
NDBC 44090[3]	Cape Cod Bay-MA	3	1,2	–	41.840	-70.329
NDBC 44020	Nantucket Sound-MA	–	1,2	–	41.493	-70.279

[1] Northeast Regional Association of Coastal Ocean Observing Systems

[2] University of New Hampshire Scripps Institute of Oceanography

[3] Woods Hole Group – Scripps Institute of Oceanography

[4] Scripps Institute of Oceanography

Table 2 (continued). Summary of the observation stations used in *The Impact of Sea Level Rise During Nor'easters in New England* study. The summary of nor'easters modeled are listed in Table 1.

Station ID	Station Name	Wind	Wave	WSE	Latitude	Longitude
NDBC BUZM3	Buzzards Bay-MA	1,2,3	–	–	41.397	-71.033
NDBC 44011	Georges Bank-MA	–	1,2,3	–	41.070	-66.588
NDBC 44097[4]	Block Island-RI	–	1,2	–	40.967	-71.126
NDBC 44008	Nantucket 54NM SE-MA	1,3	1,2,3	–	40.504	-69.248
NDBC 44017	Montauk-NY	2,3	1,2	–	40.693	-72.049
NOS 8411250	Cutler Faris Wharf-ME	1	–	2	44.657	-67.205
NOS 8413320	Bar Harbor-ME	1	–	1,2,3	44.400	-68.200
NOS 8418150	Portland-ME	–	–	1,2,3	43.682	-70.133
NOS 8443970	Boston-MA	–	–	1,2,3	42.354	-71.050
NOS 8447435	Chatham-MA	–	–	1,2	41.688	-69.948
NOS 8449130	Nantucket-MA	–	–	1,2,3	41.286	-70.095
NOS 8447930	Woods Hole-MA	–	–	1,2,3	41.509	-70.662
NOS 8510560	Montauk-NY	–	–	1,2,3	41.050	-71.967
USGS 420259070105600	Provincetown USGS-MA	–	–	2,3	42.050	-70.182

[1] Northeast Regional Association of Coastal Ocean Observing Systems

[2] University of New Hampshire Scripps Institute of Oceanography

[3] Woods Hole Group – Scripps Institute of Oceanography

[4] Scripps Institute of Oceanography

Water Level Analysis: Historical MSL

Water level data from NOAA tide gauges were used to characterize the MSL observed since the establishment of current tidal and land elevation datums. Elevation datums commonly used in the region include NAVD88 (established in 1988) and tidal datums such as MSL (established from analysis of the 1983-2001 epoch). Due to the rise of mean sea levels, we analyzed the MSL over time from the mid-1980s to the present. This analysis helped to develop an average record of MSL per year in the project study area that was used for modeling modern day historical events (e.g., storm of 2007). Additionally, the analysis enabled us to determine the offset from the mid-1980s to 2020, to add to SLR projections relative to 2020. The observed monthly mean sea levels were downloaded through the NOAA Tides and Currents Sea Level Trends pages for Bar Harbor, ME, Boston, MA, Nantucket, MA, and Woods Hole, MA, as these locations frame the study area. The sea level trend data provided by NOAA were analyzed to remove regular seasonal fluctuations, and the average of these locations was calculated for each month. The appropriate monthly value was used to define the MSL for historical events.

Water Level Analysis: SLR, Characterization of Peak Water Levels and Storm Surges

An analysis of data at NOAA tide gauges in the region was performed to characterize peak water levels and peak storm surges local to each park and help identify high impact events. The analysis was performed at (1) Bar Harbor, ME; (2) Boston, MA; and (3) Woods Hole, MA. The period of record of available data at each station is shown in Figure 3.

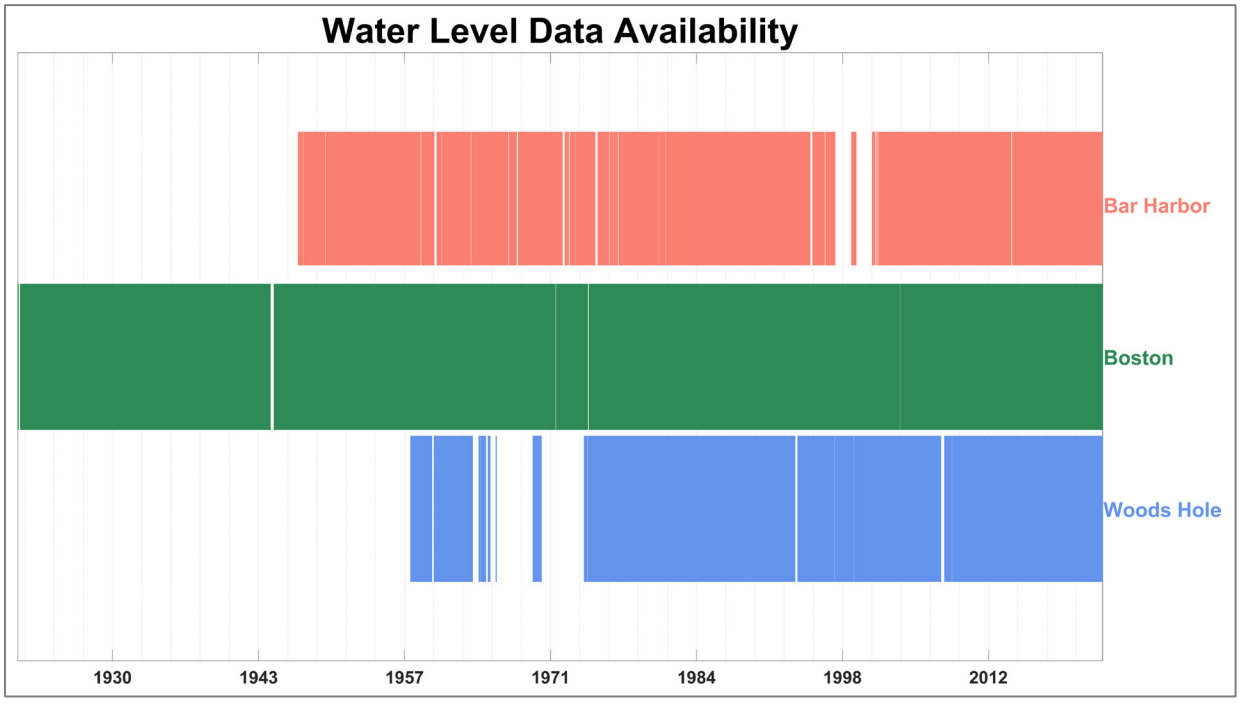


Figure 3. Water level data periods of record used for analysis of peak water level and surges at Bar Harbor, Maine, Boston, Massachusetts, and Woods Hole, Massachusetts.

The NOAA gauges provide information on both the observed water level and the theoretical water level, which is the predicted water level due to astronomical tidal forces. The recent data were available on a 6-minute time step. However, older records in the dataset are only available on an hourly (60-minute) time step. Thus, the analysis was performed using hourly records. The observed and theoretical water levels were obtained from the NOAA COASTWATCH ERRDAP server relative to the mean lower low water (MLLW) vertical datum, ensuring consistency across all sites. The observed storm surge is calculated as the difference between the observed and theoretical water level, as shown in Equation 1.

Equation 1: $Observed\ Surge = Observed - Theoretical\ (Tidal)\ Water\ Level$

For each site, the observed storm surge was calculated for every time step. The peak water level and peak surge were identified for each day of the record. Furthermore, the corresponding surge at the time of peak water level and the corresponding water level at the time of peak surge were determined. The peak water level events were ranked and plotted along with the corresponding surge. Similarly, the top surge events were ranked and plotted along with their corresponding water level. The events were color coded based on whether they are considered a tropical storm (red), an extratropical storm (blue), or a hybrid (red/blue hashed) at the gauge site.

One limitation of this analysis is that it did not remove the effects of SLR. The observed water level is influenced by tides, wind/weather conditions, and the MSL which changed over time due to SLR. The data retrieved is relative to the present tidal epoch (1983–2001).

ADCIRC-SWAN Modeling Study

The ADCIRC-SWAN modeling included several steps, such as developing the model application for the study area, validating the model simulations, and using the validated model application to simulate storms with the inclusion of SLR. Additionally, two separate modeling analyses were performed to investigate different aspects of the storm surge modeling and coastal vulnerability, including (1) the impact of waves on simulations of coastal storm surge; and (2) the impact of a barrier beach shoreline configuration on the water level and storm surge within the adjacent coastal embayments. Further details of these modeling analyses are provided in the following subsections.

Model System

Storm surge modeling was performed using the Advanced Circulation (ADCIRC Version 54.01) model coupled with the Simulating Waves in the Nearshore (SWAN Version 41.10) model. ADCIRC is a hydrodynamic model that uses the finite element method to solve the continuity equation along with the shallow water form of the momentum conservation equations to simulate water levels and water currents at mesh nodes. SWAN solves the spectral action balance for wave growth, which refers to solving the wave action balance equation for a discretized spectrum of frequencies. The model output includes calculations of spatially and temporally varying significant wave height, mean wave direction, and wave period. Details on the equations solved and the numerical implementation of the solutions, along with the description of key assumptions and the handling of boundary conditions, are provided in Luettich and Westerlink (2004) for ADCIRC and from the SWAN team (2006) for SWAN.

The ADCIRC and SWAN models are coupled using a leapfrog scheme and exchange information on the coupling timestep defined in the model run control file. ADCIRC alone is computationally intensive, and when coupled with SWAN there is an additional computational burden. Consequently, the simulations of a storm event is performed in two steps to reduce computational needs, (1) a spin-up period using ADCIRC alone to initialize the water levels from tides and (2) a storm period using ADCIRC-SWAN, which starts from the output of the spin-up run.

Model Setup

Development of the model application includes defining all model inputs such as the model mesh, model forcing, and key physical and numerical parameters.

Mesh

ADCIRC uses an unstructured mesh consisting of a collection of irregularly spaced points (referred to as nodes) which define endpoints for triangular elements. The mesh nodes store attributes, including bottom elevation, bottom roughness, as well as computational factors.

This project adopted the model setup and model mesh from NOAA's Hurricane Surge and On-Demand Forecasting System (HSOFS), a system that provides real-time guidance for storm surges and tides at the US coastlines (https://www.weather.gov/sti/coastalact_surgewg). The mesh covers a large domain spanning from the Caribbean to Nova Scotia, encompassing the offshore waters of the western Atlantic Ocean and extending landward to include coastal embayments and harbors. The large domain is used to capture the evolution of the storm, which can have far reaching effects well ahead of the arrival of the peak storm at a given location. In the study focus areas, the mesh extends over land to elevations of approximately 33 ft (10 m) above MSL to capture any potential inundation over land during peak storm surges, particularly in combination with SLR.

For this project, the HSOFS mesh was modified and refined to capture the coastline, topography, and bathymetry of the study areas more accurately. Mesh elevations in southern New England were developed from the United States Geological Survey (USGS) Coastal National Elevation Database (Danielson et al. 2018) topographic/bathymetric data set that integrates high resolution LiDAR observations from surveys performed after Hurricane Sandy. Mesh elevations outside the southern New England region were developed based on elevations from the original HSOFS mesh. The entire model mesh is presented in Figure 4, and zoomed in views local to each park are presented in Figure 5-Figure 7, where the mesh element edges are colored to reflect the mesh elevations. In areas of high resolution, the edges tend to run into one another and appear as continuous fill. However, at distances further from shore where the resolution is coarser, the spaces between edges are more apparent. The resolution varies significantly, from kilometer scale in offshore regions to tens of meters and even meters scale in the nearshore. The complex terrain in New England, highly variable bottom elevation changes over short distances, is a challenge to modeling and is most efficiently captured with an unstructured mesh such as this that can be adapted as needed.

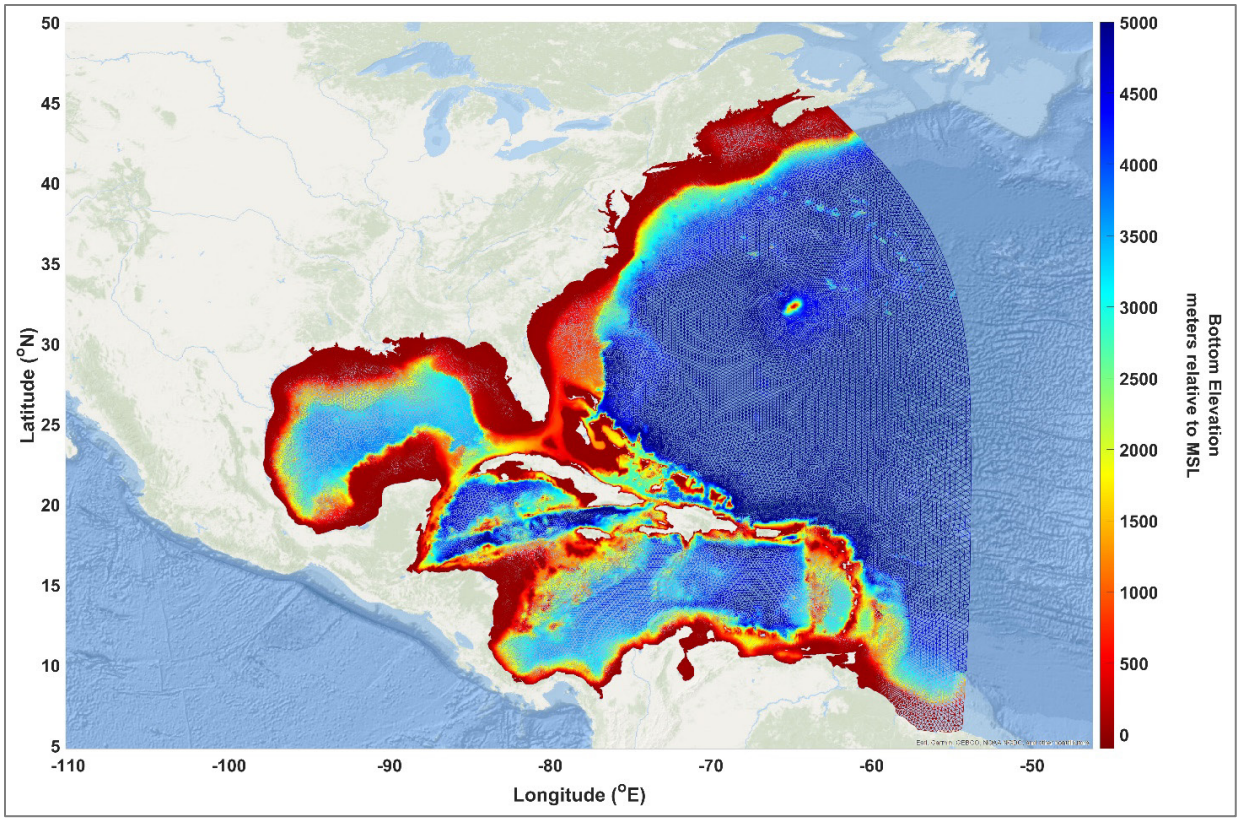


Figure 4. Advanced circulation model (ADCIRC) mesh (entire extent) plot over ESRI ocean basemap imagery with mesh elements colored by elevation (depths are positive).

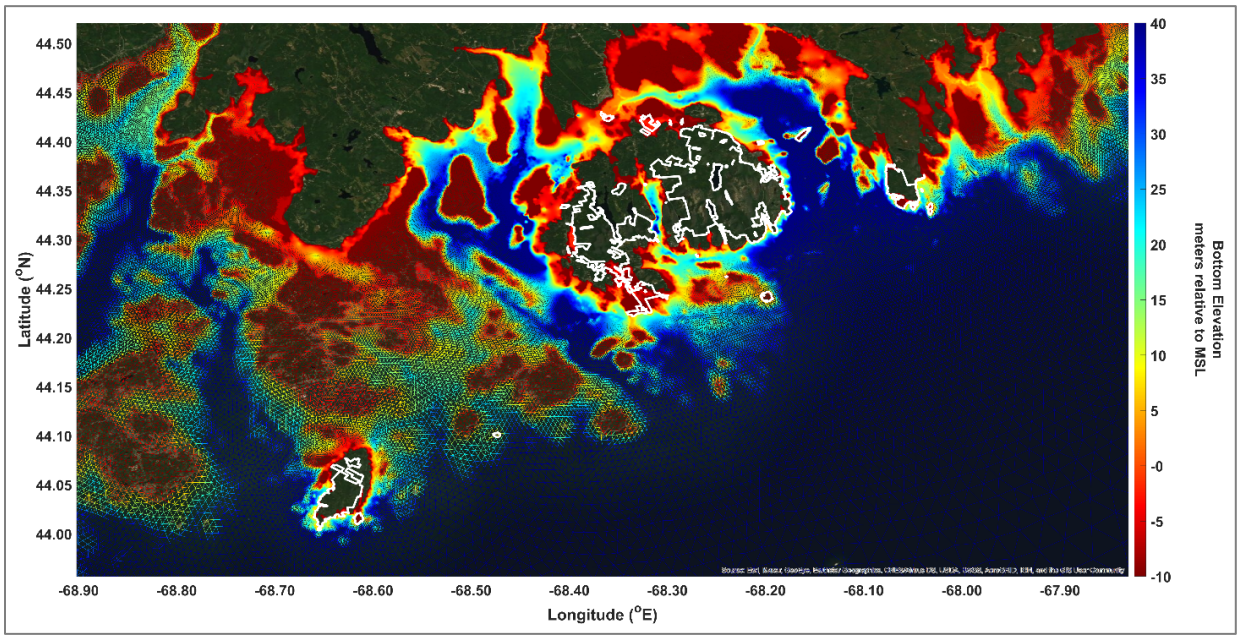


Figure 5. Advanced circulation model (ADCIRC) mesh local to Acadia National Park plot over ESRI satellite imagery with mesh elements colored by elevation (depths are positive). Park boundaries are overlain in white.

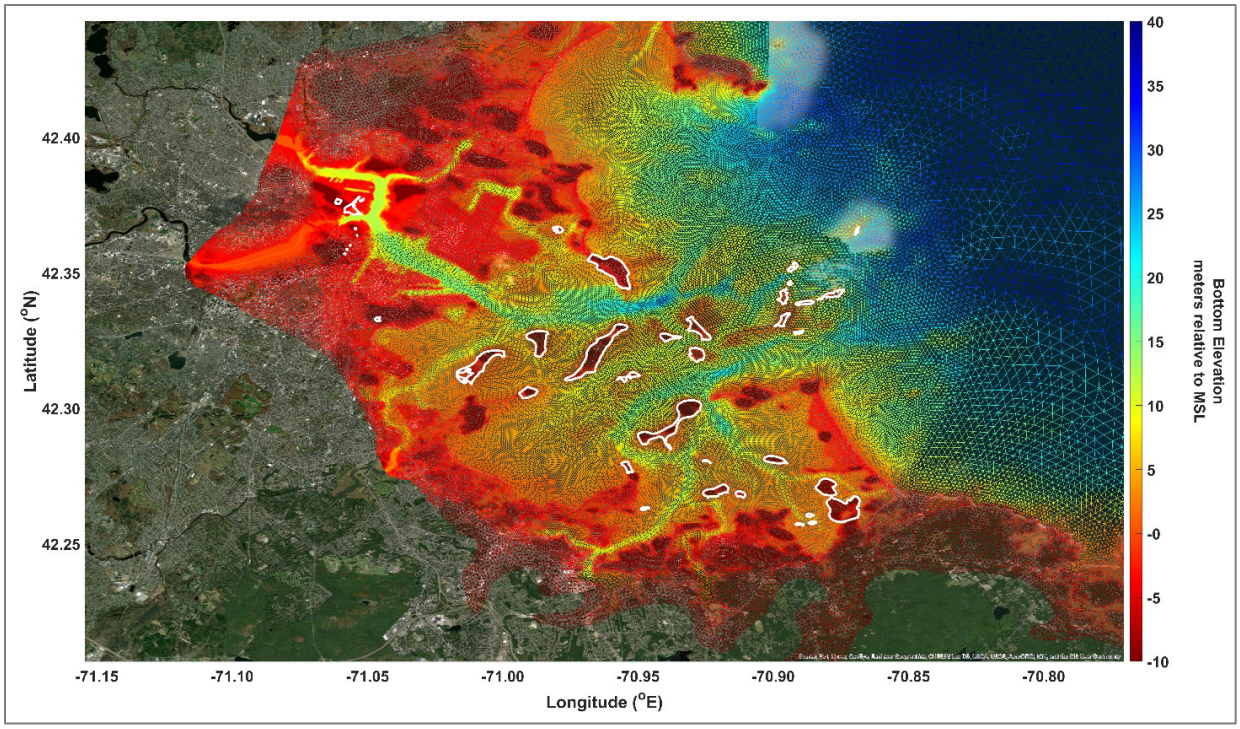


Figure 6. Advanced circulation model (ADCIRC) mesh local to the National Parks of Boston plot over ESRI satellite imagery with mesh elements colored by elevation (depths are positive). Park boundaries are overlain in white.

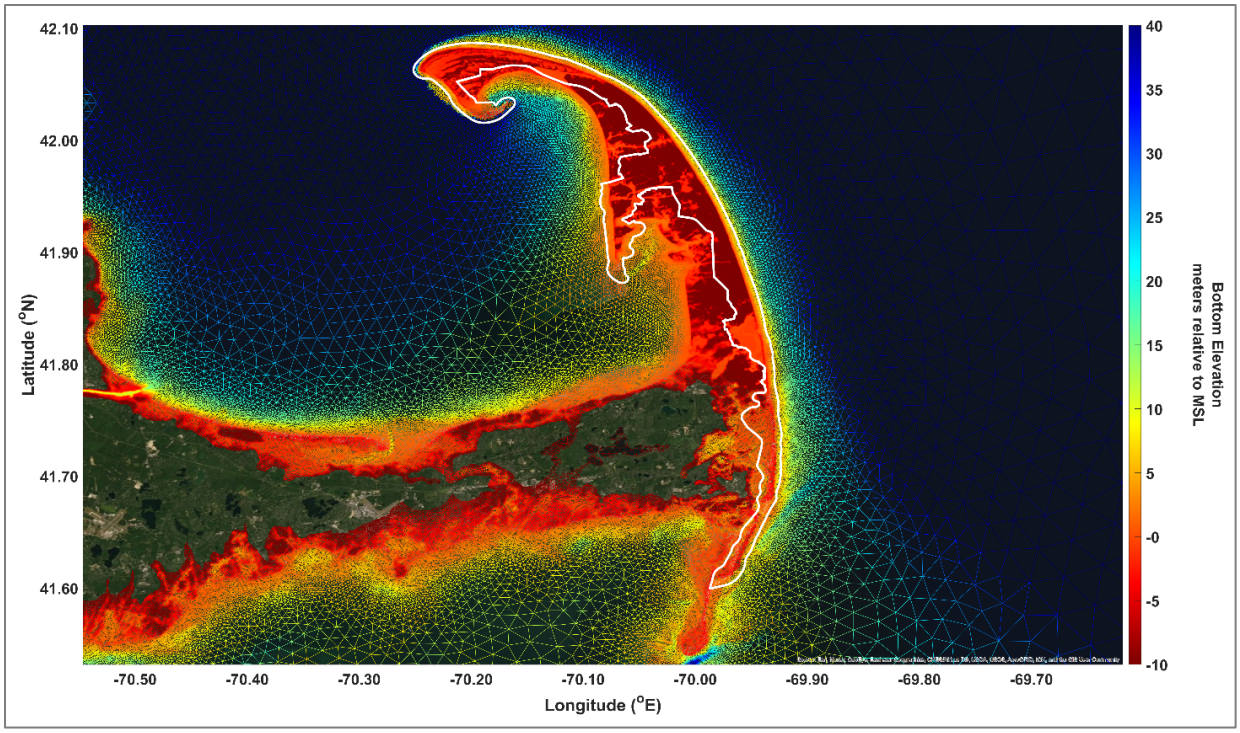


Figure 7. Advanced circulation model (ADCIRC) mesh local to Cape Cod National Seashore plot over ESRI satellite imagery with mesh elements colored by elevation (depths are positive). Park boundaries are overlain in white.

The mesh specification contains optional "nodal attributes," which are parameters related to physical and numerical processes. Table 3 provides a summary of the nodal attributes used in this application. The model input files will be included as part of the data delivery for this project as a record of the model details.

Table 3. Summary of advanced circulation model (ADCIRC) nodal attributes.

Nodal Attribute	Description
mannings_n_at_sea_floor	Bottom roughness which is used as a tuning parameter to validate the model predications of water level. Values were variable in accordance with Table 4.
sea_surface_height_above_geoid	Value applied to achieve the appropriate MSL. Spatially and temporally constant, however varied per scenario.
primitive_weighting_in_continuity_equation	Affects numerical stability and assigned using ADCIRC utility program.
advection_state	Used to enable advective terms, parameters can be set to spatially vary where the terms are considered.
elemental_slope_limiter	Used to improve model stability as it limits the slope of the water surface across nodes. Limit set to 0.01 (1%)

Table 4. Summary of Manning's n used for each modeling event.

ID	Event	Manning's n s/[$m^{1/3}$]
1	April 2007 Nor'easter	0.035
2	January 2018 Nor'easter	0.030
3	March 2018 Nor'easter	0.035

Tidal forcing

The model includes tidal forcing at the nodes along the open boundary and meteorological forcing applied to the water surface (all 'wet' nodes). The tidal boundary conditions were extracted from the HSOFS model setup. Site-specific astronomical constituent specifications are assigned at the nodes along the offshore boundary. These astronomical characteristics describe the periodic nature of the water level by specifying the amplitude and phase of each constituent at the open boundary. The model sums the contribution from all constituents and propagates these water levels through the domain; this process ensures that the appropriate water level is calculated at each node at each simulation timestep. The tidal forcing includes eight constituents (M2, S2, N2, K2, K1, O1, P1, Q1), which vary in magnitude along the open boundary.

Meteorological Forcing

The meteorological forcing is applied as spatially and time varying fields of wind (speed and direction) and atmospheric pressure for a spatial extent that encompasses the ADCIRC mesh. This forcing was developed using the European Centre for Medium Range Weather Forecasts (ECMWF) reanalysis product ERA5 (Dee et al., 2011). ERA5 is the output from the ECMWF global atmospheric model provided at a 0.25-degree spatial resolution and a one-hour temporal resolution. Figure 8 through Figure 10 show a snapshot of the meteorological conditions near the peak of the storm speed, as well as a time series of wind speed local to the different focus areas (Bar Harbor, ME, Boston, MA, and Provincetown, MA) for each event.

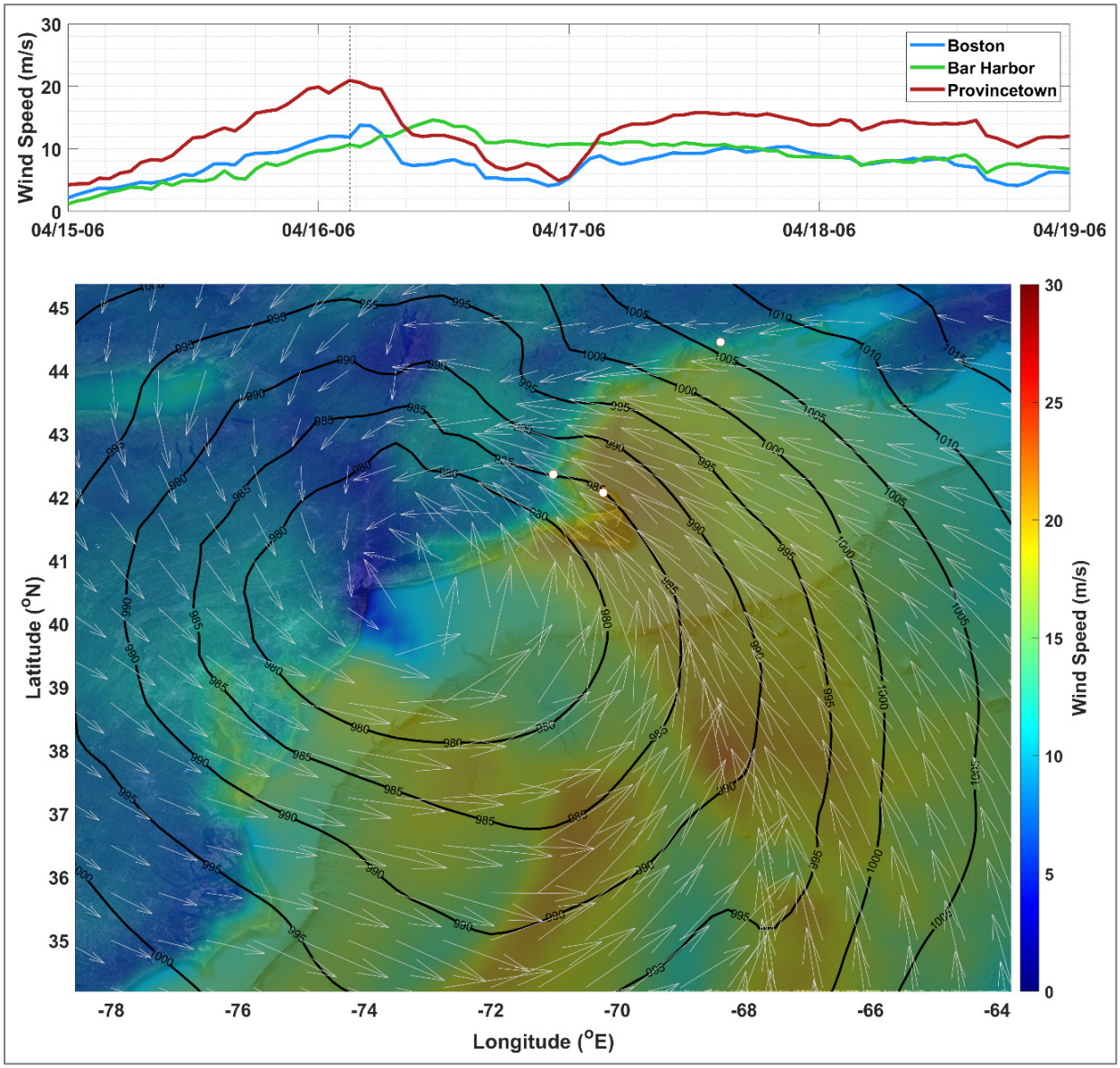


Figure 8. Snapshot of meteorological forcing during the April 2007 nor'easter from the European Center for Medium Range Forecasts Re-Analysis 5 (ERA-5) data overlaid on satellite imagery. Top plot shows time series (x-axis is month/day–hour) at the three locations denoted with white circle markers and the bottom plot shows the spatial field of wind speed (color contour) wind direction (vectors) and atmospheric pressure (contour lines with labels of pressure in mbar) at the time identified with the vertical black line in the upper plot.

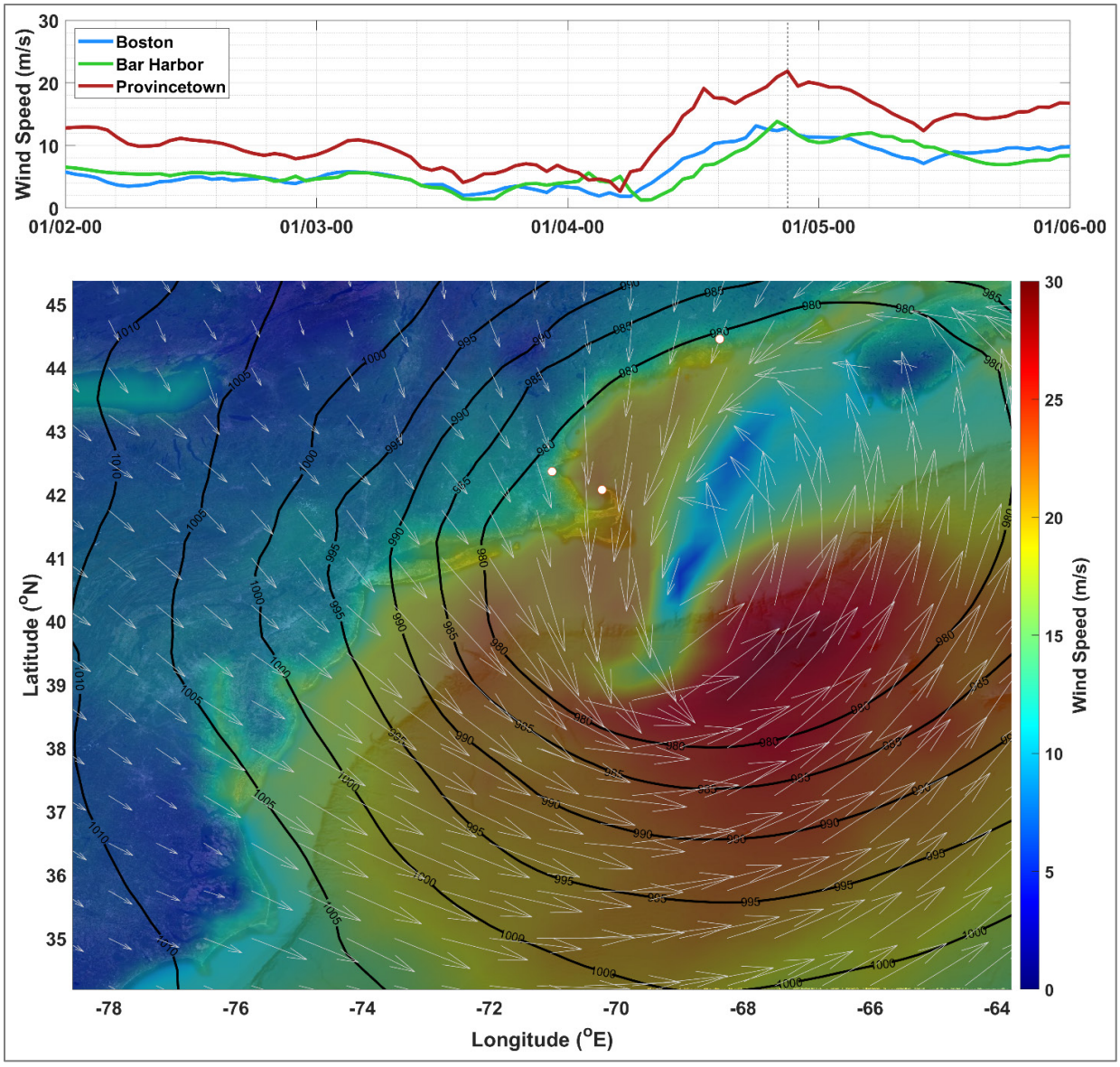


Figure 9. Snapshot of meteorological forcing during the January 2018 nor'easter from the European Center for Medium Range Forecasts Re-Analysis 5 (ERA-5) data overlaid on satellite imagery; top plot shows time series (x-axis is month/day–hour) at the three locations denoted with white circle markers and the bottom plot shows the spatial field of wind speed (color contour) wind direction (vectors) and atmospheric pressure (contour lines with labels of pressure in mbar) at the time identified with the vertical black line in the upper plot.

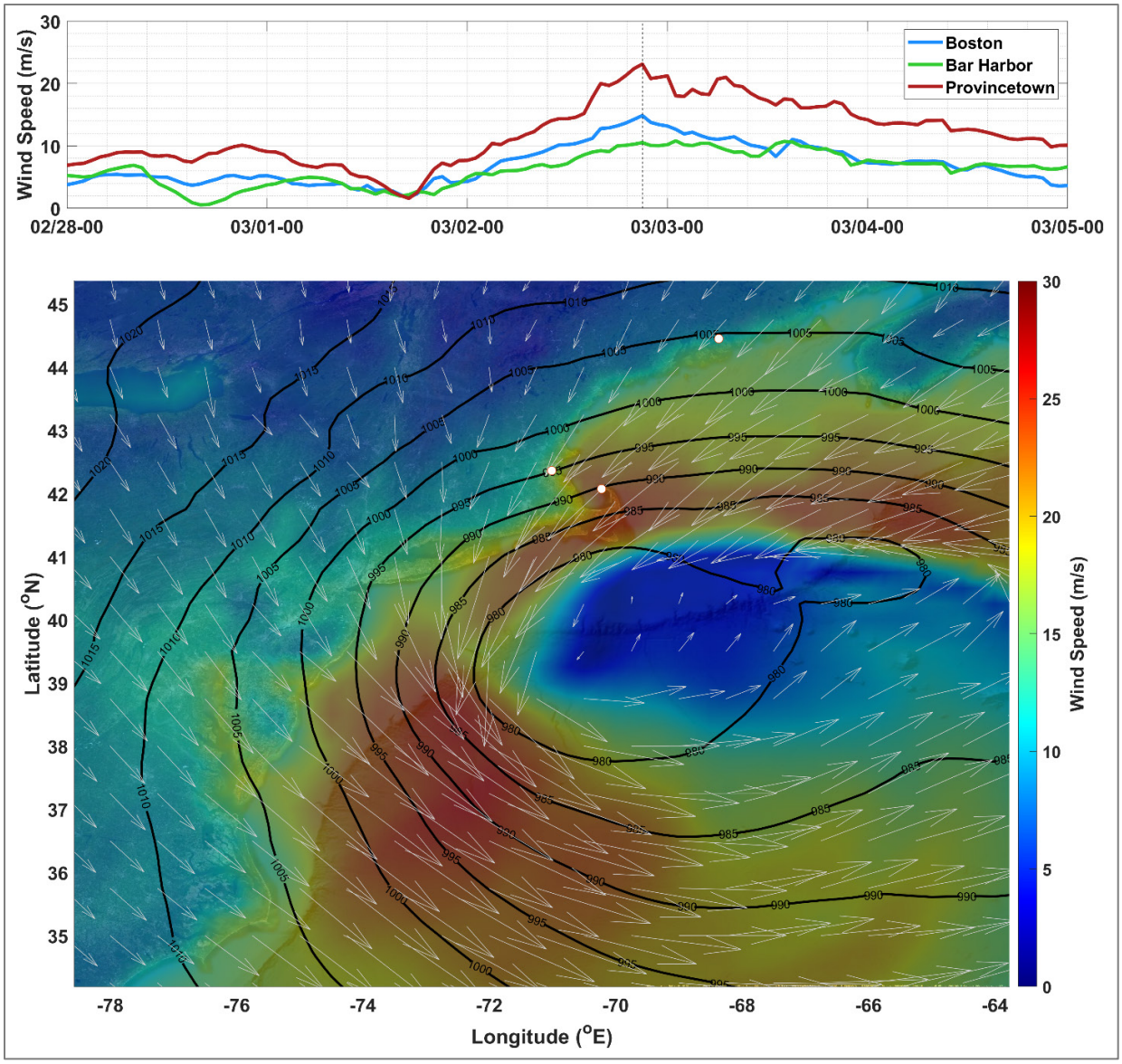


Figure 10. Snapshot of meteorological forcing during the March 2018 nor'easter from the European Center for Medium Range Forecasts Re-Analysis 5 (ERA-5) data overlaid on satellite imagery. Top plot shows time series (x-axis is month/day–hour) at the three locations denoted with white circle markers and the bottom plot shows the spatial field of wind speed (color contour) wind direction (vectors) and atmospheric pressure (contour lines with labels of pressure in mbar) at the time identified with the vertical black line in the upper plot.

Modeling Parameters

The model system has numerous required and optional parameters that have either physical or numerical significance. The model control files will be supplied as part of the data delivery for this project as a record of the model details.

Model Validation

Prior to using model results for assessing vulnerabilities and planning purposes, the modeling approach and ADCIRC-SWAN model performance were validated by comparing the meteorological forcing and results of the ADCIRC-SWAN simulations of historic events to available observations. This validation involved comparing the observed wind to the model wind speed, as well as comparing the simulated water levels, wave heights, and areas inundated to available observations. To prevent artificial flooding in the model, the validation process for tidal inundation included unsmoothing and manually assigning nodal elevations to prevent inundation over land outside intertidal regions in inland areas with clear evidence that they are not flooded regularly due to tides (e.g., developed areas). The simulations of tides alone were conducted iteratively, incorporating mesh changes until the inundation during high and low tides generally agreed with the footprint of intertidal regions as delineated on NOAA navigation charts or aligned well with the shoreline as compared to aerial imagery.

Simulations of Nor'easters

The model simulations for each event were conducted in two stages: a spinup period to ramp in the tides, followed by the storm period starting from the final step of the spinup. To assess the impact of SLR, each event was simulated with three different mean sea levels (MSLs) in addition to the actual MSL that was simulated for model validation, (1) the expected MSL for 2020; (2) with 1 foot (ft) (0.3048 m) of SLR added to the 2020 MSL; and (3) with 1 m (3.2808 ft) of SLR added to the 2020 MSL. The expected MSL for 2020 was simulated to provide a consistent baseline case across storms that is close to the present day. The choices of 1 ft and 1 m of SLR reflect midterm (~2050) and long term (~2100) projections respectively; more details supporting these choices are provided in the *Synthesis of Sea Level Rise Data and Literature* subsection of the *Results* section. The modification of MSL for each event was handled by using the "sea surface height above geoid" nodal attribute, allowing an offset relative to the MSL by which the mesh elevations were defined to achieve the desired MSL. Initial spinup simulations indicated that the tides were sufficiently ramped in within a couple of days, and for the final simulations, the spinup was conducted for a period of 5 days. The storm periods were simulated between 4–4.5 days, depending on the event. The timing of the spinup and start of the storm period were chosen such that the storm had not yet developed locally to the park, enabling the simulation of the storm's evolution. The duration was chosen to ensure the peak water levels were captured.

Analysis of the Role of Waves

We investigated the importance of including wave coupling (ADCIRC coupled with SWAN) by comparing it with running ADCIRC alone, both with and without SLR, to quantify the contribution of waves to coastal water levels and examine how it may change with SLR. Our analysis focused on the outer east coast of Cape Cod, which experiences significant storm surge and offshore waves (Figure 11). We conducted simulations of the January 2018 Nor'easter with and without wave coupling, with no SLR and with 1m SLR. Note, for this analysis, we chose only to simulate the upper bound of SLR considered in our analysis. The results were evaluated to determine the difference in peak water elevations with and without wave coupling, as well as the difference in the wave regime with and without SLR.

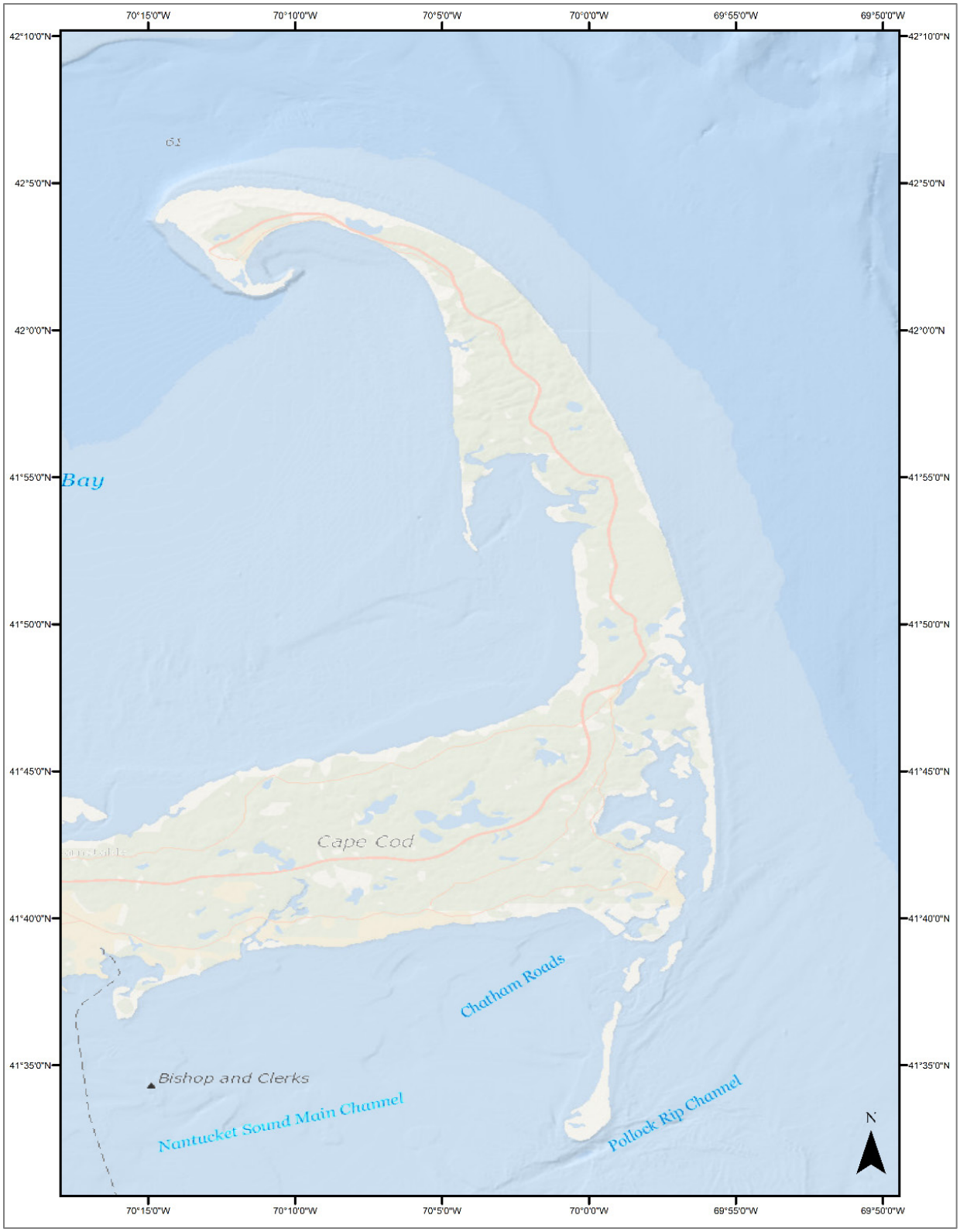


Figure 11. Wave analysis study area on the outer east coast of Cape Cod, MA, is depicted by the black box.

Analysis of the Effect of Shoreline Configuration on Storm Surge and Peak Water Level

We investigated the impact of shoreline changes on peak water levels and storm surges in the southeast Cape Cod Pleasant Bay region. This region is susceptible to significant morphological changes resulting from tides and waves. According to previous studies (Giese et al. 2009), the morphological evolution of the barrier system in this area is cyclical. However, the rate of morphological changes is not constant, and storms can cause significant changes over short intervals. Figure 12 presents satellite imagery in the southeast Cape Cod region illustrating the barrier beach changes at different times between 1986-2017.

Below is a review of the evolution of the shoreline configurations observed over time referencing Figure 12:

- 1986: This depicts the furthest southward extent of an intact barrier beach, with the main opening to the Atlantic Ocean at location B, which is more southward than eastward facing, and there is a hydraulic connection to Nantucket Sound (A).
- 1987: A strong nor'easter in 1986 resulted in a breach that formed an inlet at location C. The opening to the Atlantic (B) and hydraulic connection to Nantucket Sound (A) are the same as in 1986.
- 1992: There has been some southward migration of the barrier, and the previous barrier island (between B-C) has morphed such that there is no longer a hydraulic connection to Nantucket Sound (A). The only opening to the Atlantic from the interior embayment is an east facing inlet at location C.
- 2006: This shows some southward migration of the barriers, though the general inlet opening locations are the same as in 1992, and there is still no hydraulic connection to Nantucket Sound (A).
- 2007: A powerful nor'easter has resulted in a breach that forms a new east facing opening (D) north of C. There are now two inlets between the embayment and the Atlantic but no hydraulic connection to Nantucket Sound (A).
- 2017: Southern migration and localized morphological changes near the inlets are evident, though the most notable difference is a hydraulic connection to Nantucket Sound (A).

Changes in shoreline configuration have been linked to changes in the tidal range within the embayments (Aubrey and Weishar 2013). Further, Figure 12 illustrates that these morphological changes can sometimes be significant and result in changes to the hydraulic connection between the Atlantic Ocean, Nantucket Sound, and the embayments behind the barrier beach (Chatham Harbor, Pleasant Bay, and Little Pleasant Bay). In this study, we analyzed the historic shoreline configurations and used the ADCIRC-SWAN modeling system to investigate how they influence vulnerability to coastal flooding during the January 2018 Nor'easter.

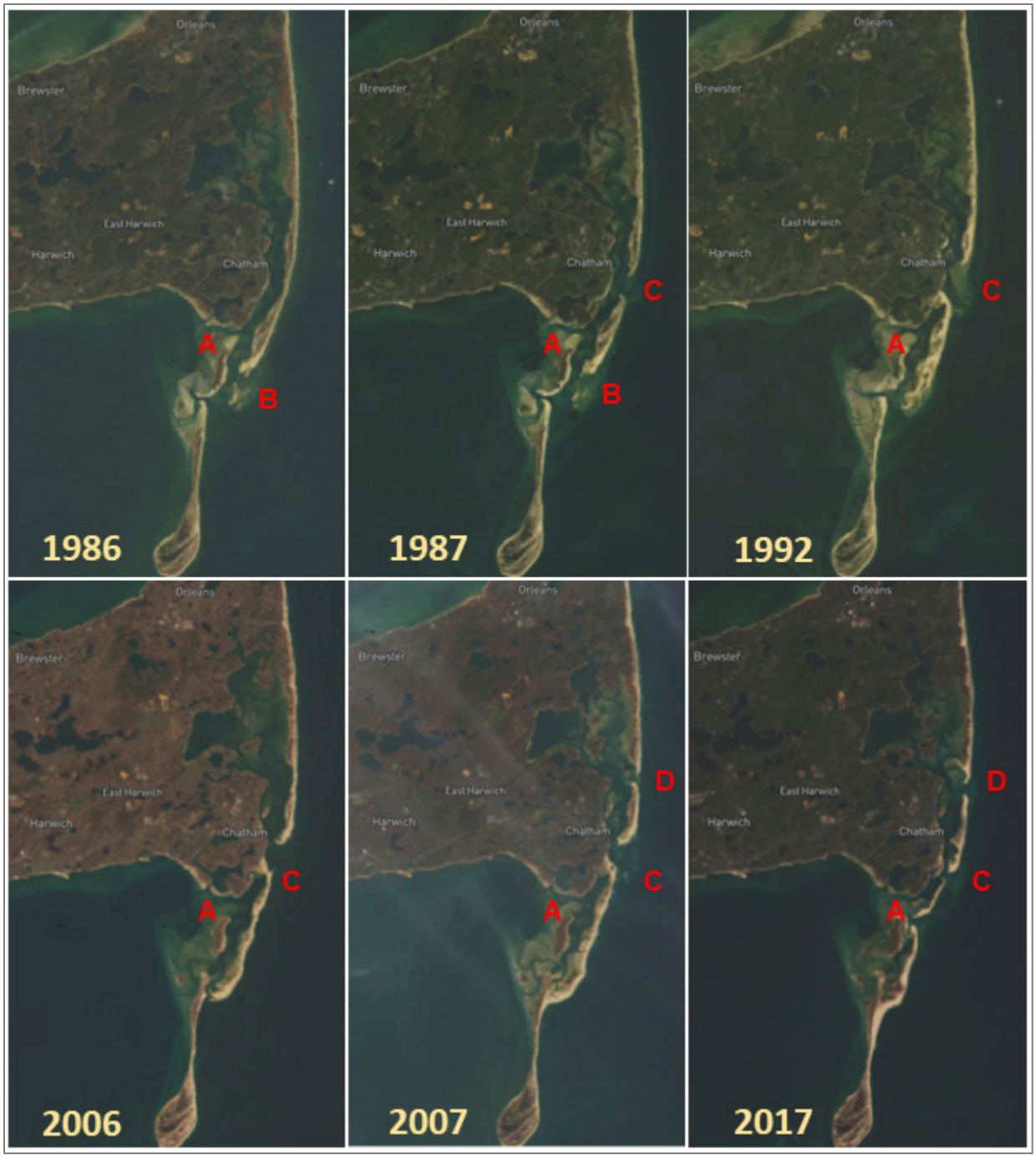


Figure 12. Satellite imagery from the United Stats Geological Survey Land Process Distributed Active Archive Center showing southeastern Cape Cod, MA, for different years showing different shoreline configurations. Letter A marks a point along the southern Cape above the spit of Monomoy National Wildlife Refuge on the Nantucket Sound side, letter B marks the approximate location of the southern entrance on the Atlantic Ocean side circa 1987-1987, letter C marks a second opening on the Atlantic side that formed in 1987, and letter D marks the approximate location of a new inlet formed in 2007.

We first analyzed historical shoreline configurations by reviewing satellite imageries. While these images do not provide bottom elevations and the tidal phase associated with each image is unknown,

they were used to estimate a mean shoreline for a specific year with distinctly varying features. We assumed that light sandy areas are above the tidal range, and darker sediments and areas covered with water are below the low end of the tidal range. The mean shoreline was delineated by hand between these features. For each configuration, the approximate inlet widths were measured, and the presence of a hydraulic connection between Chatham Harbor and Nantucket Sound was noted, as these are important variables that can affect the water levels within the embayments behind the barrier system. A summary of the years analyzed, and the associated metrics is provided in Table 5.

Table 5. Summary of shoreline configurations assessed at Pleasant Bay, MA.

Year	Hydraulic Connection to Nantucket Sound	Total Width Open to Atlantic (m)	Total Width Open to Nantucket Sound (m)	Total Opening Width (m)
1986	Yes	600	350	950
1987	Yes	1876	440	2316
2002	No	1230	NA	1230
2006	No	1220	NA	1220
2008	No	1930	NA	1930
2016	No	517	NA	517
2021	Yes	1530	191	1721

Based on our analysis of historical shoreline configurations, we developed three hypothetical shorelines to represent the following configurations that bounded the variability. These configurations are shown in Figure 13 and a description is provided below:

- Configuration 1: Small opening to the Atlantic Ocean and no opening to Nantucket Sound
- Configuration 2: Large opening to the Atlantic Ocean and no opening to Nantucket Sound
- Configuration 3: Large opening to the Atlantic Ocean with an opening to Nantucket Sound

These shoreline configurations are treated as hypothetical since historical elevation information was not consistently available. Note that only the key shoreline features used to distinguish the different configurations are delineated in Figure 13.

The model mesh and setup for this analysis are described in previous sections, with the exception that in this region the mesh nodal elevations were adjusted to reflect different hypothetical shoreline configurations. For each shoreline configuration, a separate ADCIRC mesh was generated to represent the specified shoreline features. Areas designated to be permanently dry were assigned an elevation of 3 m above MSL, and areas designated as inlets were assigned a depth of 2 m below MSL, with some transitioning to adjacent nodes. The mesh resolution in this region is shown in the leftmost panel of Figure 14 and the mesh nodal elevations for the three configurations are shown in the three panels on the right.

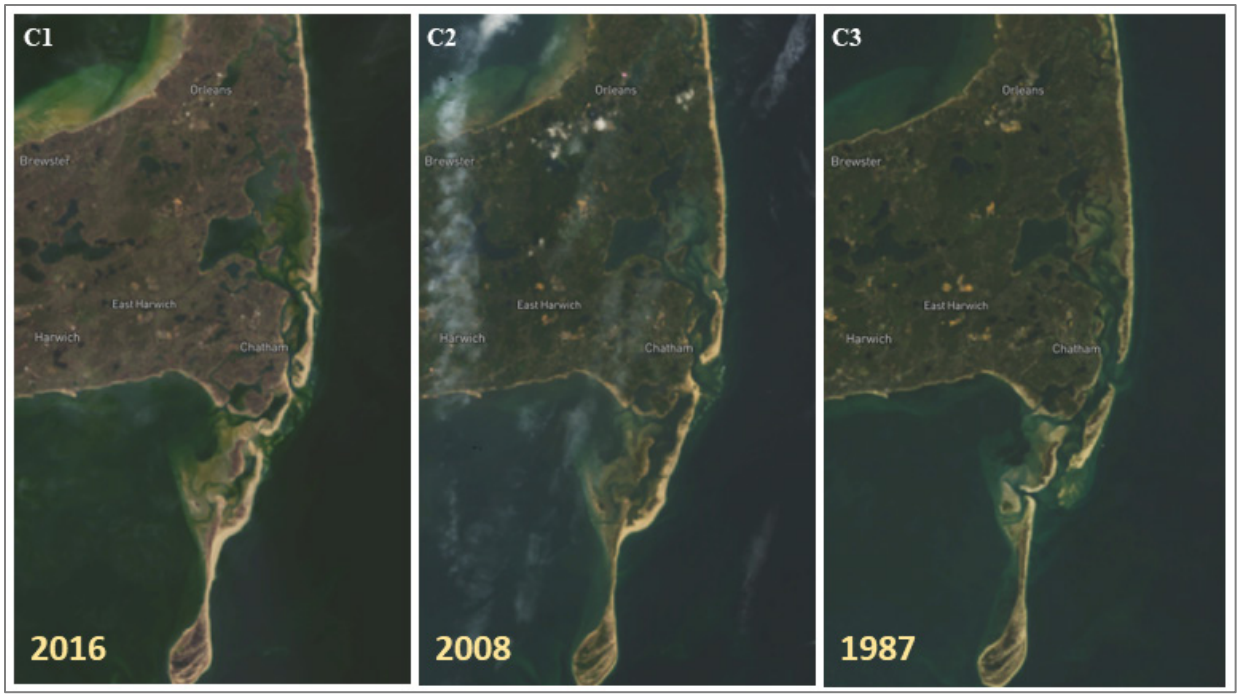


Figure 13. Delineated mean shoreline for analysis configurations shown over satellite imagery from the United Stats Geological Survey Land Process Distributed Active Archive Center.

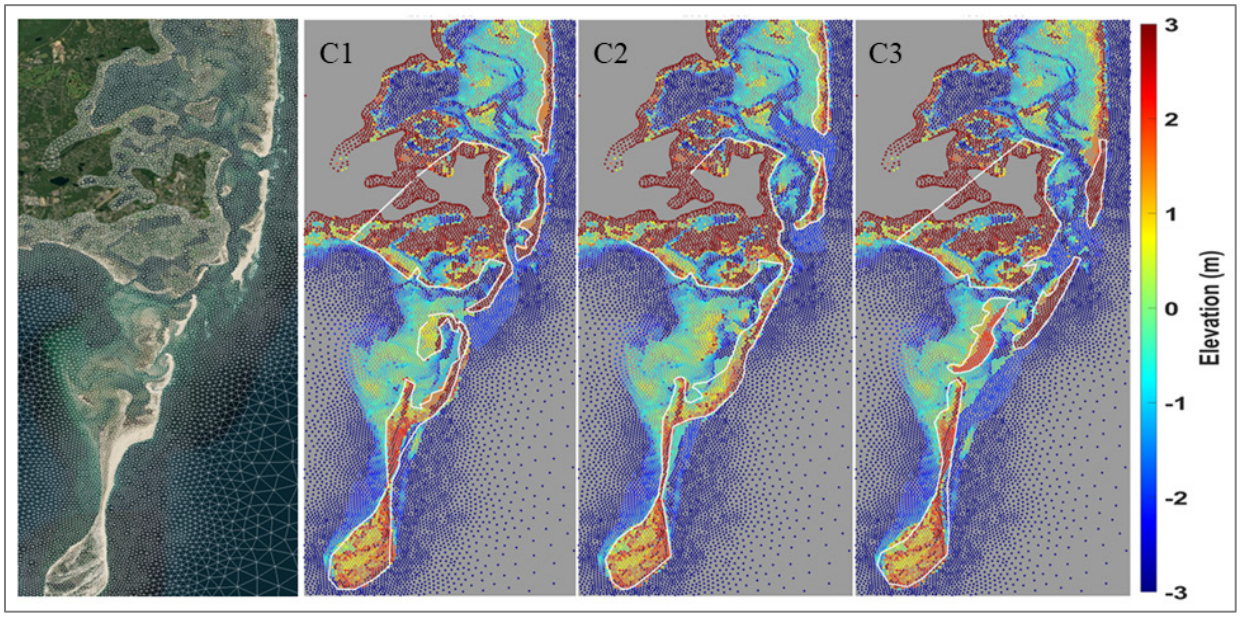


Figure 14. Mesh resolution shown over satellite imagery from ESRI (left) and modified mesh elevations for configuration 1 (middle-left), 2 (middle-right) and 3 (right) for the Pleasant Bay region located in southeastern Cape Cod. The delineated shoreline of the reference historical mean sea level is overlaid in white for reference.

For each configuration, we conducted three simulations, (1) a tidal spinup period; (2) a storm period with wind forcing; and (3) a storm period without wind forcing. We used the difference

between the runs with and without wind forcing to estimate storm surge, as it removes the influence of the tides and isolates the wind driven effect. The results were analyzed to characterize the peak water level and surge in different locations for a relative comparison of the three configurations.

3D Visualization

Realistic 3D visualizations for select areas have been created to communicate the impacts of Nor'easters. These visualizations were created by combining ADCIRC model outputs with geographic information provided by the United States Geological Survey (USGS), National Park Service, and the US Department of Agriculture. This was accomplished using a combination of platforms, including McNeal Rhino, RhinoTerrain SAS RhinoTerrain, Avenza Geographic Imager, and driven by ADCIRC outputs using custom scripts written in the R and Python program language. Visualization methods are described in more detail in Stempel et. al. 2023 and Stempel et.al. 2018. The combined work forms a visualization infrastructure that was applied to create multiple visualization products at the direction of NPS representatives. A summary of visualizations developed for the project is provided in Table 6.

Table 6. Summary of three-dimensional visualizations developed for *The Impact of Sea Level Rise During Nor'easters in New England* study.

Park	Sites Visualized	Storm Scenarios
Acadia National Park	Trenton Bridge	Existing conditions / March 2018 Nor'easter / +1m SLR
Acadia National Park	Sand Beach	Jan 2018 Nor'easter / +1m SLR
Cape Cod National Seashore	Eastham	March 2018 Nor'easter / +1m SLR
Cape Cod National Seashore	Orleans Circle	Jan 2018 Nor'easter / +1m SLR
Cape Cod National Seashore	Race Point Light	Jan 2018 Nor'easter / +1m SLR
Cape Cod National Seashore	Race Point Bathhouse	Jan 2018 Nor'easter / +1m SLR
Cape Cod National Seashore	Province Town (Wood End)	March 2018 Nor'easter / +1m SLR
Boston National Historical Park	Charlestown Navy Yard	Jan 2018 Nor'easter / +1m SLR
Boston Harbor Islands National Recreation Area	Georges Island	Existing / March 2018 Nor'easter / +1m SLR

Results

Literature Review of Extratropical Cyclones ("Nor'easters') and Associated Storm Surges in New England

Meteorologically, New England is situated in a transitional zone between continental and marine climate types and experiences both tropical cyclones (TCs) and extratropical cyclones (ETCs) depending on the time of year. TCs generally originate in the tropical and subtropical waters to the south-southeast during summer through mid-fall, occasionally causing major coastal flooding to the region, as seen most recently from Hurricane Sandy (2012). TCs typically bring stronger winds and higher surges, while ETCs tend to impact larger stretches of coastline. ETCs typically impact an area for a longer duration than TCs.

ETCs that affect New England typically originate from the west-northwest during late autumn through spring seasons. The intensification and storm track of ETCs are often determined by the relative position of troughs and ridges in the jet stream. The primary energy source of ETCs is a temperature difference between the cold air over land and the relatively warmer air over the ocean. Warmer air holds more moisture and northeast winds blow this moisture-laden air onshore when the storm approaches the coast, resulting in heavy rain and snow and strong winds (Hirsch et al. 2001; Zhang et al. 2000; Thompson et al. 2013). The strongest ETCs, commonly known as nor'easters, often intensify offshore and follow a more meridional path, causing them to travel slower and impact the region for longer periods (Dolan and Davis 1992; Zhang et al. 2000; Bernhardt and DeGaetano 2012; Colle et al. 2015; Booth et al. 2016; Catalano and Broccoli 2018). Nor'easters are responsible for most coastal flood events in New England as compared with TCs. Forecasting the intensity and size of nor'easters can be challenging, and they can rapidly strengthen near or directly onshore while tracking northeastward along the coastal front, thereby amplifying their impact. This challenge extends to hybrid storms, which exhibit characteristics of both TC and ETCs, as exemplified by Hurricane Sandy in 2012.Under current global warming scenarios, it is projected that the intensity (maximum wind speed and central pressure) of TCs and frequency of major hurricanes in the Atlantic Basin will increase in the future (Knutson et al. 2019; Knutson et al. 2020). However, projections regarding intensity, size, and storm track positions of ETCs due to changes in synoptic atmospheric patterns in the future climate remain inconclusive (Michaelis et al. 2017; Dupigny-Giroux et al. 2018; Lin et al. 2019).

Several studies investigated the differences between TCs and ETCs in coastal flood events. However, very few have focused on New England. Booth et al. (2016) examined extreme storm surge events (greater than 1-yr return level) at selected tide gauges from Duck, North Carolina to Portland, Maine. They found that for broad coastal flood events, tropical systems were the primary cause, whereas for less severe events and coverage, the importance of TCs decreased, and that of ETCs increased, with higher frequencies of TCs in southern regions. Catalano and Broccoli (2018) focused on the large-scale atmospheric influences on ETC surge events at three locations along the U.S. East Coast (Boston, Massachusetts; the Battery, NYC; and Sewells Point, Virginia). They noted that surge events in Boston and Sewells Point occur primarily during El Niño conditions. Strong El Niños produce anomalous northeasterlies along the East Coast, which is the predominant wind direction for

the largest surge events in those regions. However, Catalano and Broccoli (2018) did not observe any significant correlations between ENSO and storm-surge height among the top 100 surge events.

Using the ADCIRC hydrodynamic model, observations, and climate projections from seven climate models, Lin et al. (2019) investigated changes in ETC storm surges between a historical period (1979–2012) and a future period (2054–2079, RCP8.5 emission scenario) at several sites along the northeast coast of the United States, including Boston. The study found significant discrepancies among climate model projections, with some models predicting only minor increases or decreases in 10- and 50-year storm surge levels, while others forecast substantial increases at all sites (up to 27% and 36% increase in 10- and 50-year surge levels, respectively). However, this study has several limitations. Directly applying the atmospheric wind and pressure fields projected by climate models, which have limited resolutions and possible biases, induces uncertainties in the surge estimation. The hydrodynamic model also has a limited resolution (~1 km along the coast) and neglects factors such as surface waves.

In summary, previous studies have mainly focused on ETC storm surge, which is one of several contributors to coastal flooding. The total flood level is a combination of storm surge, astronomical tide, and sea level rise. To our knowledge, limited studies have yet examined the combined effects of these factors on coastal flooding during ETC events along the northeast coast of the United States. This project aims to fill this gap and investigate the impact of these factors on coastal flooding in the focus parks (CACO, BOHA, BOST, and ACAD).

Sea Level Rise Literature Review and Data Analysis

We reviewed the interagency 2022 Sea Level Rise Technical Report led by NOAA (Sweet et al., 2022) to synthesize data related to the study area. The report provides regional scale projections of SLR aligned with the latest shared socioeconomic pathway (SSP) scenarios from the Intergovernmental Panel on Climate Change (IPCC). The IPCC defines five SSPs that vary in terms of greenhouse gas emissions and socioeconomic factors, resulting in varying levels of expected global sea level rise. The interagency study uses the global sea level rise projections associated with each SSP from IPCC, renamed in accordance with SLR severity from low to high. It also integrates recent observations and improved modeling and analysis techniques to provide estimates of regional scale SLR for each scenario. The projections for each scenario (e.g., low) are provided at three different confidence intervals, represented as percentiles (17^{th}, 50^{th} and 83^{rd}). The 50^{th} percentile value represents the expected value, although due to uncertainty in modeling accuracy, values may be lower (17^{th} percentile) or higher (83^{rd} percentile).

The projections of the expected values for the interagency intermediate scenario, adjusted to be relative to the 2020 MSL, are presented in Figure 15 for various Northeast locations. While there is some minor variability across the region, it is small relative to the variability expected over time. Figure 16 presents an example of projections for the low, intermediate, and high emissions for the expected (50^{th} percentile) and low and high uncertainties (17^{th} and 83^{rd} percentile) at Boston, MA. This demonstrates that the uncertainty in projections can be significant relative to the incremental differences in the severity scenario. For some timeframes, the uncertainty between severity scenarios

overlaps. However, with increased time, the difference between scenarios becomes greater because of the cumulative effects of the pathways assumed for the scenario.

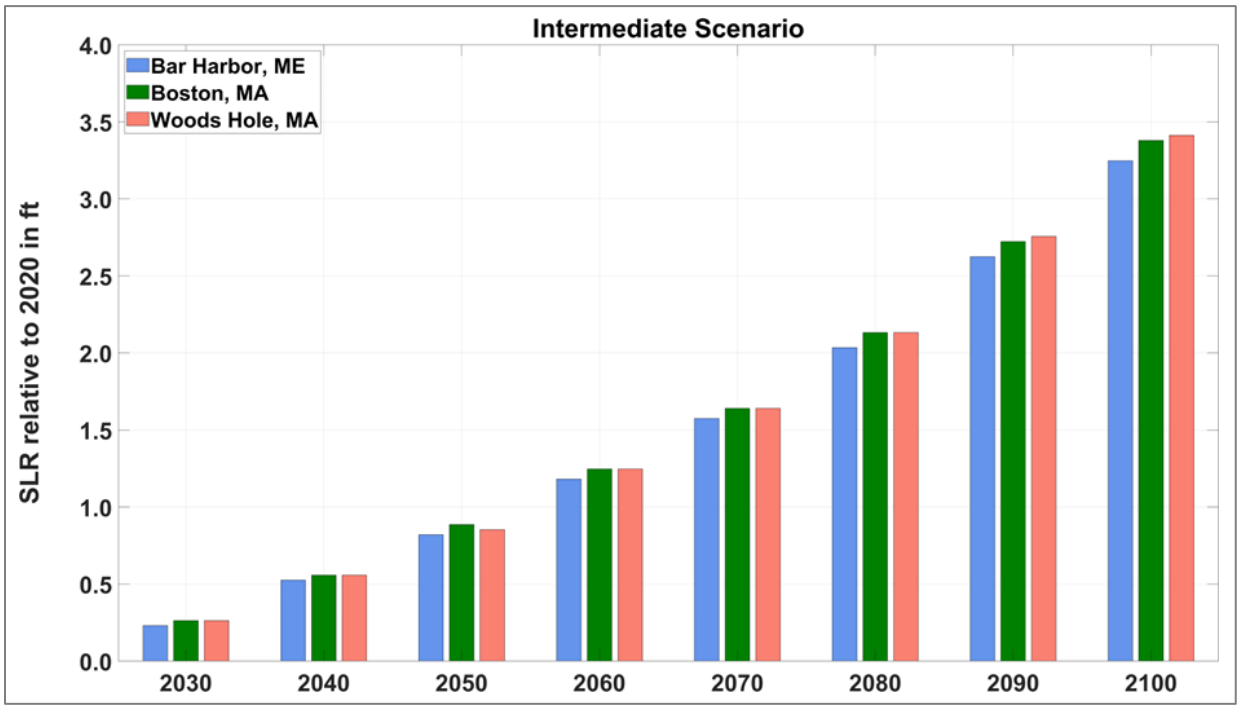


Figure 15. Projections of sea level rise for the intermediate scenario over time at multiple New England locations relative to 2020 mean sea level.

Based on our analysis of the interagency report, the following findings are specific to the study area:

- The mean sea level (MSL) rise in the northeast is projected to increase more than the global MSL.
- Specific MSL rise projections vary across the northeast.
- There is significant uncertainty in the projections, which increase with time from the present.
- The MSL projections vary spatially, albeit to a small degree. For example, considering Woods Hole, Boston, and Bar Harbor the projections vary by 0.02 m (0.066 ft) and 0.05 m (0.164 ft) for the expected value of the intermediate scenario relative to 2020 for 2050 and 2100 respectively.
- Using Boston as a proxy for the study area:
    - The projected MSL by 2050 relative to 2020 ranges from 0.13 – 0.48 m (0.43 – 1.58 ft). The expected value for the intermediate scenario is 0.28m (0.919 ft).
    - The projected MSL by 2100 relative to 2020 ranges from 0.20 – 2.08 m (0.66 – 7.15 ft). The expected value for the intermediate scenario is 0.72m (2.36 ft)

- Considering the projected values from the intermediate scenario for Boston, 1 ft (0.3048 m) and 1m (3.2808 ft) are our choices for proxies of mid-term (2050) and long-term (2100) projections and thus the values we used in the modeling.

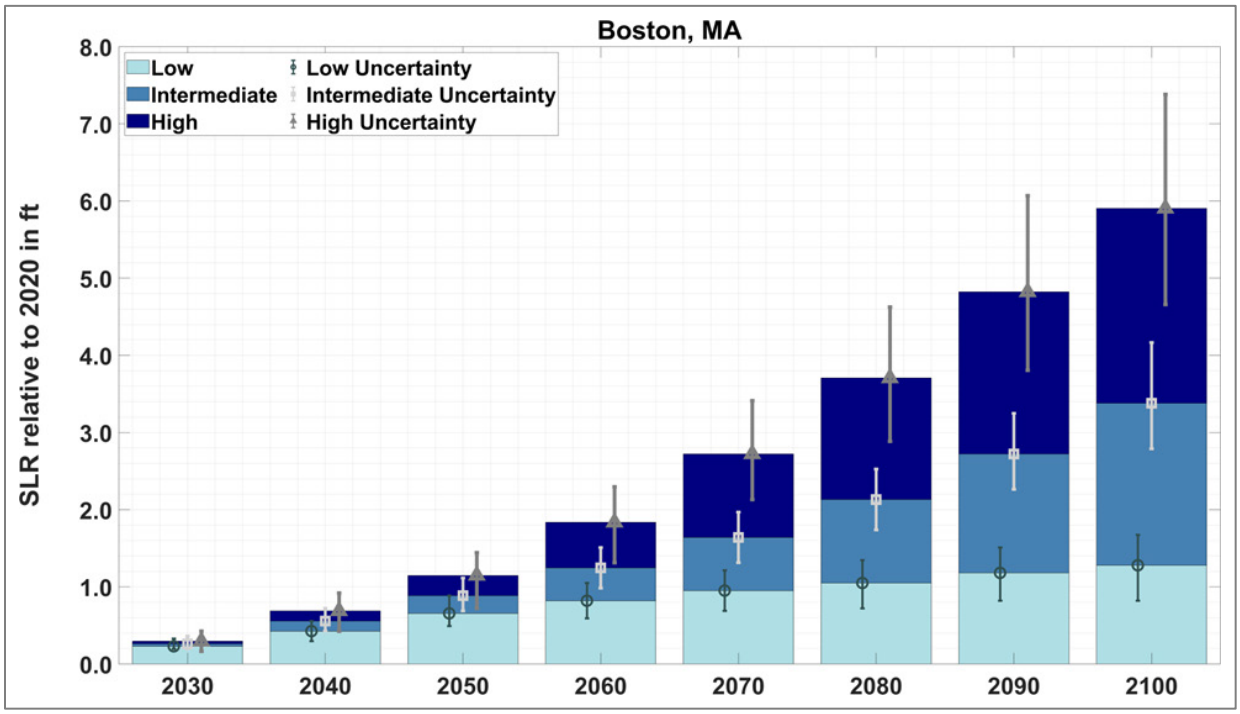


Figure 16. Projections of low, intermediate, and high sea level rise at Boston, MA, relative to 2020 mean sea level along with error bars representing uncertainty.

Results of Historical Water Level Analysis

Water Level Analysis: Historical MSL

The monthly average MSL from tide gauges local to the parks is shown in Figure 17. The dashed black line represents the regional average used to establish the historic MSL.

The historic MSL and the projections of SLR were used to determine the offsets from the present datum of MSL for use in the modeling. A summary of these offsets is presented in Table 7.

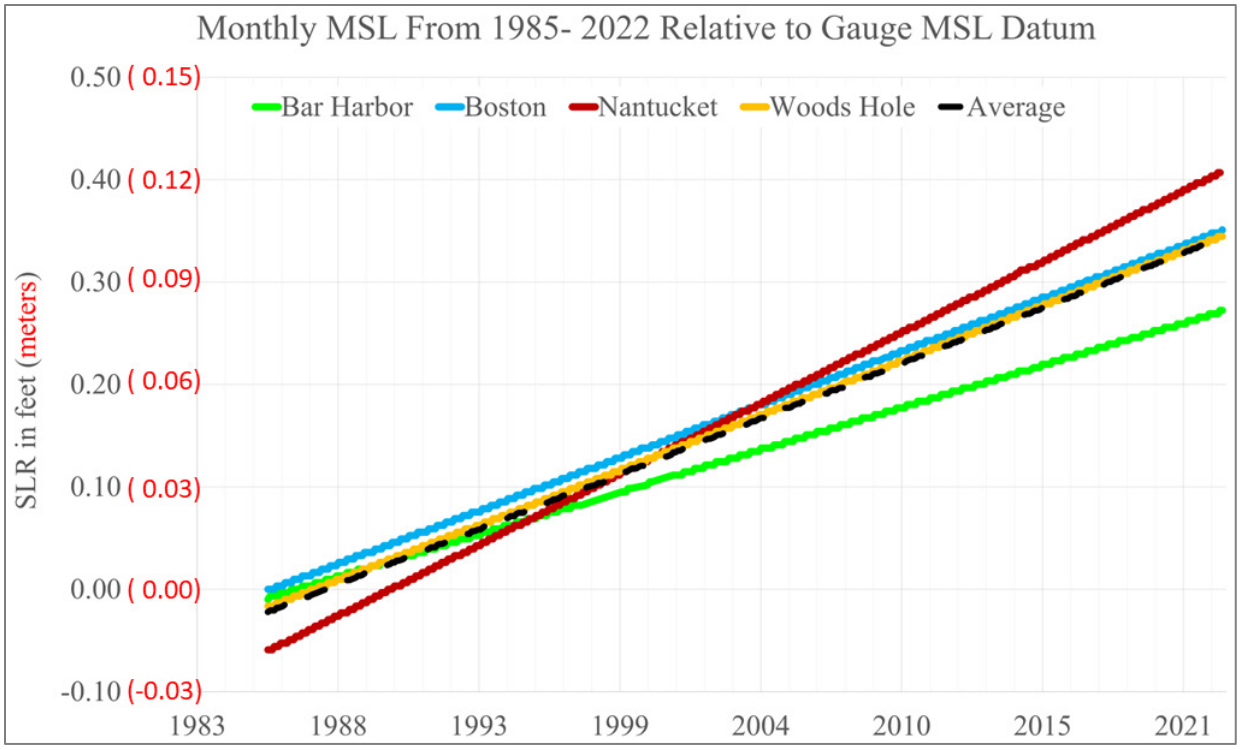


Figure 17. Observed monthly mean sea level at multiple New England locations and their average relative to established mean sea level datum at tide gauges local to the study focus areas.

Table 7. Summary of offsets of mean sea level for historic and future events assumed for the New England region.

Description	Date	Offset of MSL in ft	Offset of MSL in m
Mid-late 1980s MSL[1]	~January 1988	0.000	0.000
Offset from Reference for April 2007 Nor'easter	April 2007	0.190	0.058
Offset from Reference for January 2018 Nor'easter	January 2018	0.296	0.090
Offset from Reference for March 2018 Nor'easter	March 2018	0.297	0.091
Offset from Reference for 2020[2]	January 2020	0.316	0.096
2020–2050 rise of 1 ft (0.304804 m) Relative to Reference	January 2050	1.316	0.401
2020–2050 rise of 3.2808 ft (1m) Relative to Reference	January 2050	3.597	1.096

[1] Zero Reference Point

[2] Reference year for Interagency Projections

Water Level Analysis: Characterization of Peak Water Levels and Storm Surges

We analyzed historic peak water levels and storm surges using NOAA tide gauge measurements at Bar Harbor, ME, Boston, MA, and Woods Hole, MA. The results are presented in Figure 18 through Figure 23, with each site having two figures, each with two subplots. The first figure shows the top fifty water level events, with the corresponding surge associated with each event presented in the bottom subplot. The second figure shows the top fifty surge events, with the corresponding water

level associated with each peak surge presented in the top subplot. The individual bars are color-coded red for tropical storms, blue for nor'easters, and light purple for hybrid storms or nor'easters during the tropical storm season. Additionally, each upper plot of water level shows a dashed black line representing mean higher high water (MHHW).

The record lengths at each site are variable (Figure 3). Despite some gaps in the records, the general trends at each site are well captured. Reviewing each set of plots individually and collectively provide several important insights:

- Peak water levels oftentimes do not coincide with peak surges, and vice versa. Although all presented peak water levels exceed MHHW and have an associated notable surge, noticeably fewer water levels associated with peak surges cross the MHHW threshold.
- Extratropical storms produce more frequent peak water levels and surges than tropical storms. This is particularly true in Boston, which is a proxy for BOHA, BOST, and the majority of CACO (eastern facing shoreline and Cape Cod Bay).
- Tropical storms produce the most severe surges and water levels at Woods Hole, which is along the vulnerable south facing coast of MA, while the other analyzed stations are along east facing shorelines north of Cape Cod.
- The surge magnitude varies across the three sites, with the top 50 peak events ranging from approximately 0.8–1.5m in Bar Harbor, 1–2m in Boston, and 0.75–1.6m in Woods Hole.
- The peak water level also varies across the sites, mostly in response to the varied tide range. Although all peak water levels exceed the local MHHW, few water levels corresponding to peak surges at Bar Harbor and Boston exceed MHHW. However, all peak surges have corresponding water levels that exceed MHHW at Woods Hole, which has the smallest tidal range of the three sites. This illustrates how a larger tidal range can potentially provide more protection extreme water levels during storms.

Our analysis revealed that the January 2018 nor'easter caused one of the most significant water levels at all parks and a relatively large surge observed at all parks. Specifically, the hourly peak water level data in Boston shows it to be the second highest water level event, surpassed only by the blizzard of 1978. However, upon examining the 6-minute data, it becomes clear it is the highest water level recorded at that site. Given the significance of the January 2018 nor'easter and observed coastal flooding in Boston and Cape Cod, we deemed this nor'easter to be an excellent storm event for our modeling study.

Our analysis shows that nor'easters are the most frequent cause of large surges and high-water levels in the study area. Notably, the surges from nor'easters in Boston have been larger than those from tropical storms. These findings highlight the importance of studying nor'easters in the region.

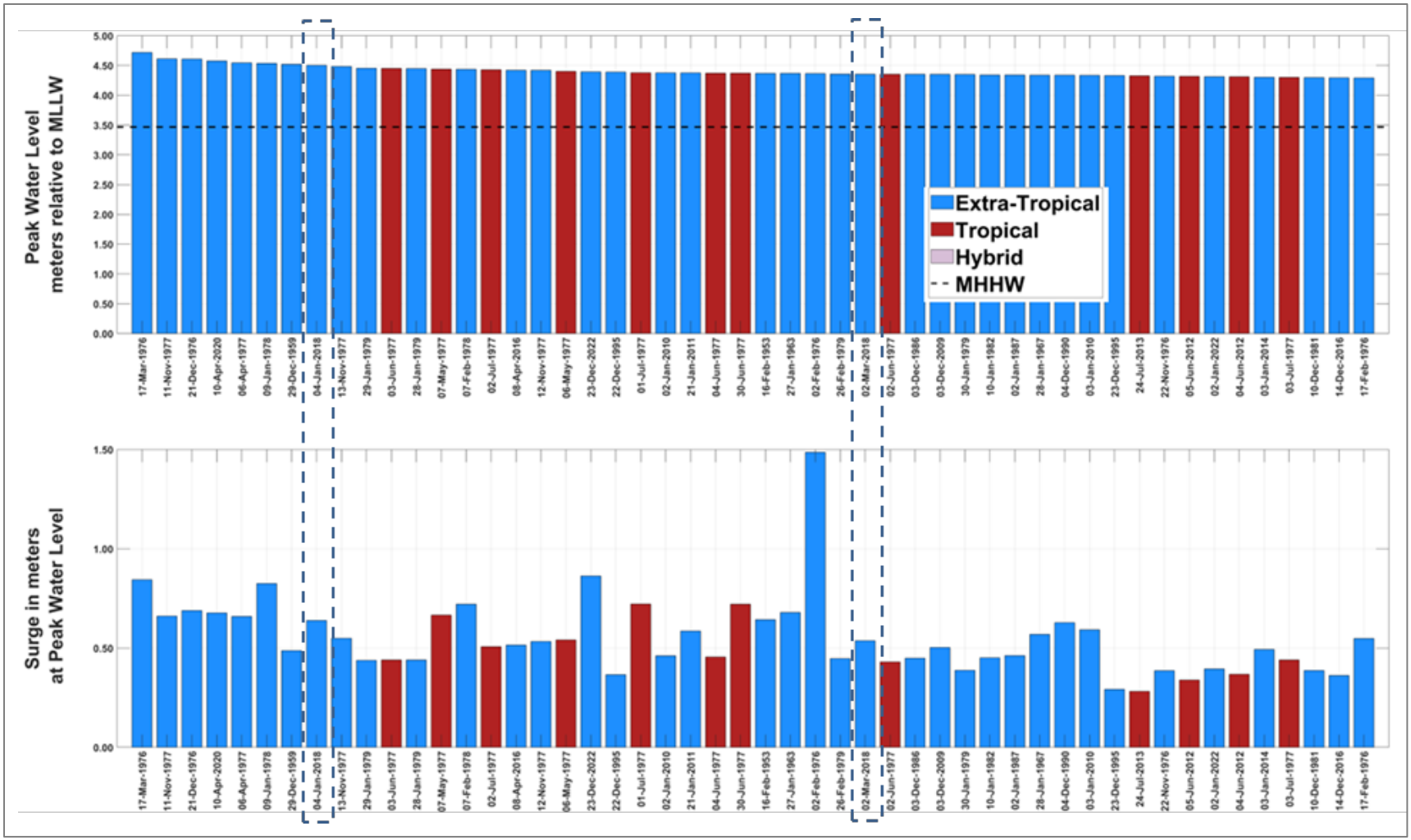


Figure 18. Peak water level (top) and corresponding storm surge (bottom) at Bar Harbor, ME. Dashed lines delineate storms modeled in this study.

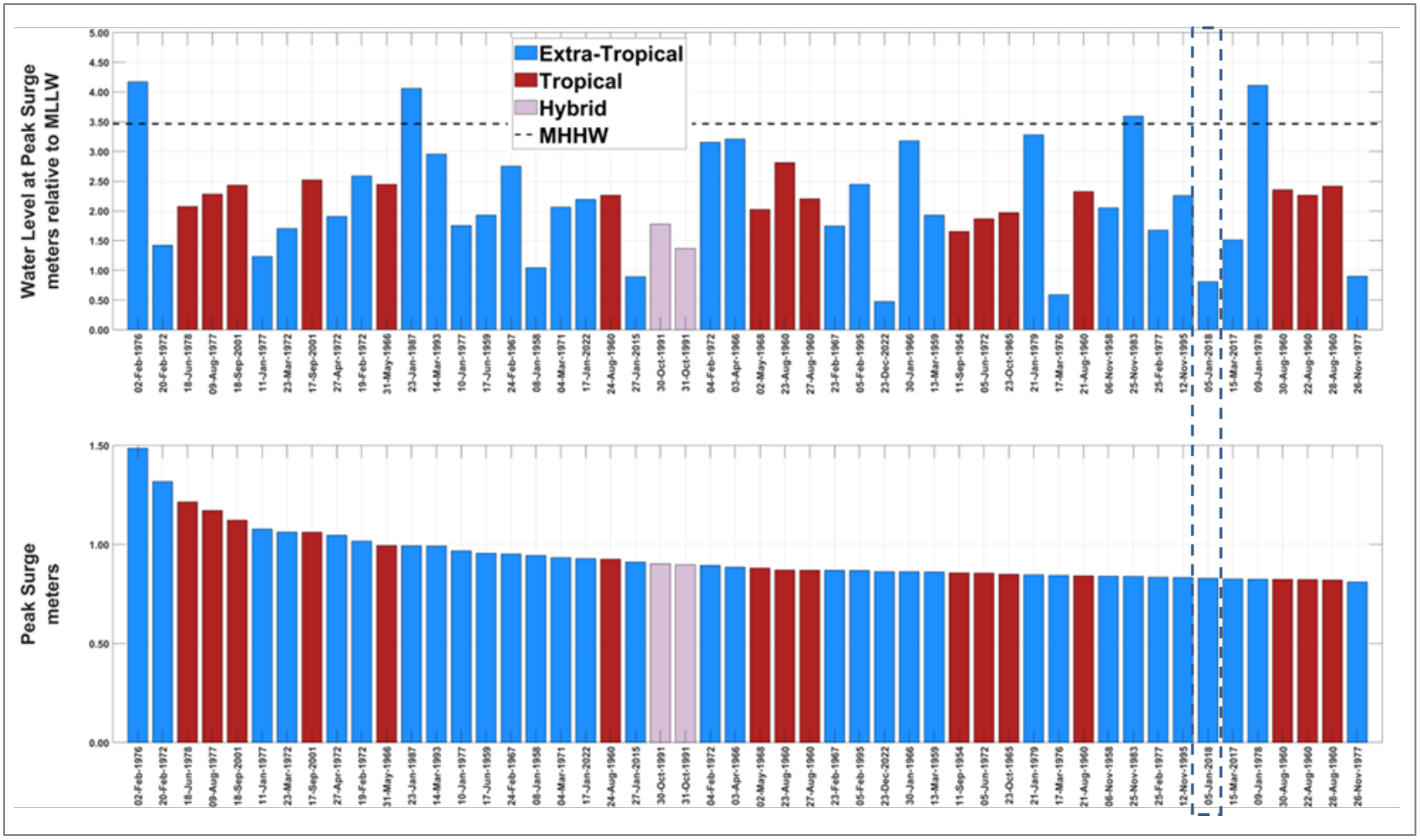


Figure 19. Water level corresponding to peak surge (top) and peak storm surges (bottom) at Bar Harbor, ME. Dashed lines delineate storms modeled in this study.

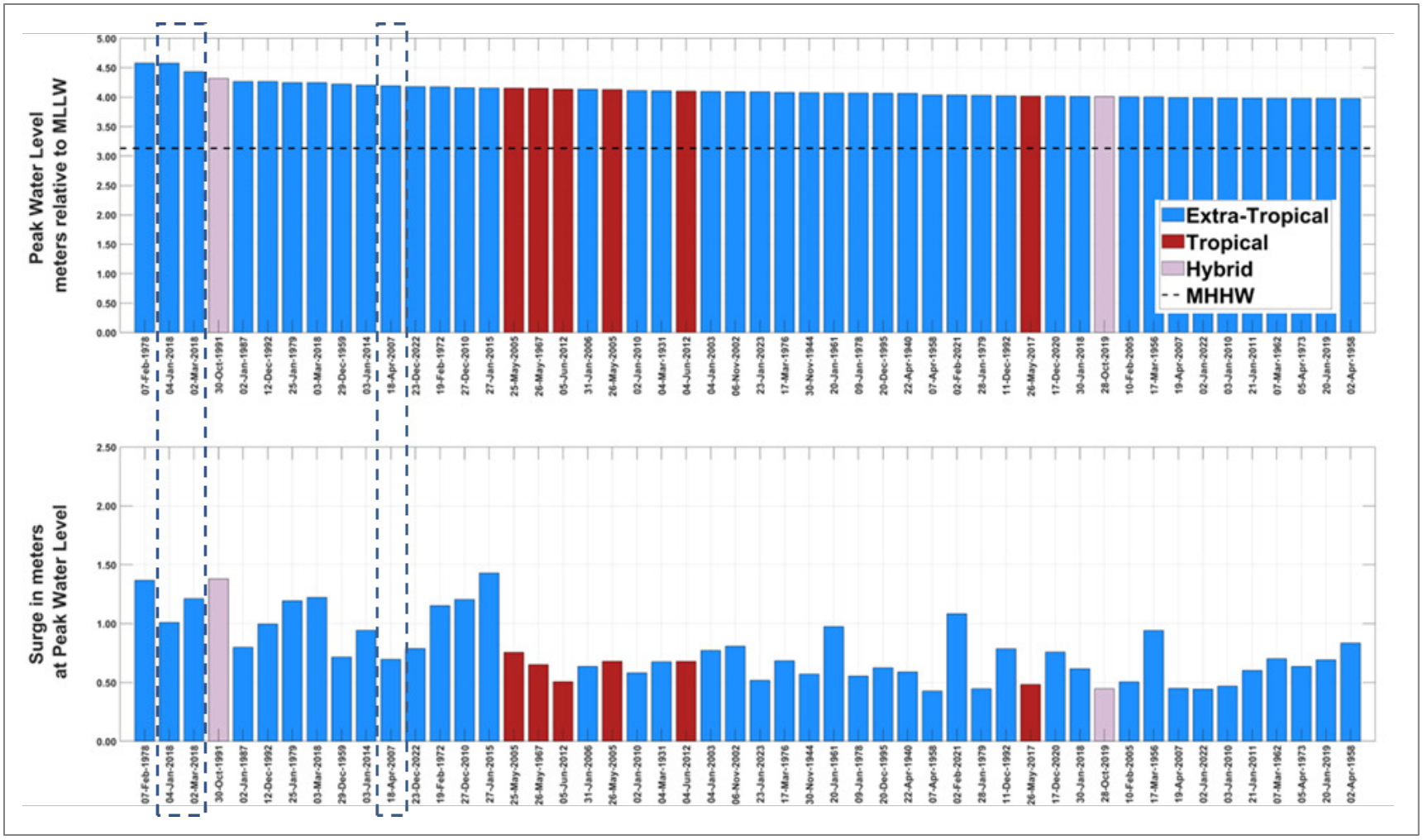


Figure 20. Peak water level (top) and corresponding storm surge (bottom) at Boston, MA. Dashed lines delineate storms modeled in this study.

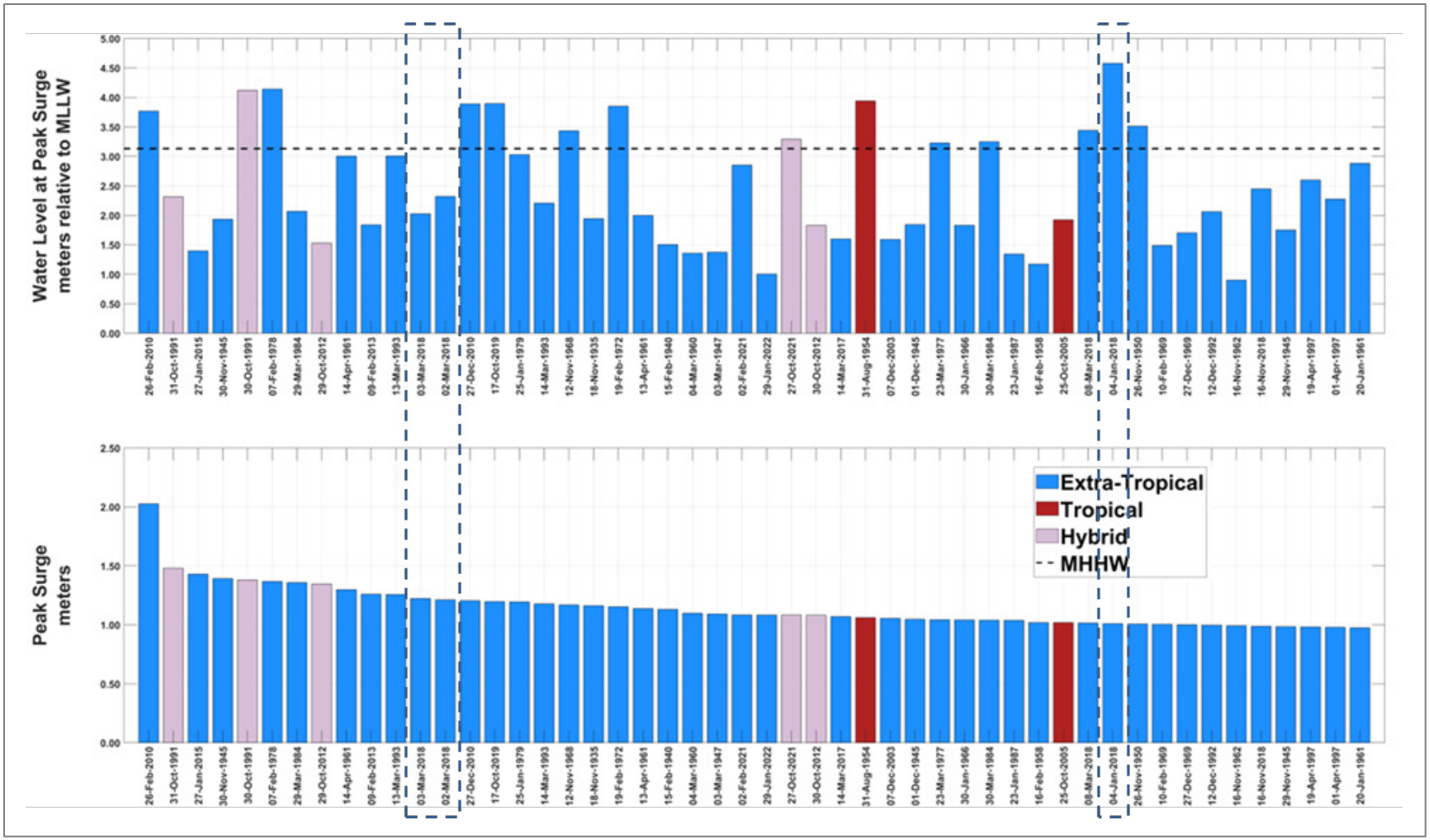


Figure 21. Water level corresponding to peak surge (top) and peak storm surges (bottom) at Boston, MA. Dashed lines delineate storms modeled in this study.

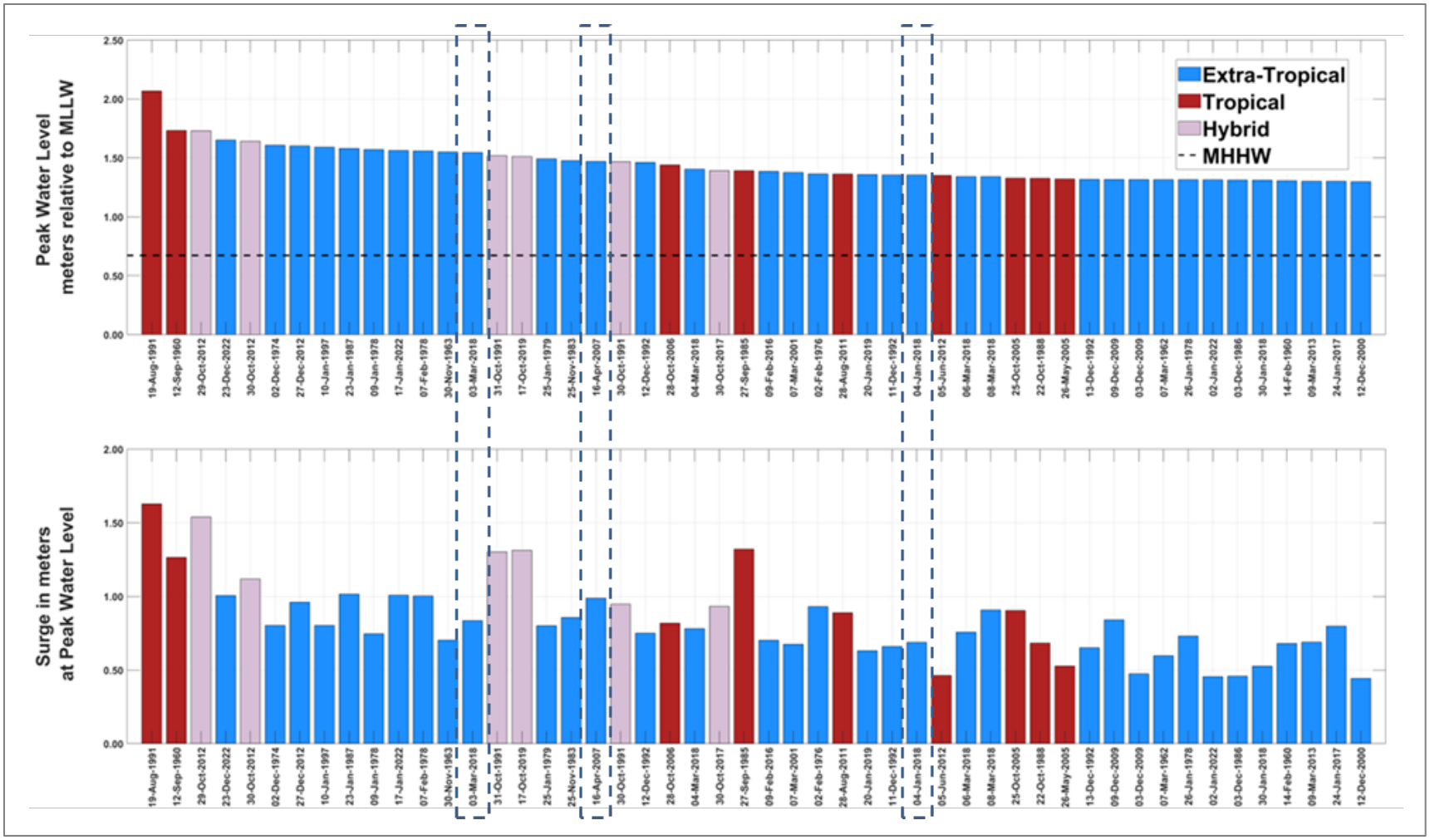


Figure 22. Peak water level (top) and corresponding storm surge (bottom) at Woods Hole, MA. Dashed lines delineate storms modeled in this study.

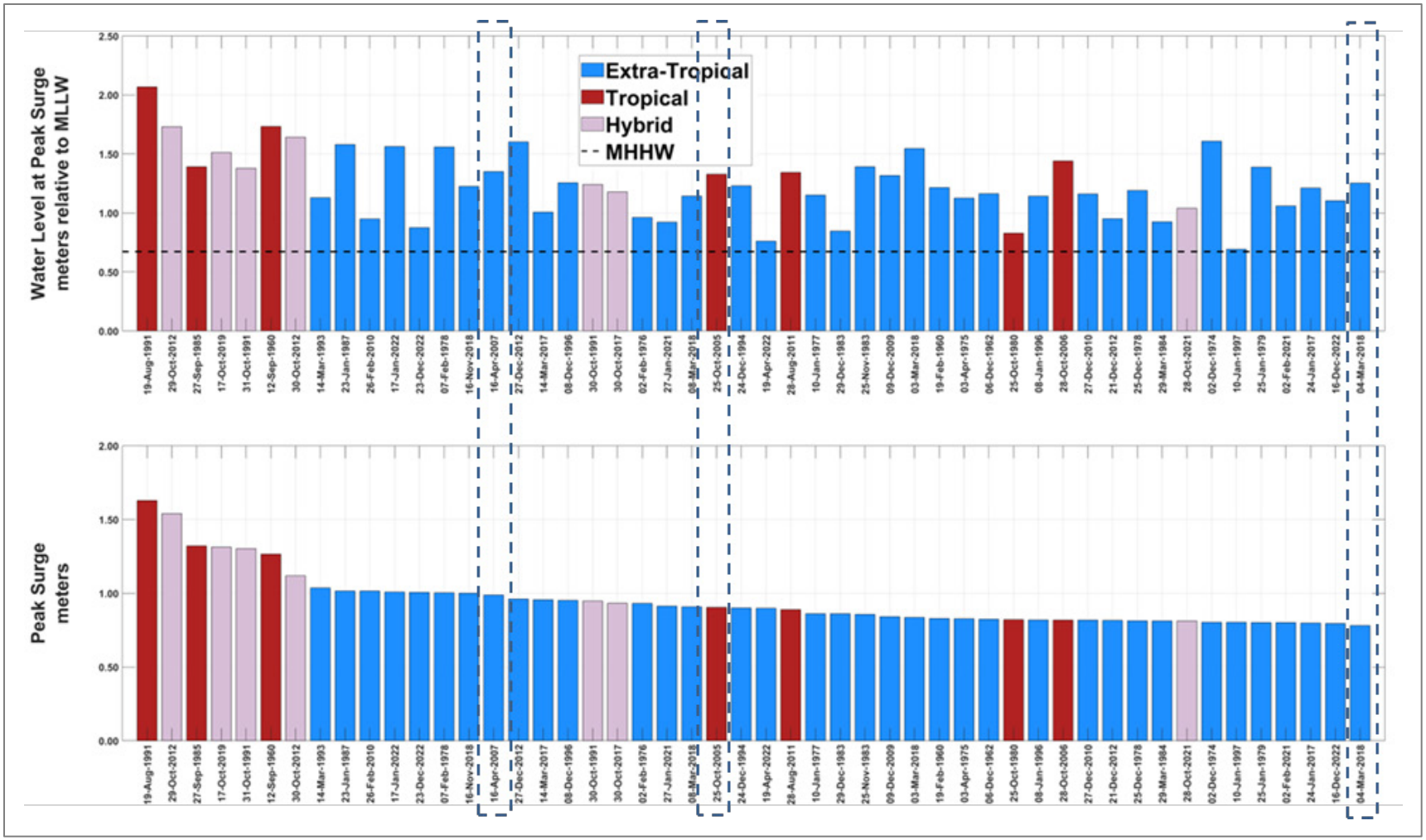


Figure 23. Water level corresponding to peak surge (top) and peak storm surges (bottom) at Woods Hole, MA. Dashed lines delineate storms modeled in this study.

Results of Model Validation

Tidal Validation

The tidal spinup portion of each simulation was compared to NOAA astronomical water level predictions and not observations. This is because the observed water level is impacted by wind, which is not included in the forcing of the ADCIRC tidal spinup run. Comparisons of the tidal water levels at local water level stations within the study area (Figure 2) are presented in Figure 24 for the April 2007 nor'easter. This figure illustrates that the model is capable of accurately simulating the spatial variability and magnitudes of tides across the domain and local to each park. The simulated water levels at other sites in the domain and for the other spinup periods similarly matched well to the NOAA astronomical tidal predictions.

In addition to comparing water levels, the extent of inundation during high and low tide was assessed by comparing it to navigational charts that delineate intertidal marsh areas in the Boston Harbor region (Figure 25) and the Provincetown Harbor region (Figure 26). On these charts, the green areas delineate marsh regions that are either flooded or dry depending on the water level. The comparison of the navigation charts to the ADCIRC simulated inundation extents show that model reproduces the trend of the intertidal zone by inundating up to the inland extent of the marsh areas during high tide and receding to the offshore extent of the marsh areas at low tide.

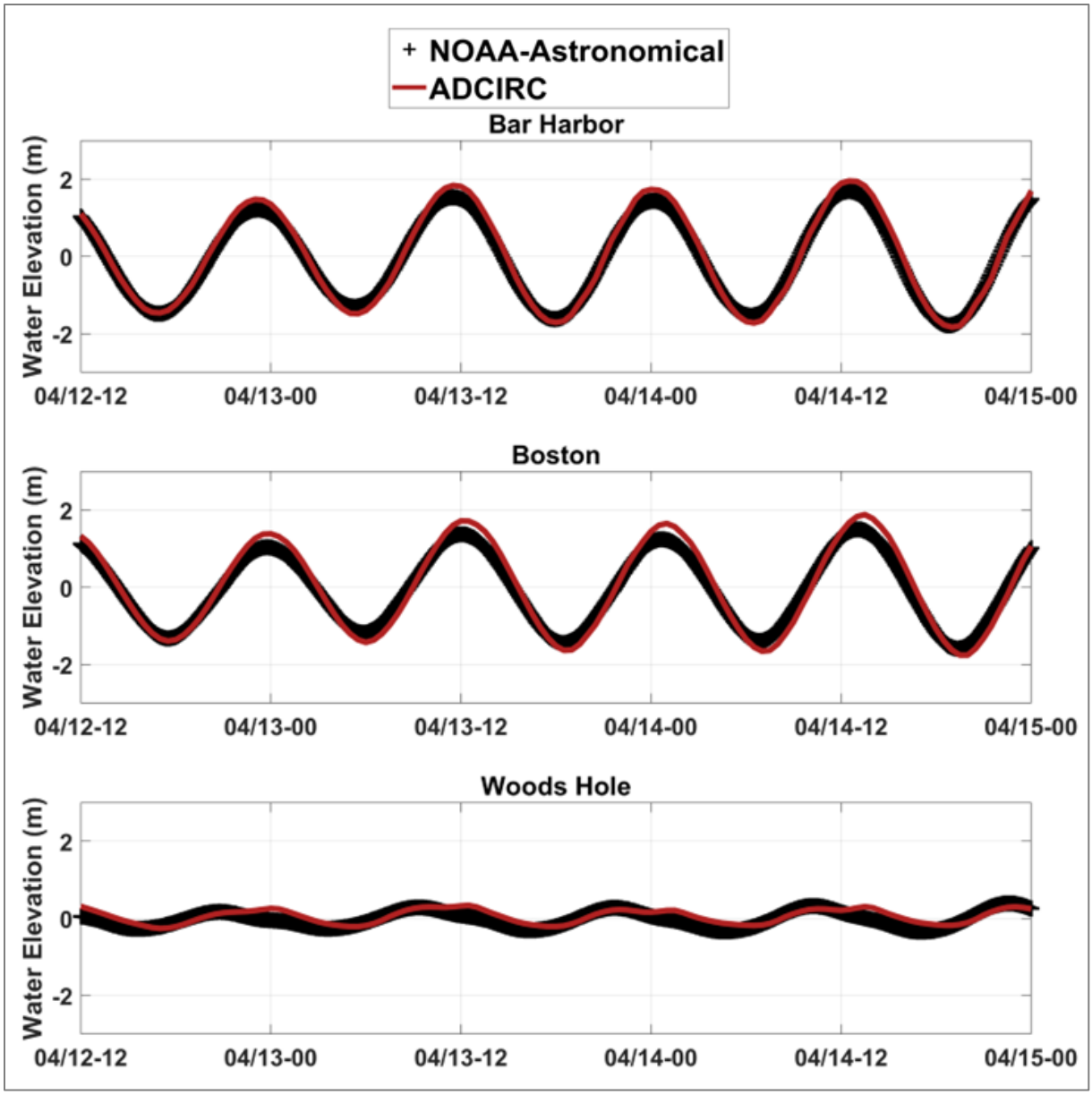


Figure 24. Comparison of astronomical tidal water predictions from National Oceanic and Atmospheric Administration (NOAA) versus simulated advanced circulation model (ADCIRC) at Bar Harbor, ME (top), Boston, MA (middle) and Woods Hole, MA (bottom) for a period prior to the April 2007 nor'easter. Time is UTC.

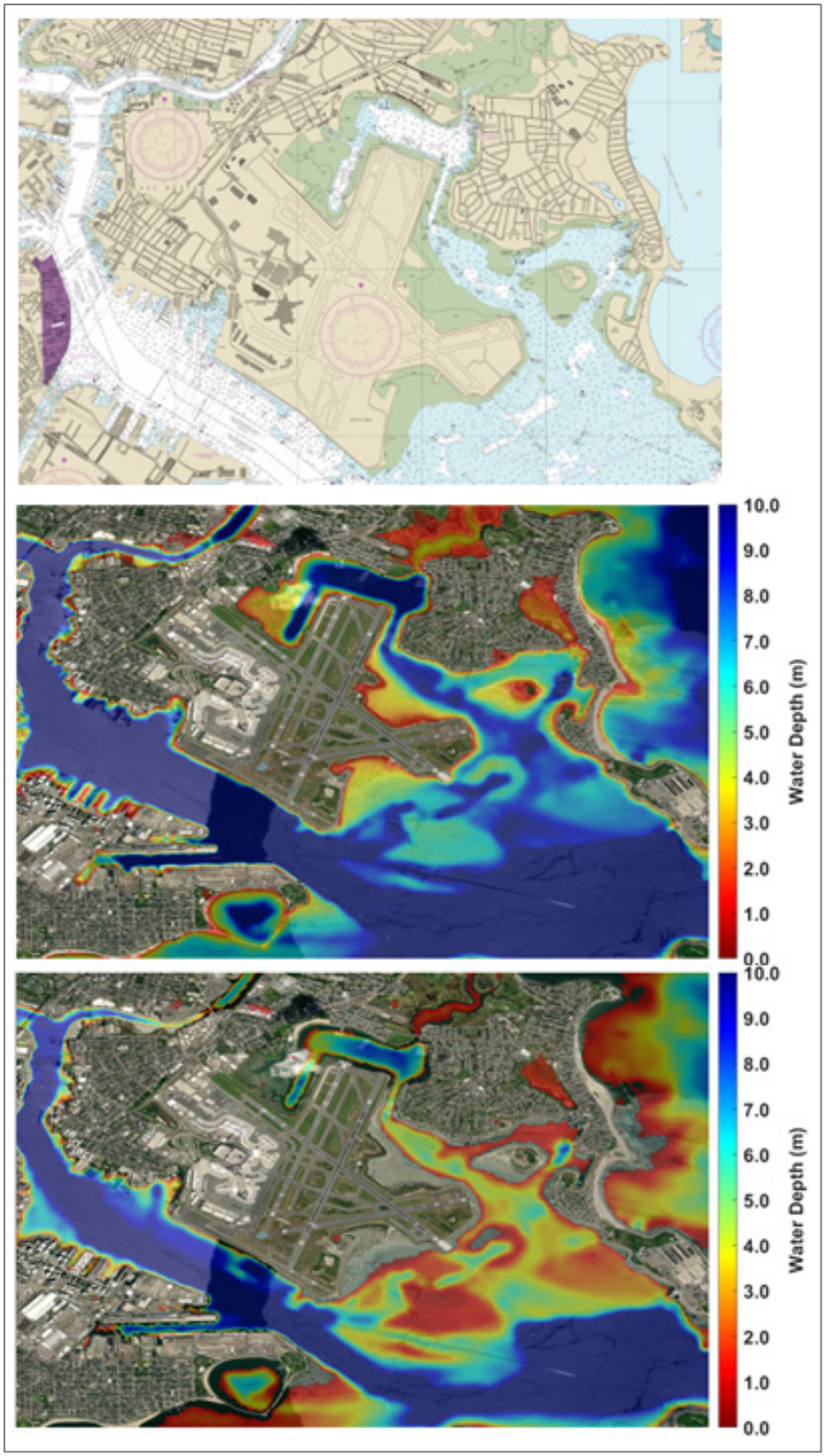


Figure 25. Navigation Chart (top), Advanced circulation model (ADCIRC) simulated inundation at high tide (middle), and low tide (bottom) in Boston Harbor, MA, near Logan Airport.

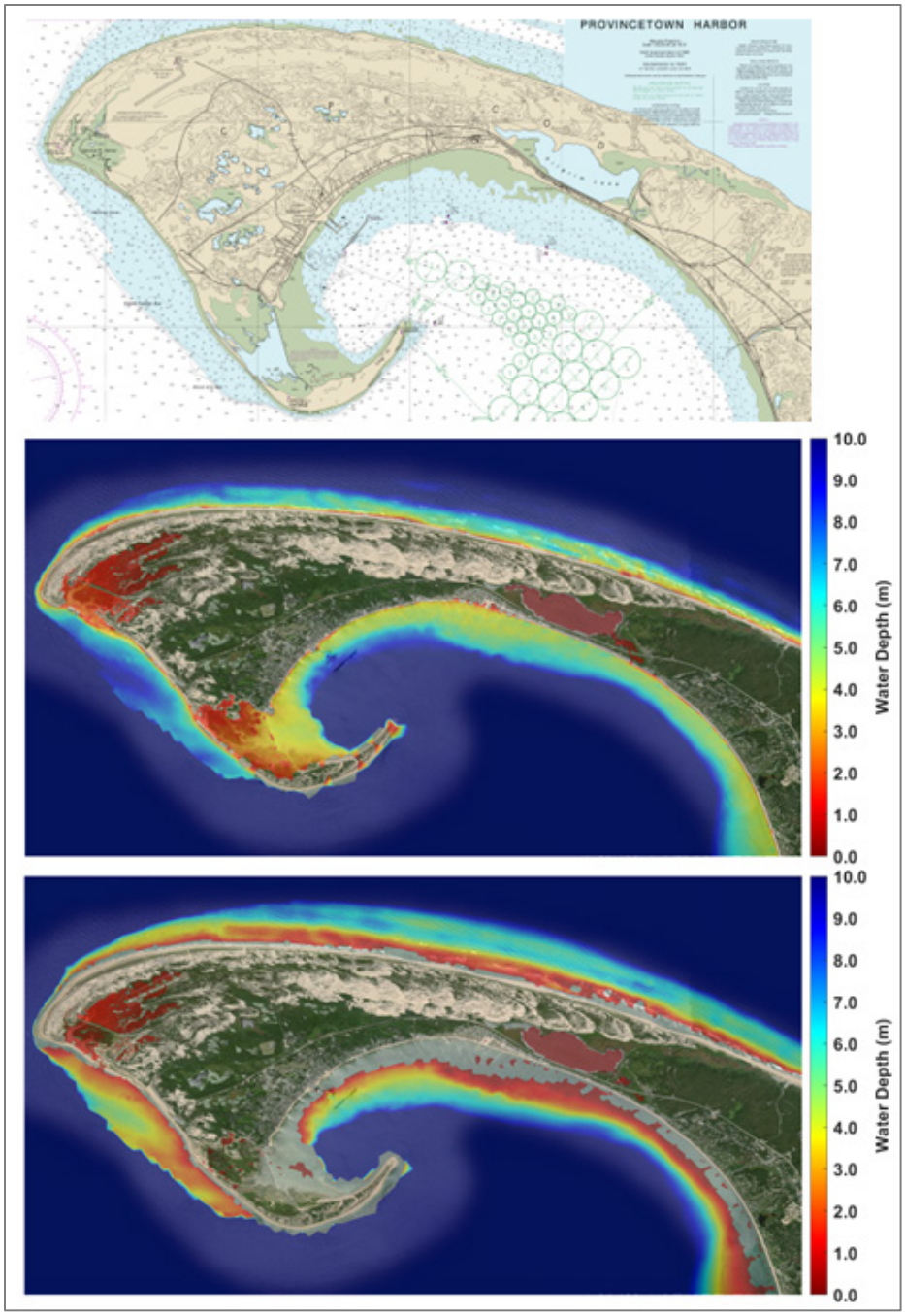


Figure 26. Navigation chart (top), advanced circulation model (ADCIRC) predicted inundation at high tide (middle), and low tide (bottom) of Provincetown Harbor, MA, region.

Storm Validation

Validation was performed by comparing model predictions to observations. A subset of comparisons at stations shown in Figure 27 are presented here. Figure 28, Figure 29, and Figure 30 present a comparison of the wind speed to wind observations for the April 2007, January 2018, and March 2018 nor'easters, respectively. These figures show that the ERA5 data matches the spatial and temporal character of the storms well. There are some differences between the ERA5 and

observations, and in most cases, the observations at the peak of the storm are greater than the ERA5 value, though most ERA5 values are within less than 5 m/s of the observations. The comparison of observed versus ERA5 values across a large domain, such as the span of Cape Cod to Maine, demonstrates that the ERA5 data capture the key features of the storms. The differences between the ERA5 and observations does not perfectly represent the observed storm, and this contributes to errors in simulated physical parameters that are sensitive to wind, such as the wind driven water levels and waves.

Comparisons of observed water level to ADCIRC-SWAN simulated values for the April 2007, January 2018 and March 2018 nor'easters are presented in Figure 31, Figure 32, and Figure 33, respectively. These figures indicate that the model effectively captured the spatial variability of tidal amplitude well (comparing the small amplitude at Woods Hole to that at the other sites) and also captured the amplitude and phase of each site accurately, similar to what was demonstrated for the tidal validation. The storm signal on water level is less pronounced than in the wind and waves results, where the peak storm conditions are 5-10 times stronger than normal conditions. However, these figures do show that the model was able to capture the storm influence, which shifts the time series to greater values. There are some differences in the overall tide range at times, however, for each storm, the peak observed water level during the event was captured well, as demonstrated by the observed versus simulated water levels on January 4th at ~16:00 in Figure 32. Capturing the peak water levels is important for this study as they result in the greatest coastal inundation.

Figure 34, Figure 35, and Figure 36, illustrate a comparison of significant wave height observations to ADCIRC-SWAN simulated values for the April 2007, January 2018 and March 2018 nor'easters, respectively. These figures show that the ADCIRC-SWAN model effectively recreated the spatial and temporal trends of the storms. However, like wind, there are some differences between the observed and simulated values, and most peak significant wave heights are underestimated. This is reasonable since the ERA5 wind forcing generally underestimated the peak winds during the storms.

Reviewing the observed versus model wind of simulated values across the three storms from a qualitative perspective, the comparisons are similar, meaning there is not a storm that looks significantly better or worse than the others. While some differences arise between observed and model simulated values, the simulations produce reasonable values of water levels and waves during a nor'easter. Further, since the goal of this study is to use the model for relative comparisons of scenarios with and without sea level rise, where the error is included in both sets of results, it does not significantly influence the comparative analysis. Lastly, while only a subset of stations is presented here to demonstrate the model skill more efficiently, comparisons at other locations were similar to the subset.

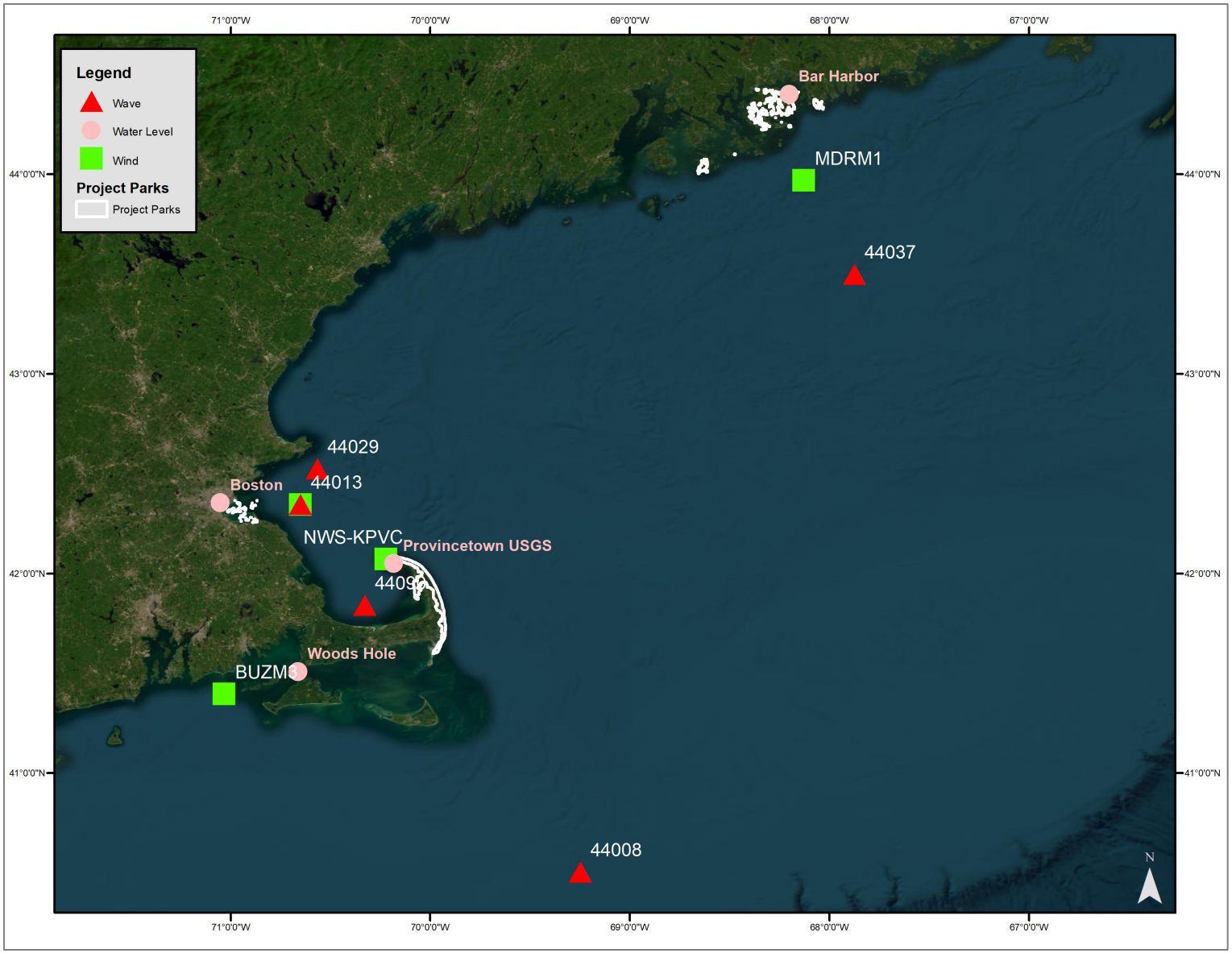


Figure 27. Subset of wave, wind and water level observation stations in the New England region used for to validate storm conditions.

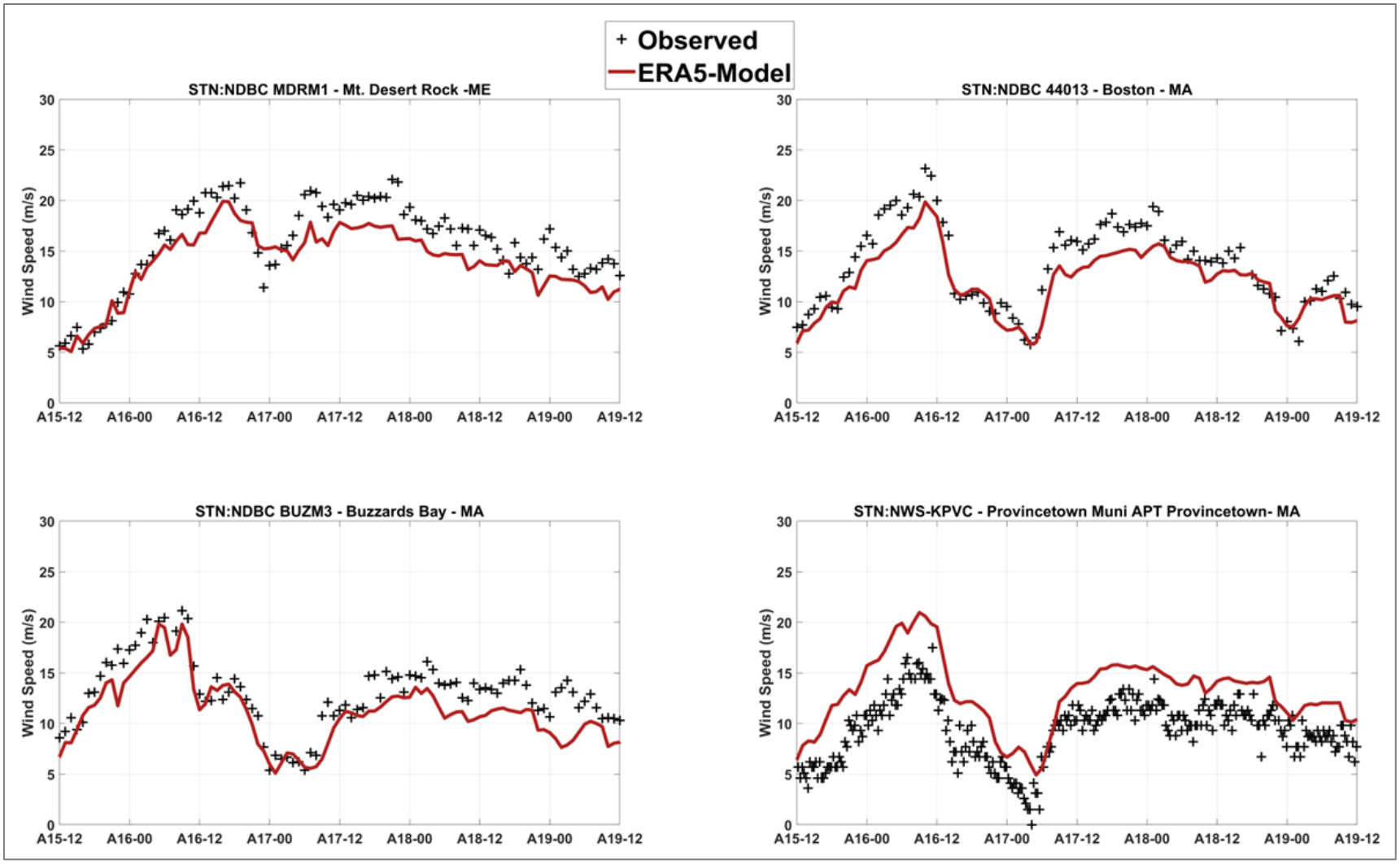


Figure 28. Comparison of observed vs European Center for Medium Range Forecasts Re-Analysis 5 (ERA-5) wind speed used in advanced circulation-simulating waves in the nearshore (ADCIRC-SWAN) model forcing of the April 2007 nor'easter. Comparisons are shown for Mt. Desert Rock, ME (top left), Boston, MA (top right), Buzzards Bay, MA (bottom left) and Provincetown Airport (bottom right). Time (x-axis) is UTC, format is Month (letter), day–hour.

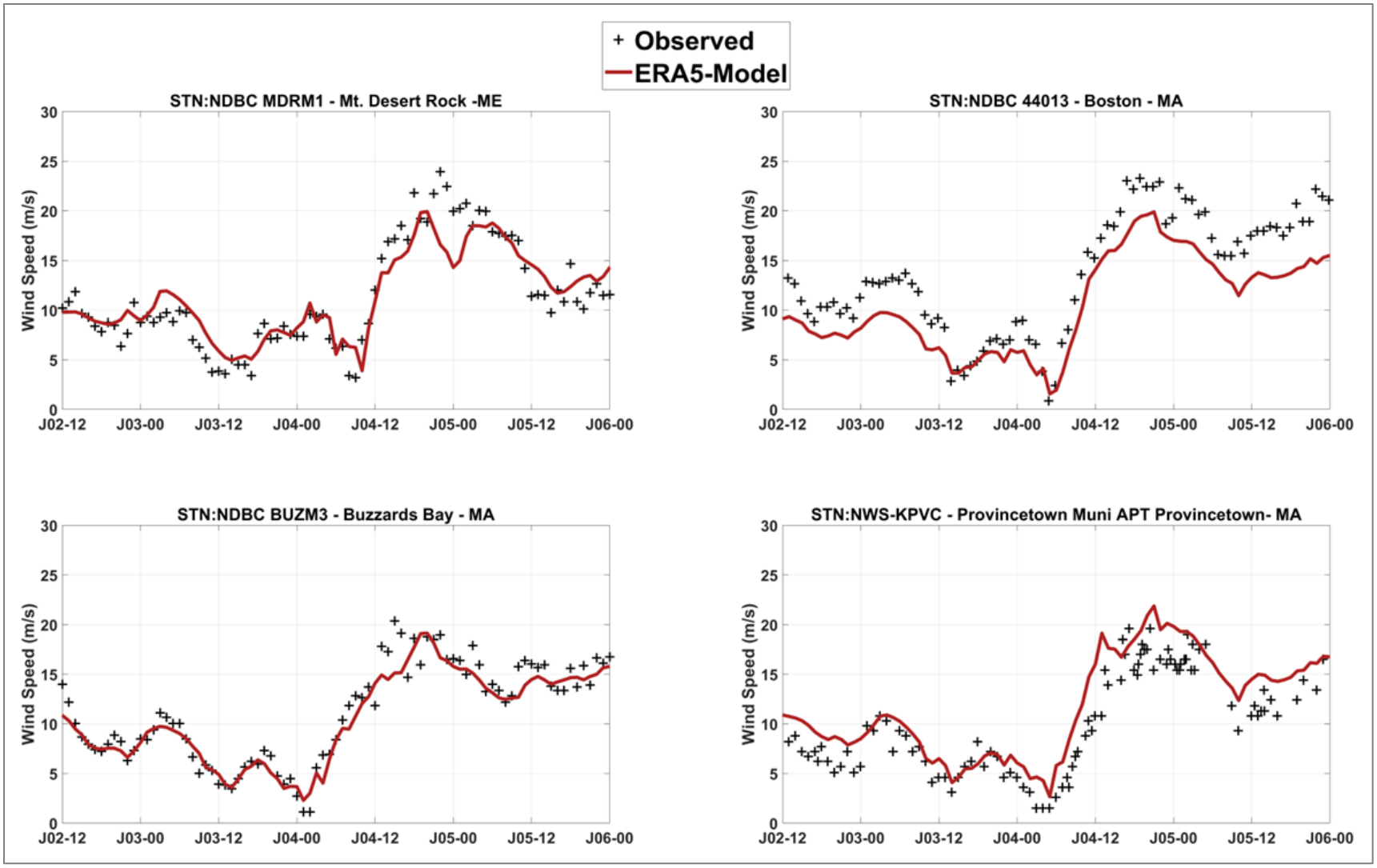


Figure 29. Comparison of observed vs European Center for Medium Range Forecasts Re-Analysis 5 (ERA-5) wind speed used in advanced circulation-simulating waves in the nearshore (ADCIRC-SWAN) model forcing of the January 2018 nor'easter. Comparisons are shown for Mt. Desert Rock, ME (top left), Boston, MA (top right), Buzzards Bay, MA (bottom left) and Provincetown Airport (bottom right). Time (x-axis) is UTC, format is Month (letter), day-hour.

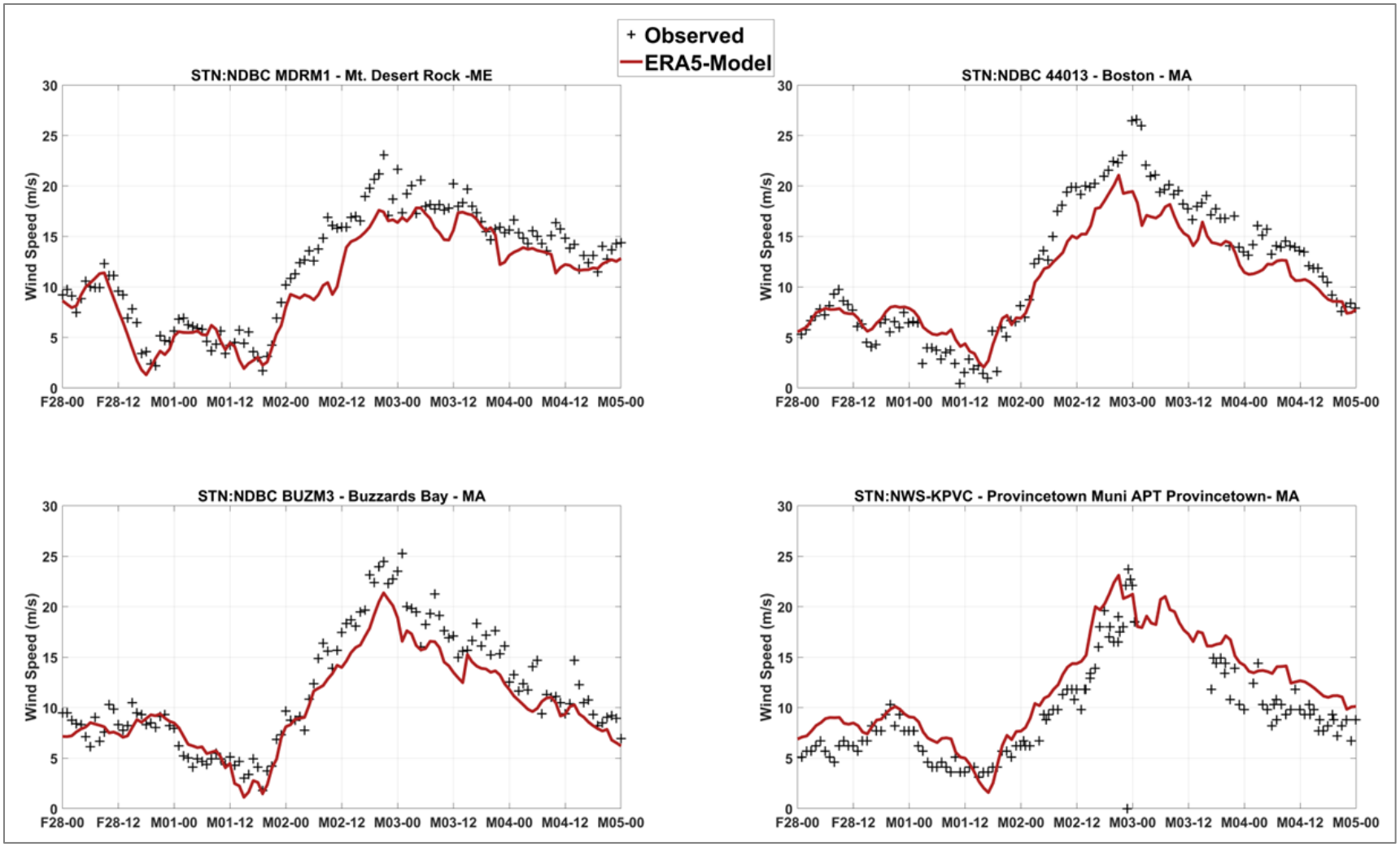


Figure 30. Comparison of observed vs European Center for Medium Range Forecasts Re-Analysis 5 (ERA-5) wind speed used in advanced circulation-simulating waves in the nearshore (ADCIRC-SWAN) model forcing of the March 2018 nor'easter. Comparisons are shown for Mt. Desert Rock, ME (top left), Boston, MA (top right), Buzzards Bay, MA (bottom left) and Provincetown Airport (bottom right). Time (x-axis) is UTC, format is Month (letter), day-hour.

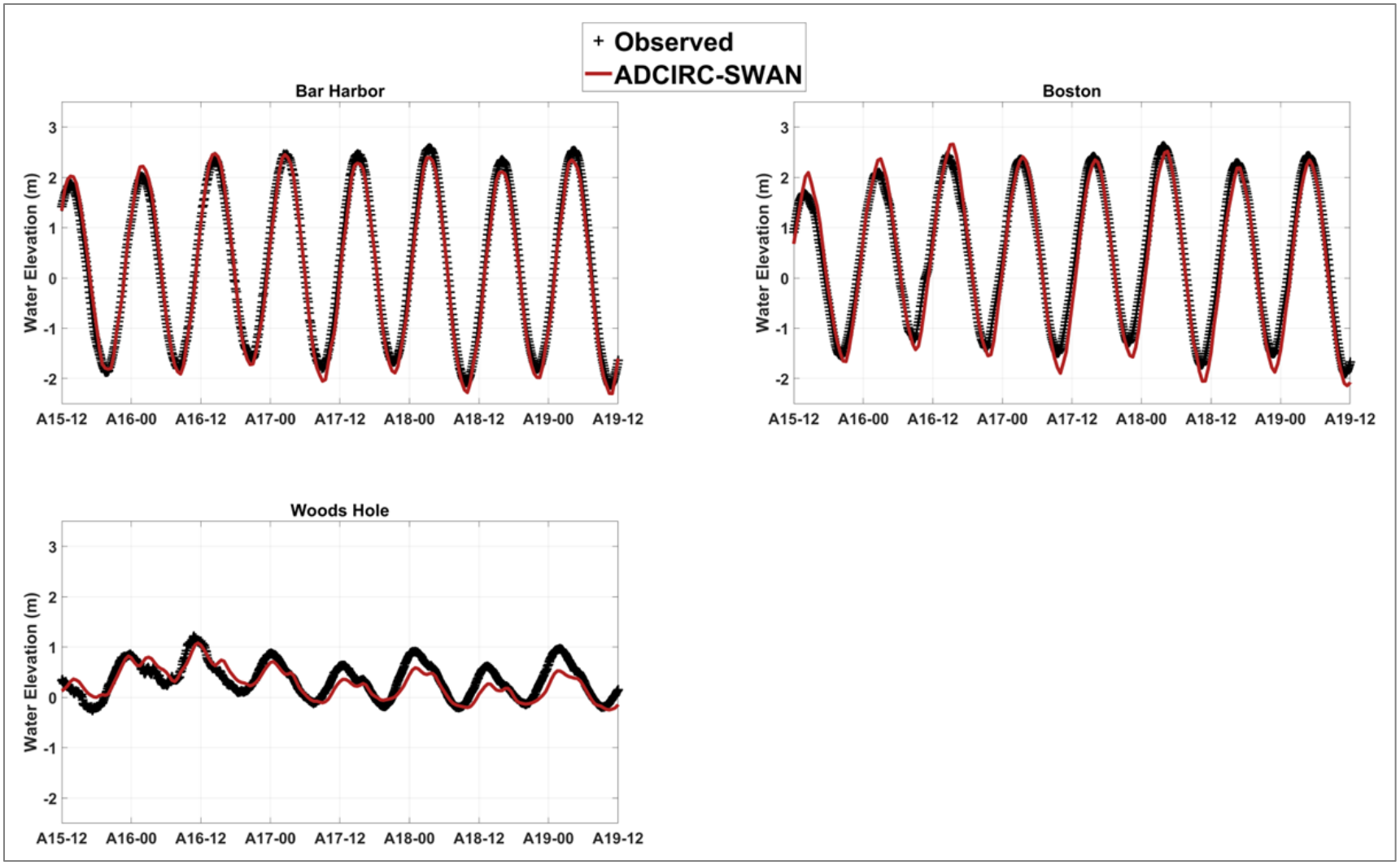


Figure 31. Comparison of observed versus advanced circulation-simulating waves in the nearshore (ADCIRC-SWAN) model simulated water levels for the April 2007 nor'easter. Comparisons are shown for Bar Harbor, ME (top left), Boston, MA (top right), and Woods Hole, MA (bottom left). Time (x-axis) is UTC, format is Month (letter), day-hour.

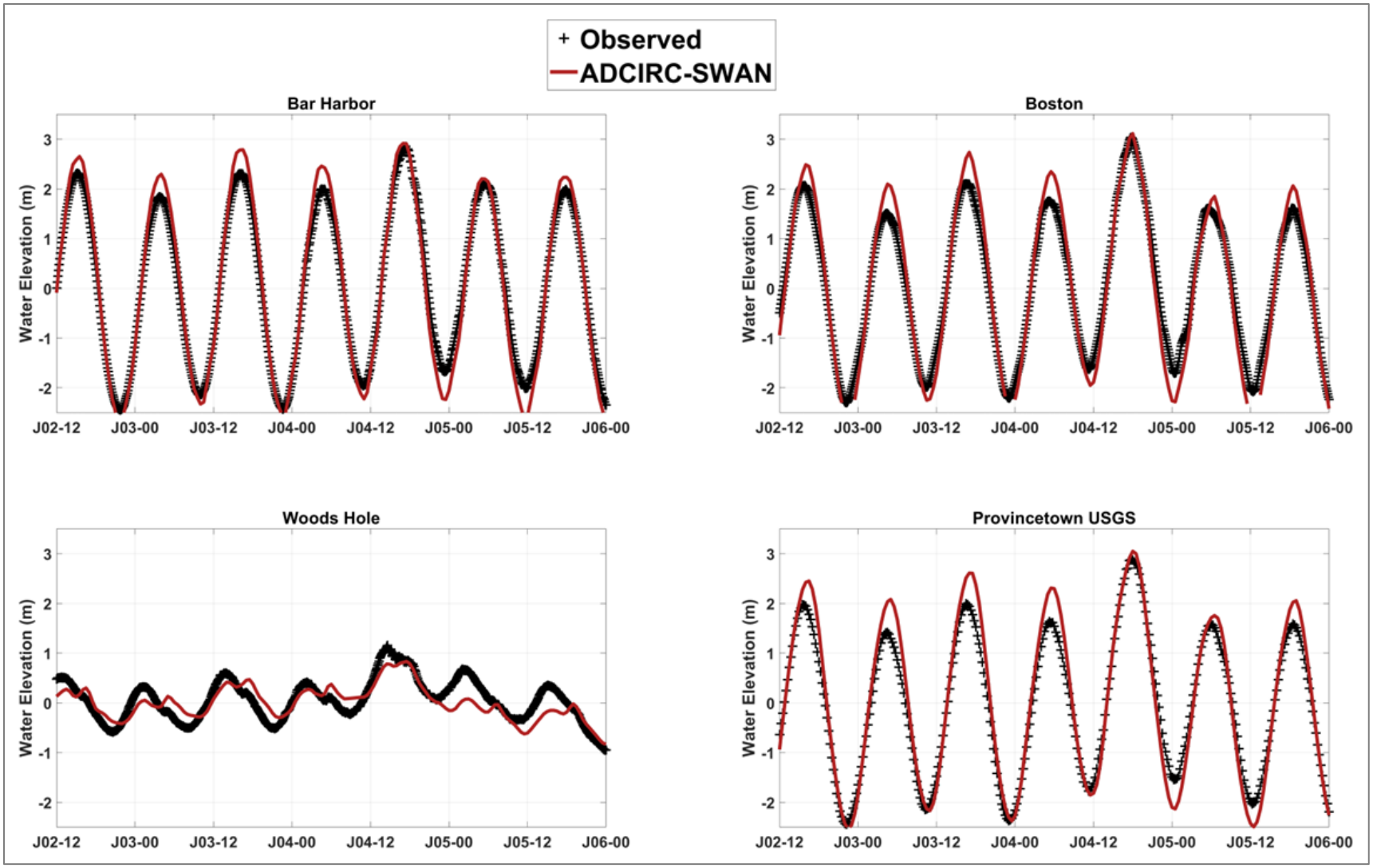


Figure 32. Comparison of observed versus advanced circulation-simulating waves in the nearshore (ADCIRC-SWAN) model simulated water levels for the January 2018 nor'easter. Comparisons are shown for Bar Harbor, ME (top left), Boston, MA (top right), Woods Hole, MA (bottom left), and Provincetown, MA (bottom right). Time (x-axis) is UTC, format is Month (letter), day-hour.

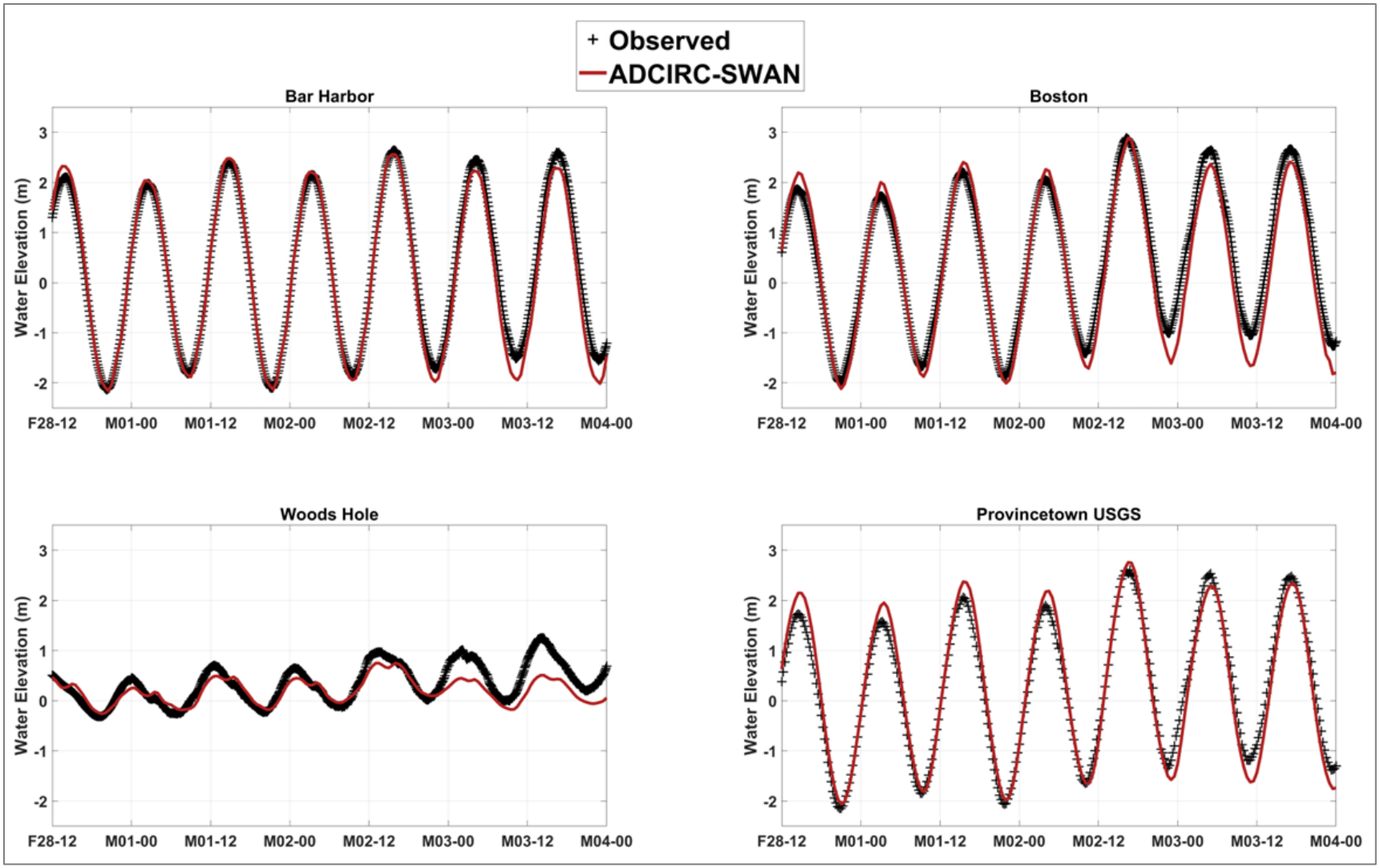


Figure 33. Comparison of observed versus advanced circulation-simulating waves in the nearshore (ADCIRC-SWAN) model simulated water levels for the March 2018 nor'easter. Comparisons are shown for Bar Harbor, ME (top left), Boston, MA (top right), Woods Hole, MA (bottom left), and Provincetown, MA (bottom right). Time (x-axis) is UTC, format is Month (letter), day-hour.

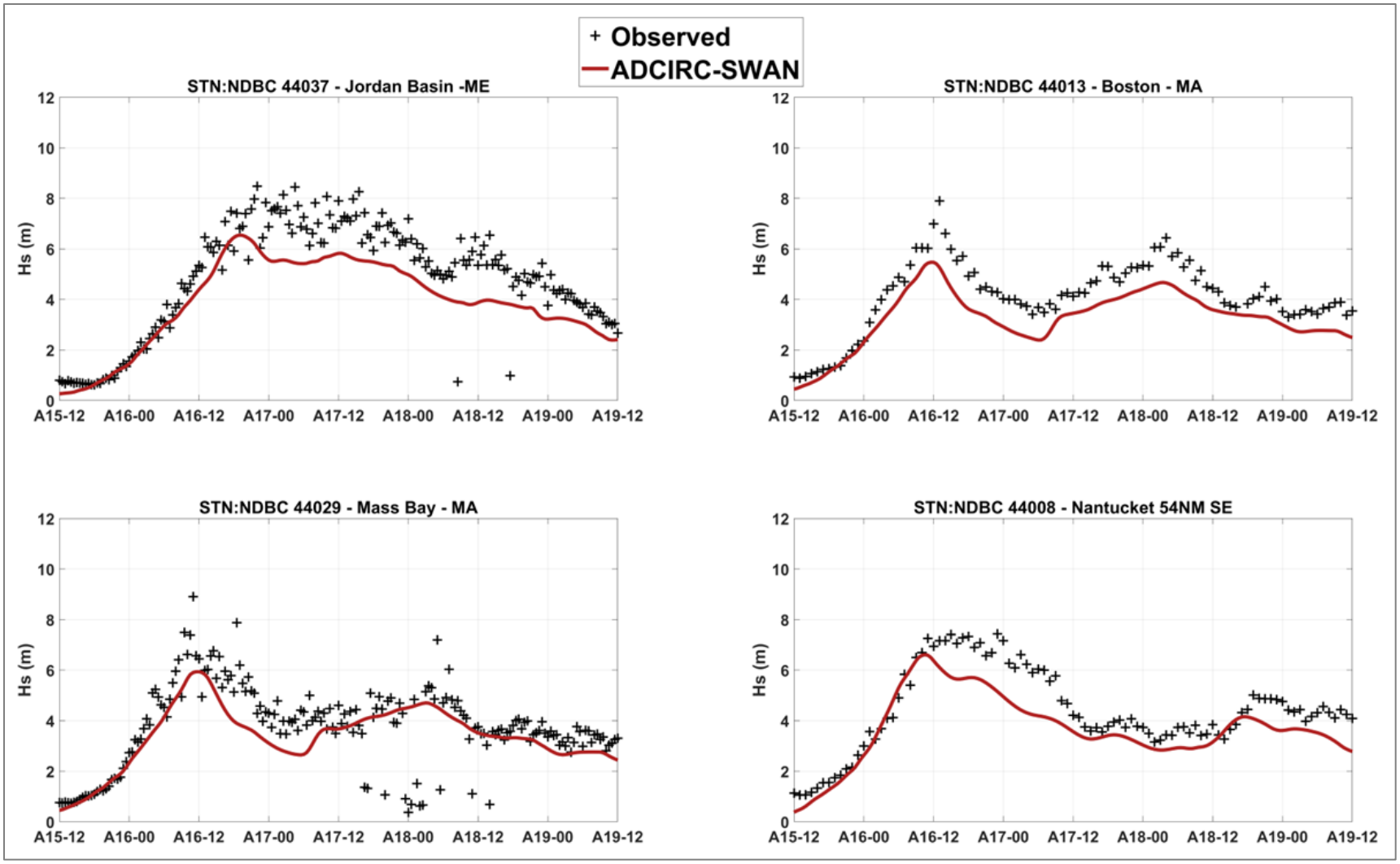


Figure 34. Comparison of observed versus advanced circulation-simulating waves in the nearshore (ADCIRC-SWAN) model simulated significant wave height for the April 2007 nor'easter. Comparisons are shown for Jordan Basin, ME (top left), Boston, MA (top right), Mass Bay, MA (bottom left), and Offshore Nantucket, MA (bottom right). Time (x-axis) is UTC, format is Month (letter), day-hour.

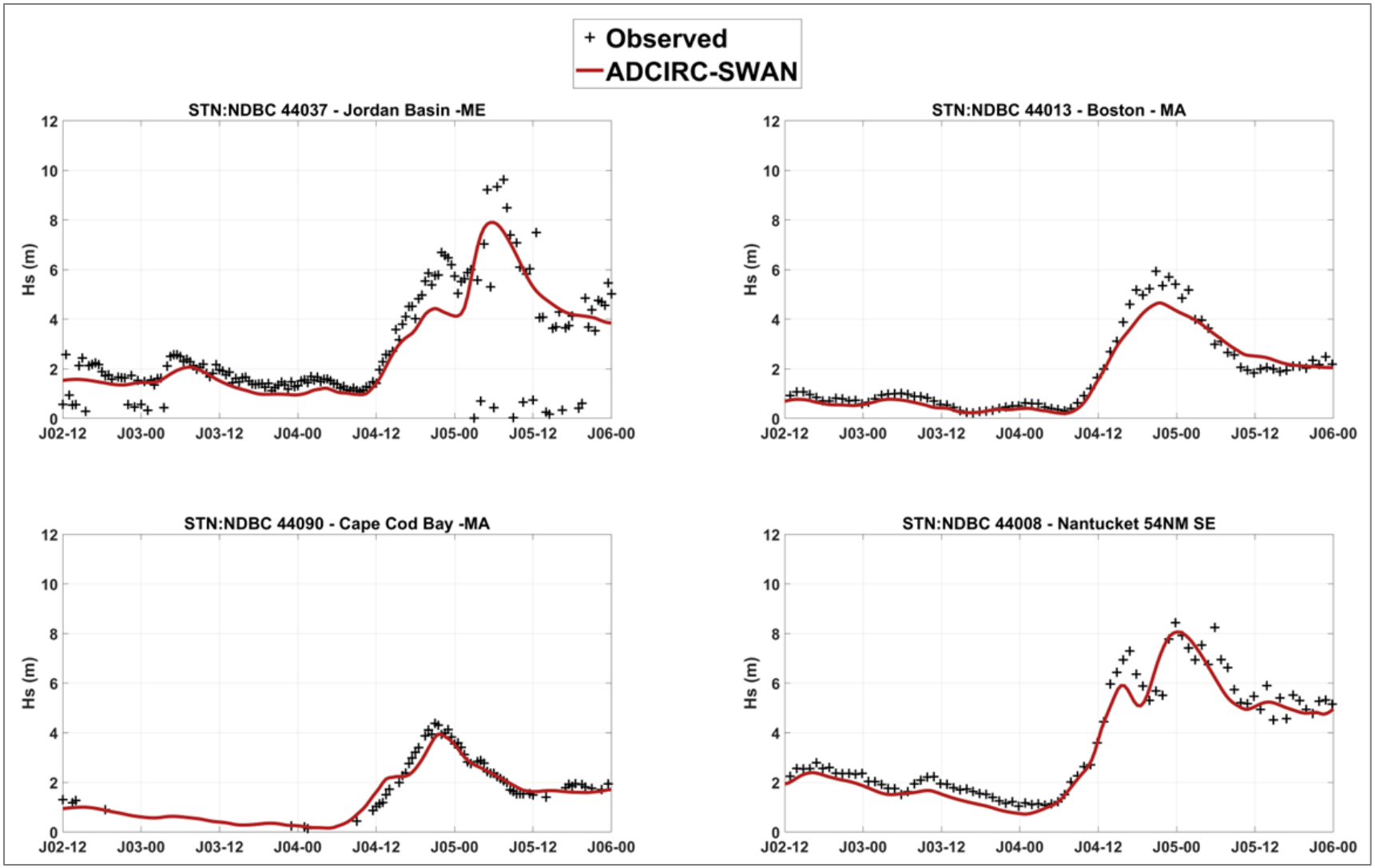


Figure 35. Comparison of observed versus advanced circulation-simulating waves in the nearshore (ADCIRC-SWAN) model simulated significant wave height for the January 2018 nor'easter. . Comparisons are shown for Jordan Basin, ME (top left), Boston, MA (top right), Cape Cod Bay, MA (bottom left), and Offshore Nantucket, MA (bottom right). Time (x-axis) is UTC, format is Month (letter), day-hour.

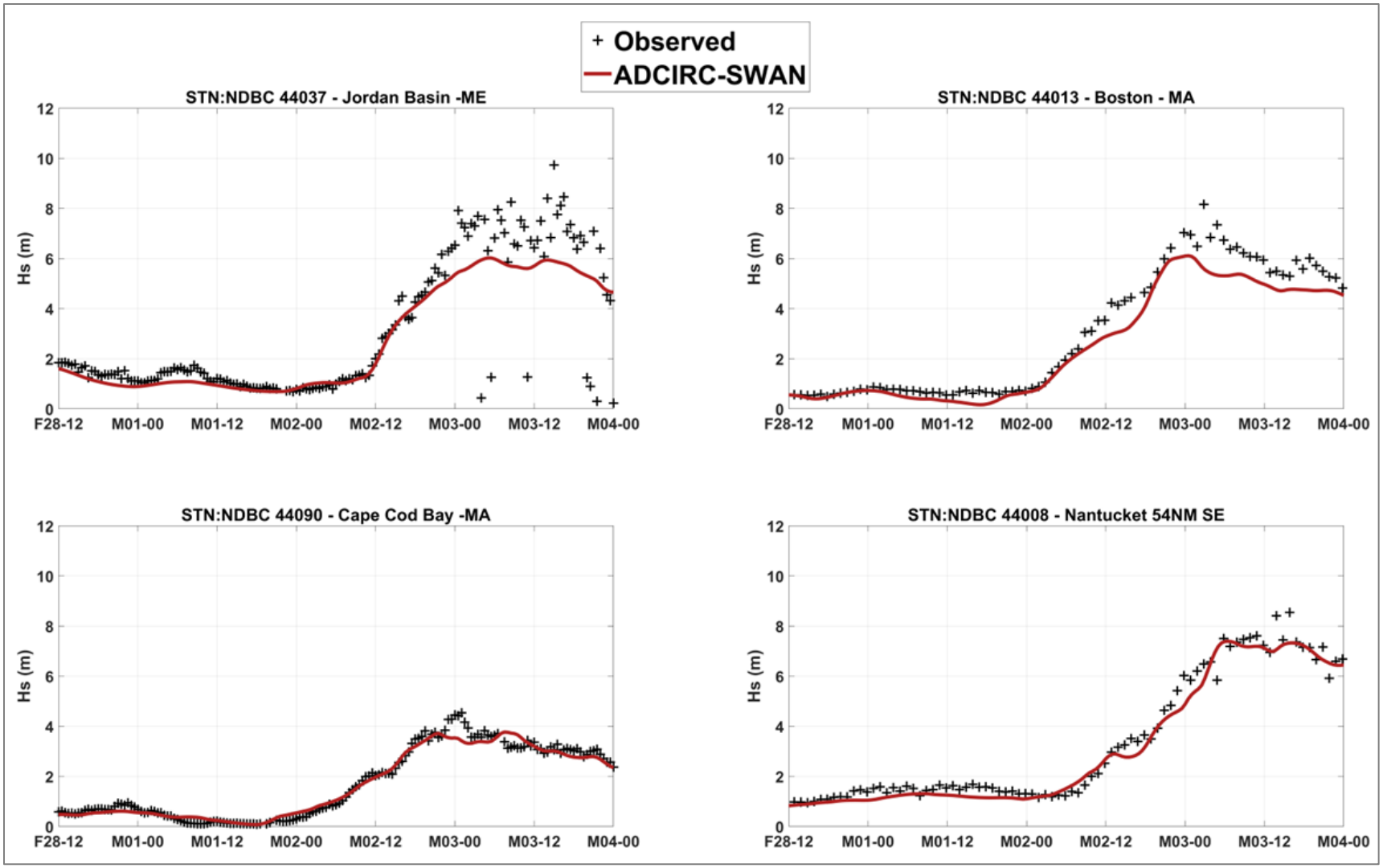


Figure 36. Comparison of observed versus advanced circulation-simulating waves in the nearshore (ADCIRC-SWAN) model simulated significant wave height for the March 2018 nor'easter. Comparisons are shown for Jordan Basin, ME (top left), Boston, MA (top right), Cape Cod Bay, MA (bottom left), and Offshore Nantucket, MA (bottom right). Time (x-axis) is UTC, format is Month (letter), day-hour.

Results of Simulations of Nor'easters with Sea level Rise

The validated model application for each storm event was used to simulate scenarios of near present MSL (2020), near present plus 1ft SLR, and near present plus 1m of SLR. In each case, a tidal spinup and storm were simulated. However, the focus of the post-processing and analysis is on the results from the storm portion of the run. A summary of the storm runs is provided in Table 8.

Table 8. Summary of simulations for analysis of nor'easters with sea level rise.

Storm Meteorological Forcing	Mean Sea Level (MSL)	Sea Level Rise Relative to Present Epoch MSL (m)
April 2007	2020	0.096
April 2007	2020+ 1ft	0.401
April 2007	2020 + 1 m	1.096
January 2018	2020	0.096
January 2018	2020+ 1ft	0.401
January 2018	2020 + 1 m	1.096
March 2018	2020	0.096
March 2018	2020+ 1ft	0.401
March 2018	2020 + 1 m	1.096

The modeling results are summarized in two nine-paneled figures for each park (Figure 37 through Figure 42), with one figure summarizing water levels and the other significant wave heights for all three storms.

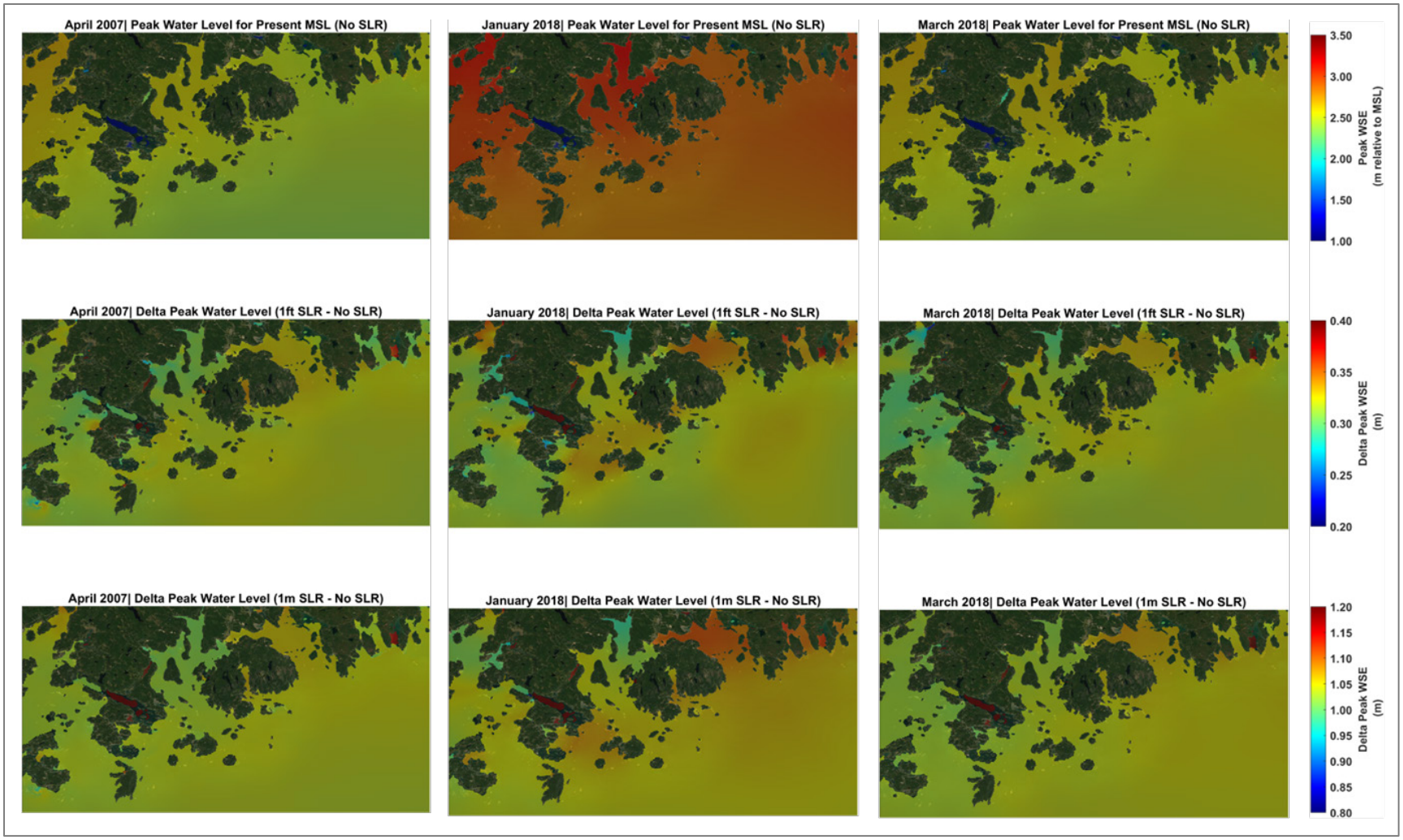


Figure 37. Advanced circulation-simulating waves in the nearshore (ADCIRC-SWAN) results of the April 2007 (left), January 2018 (center), and March 2018 (right) nor'easters at Acadia National Park; peak water levels from the simulation using 2020 MSL (top), change in peak water levels when 1 ft (0.3048m) of SLR is simulated (middle), and change in peak water levels when 1 m of SLR simulated (bottom).

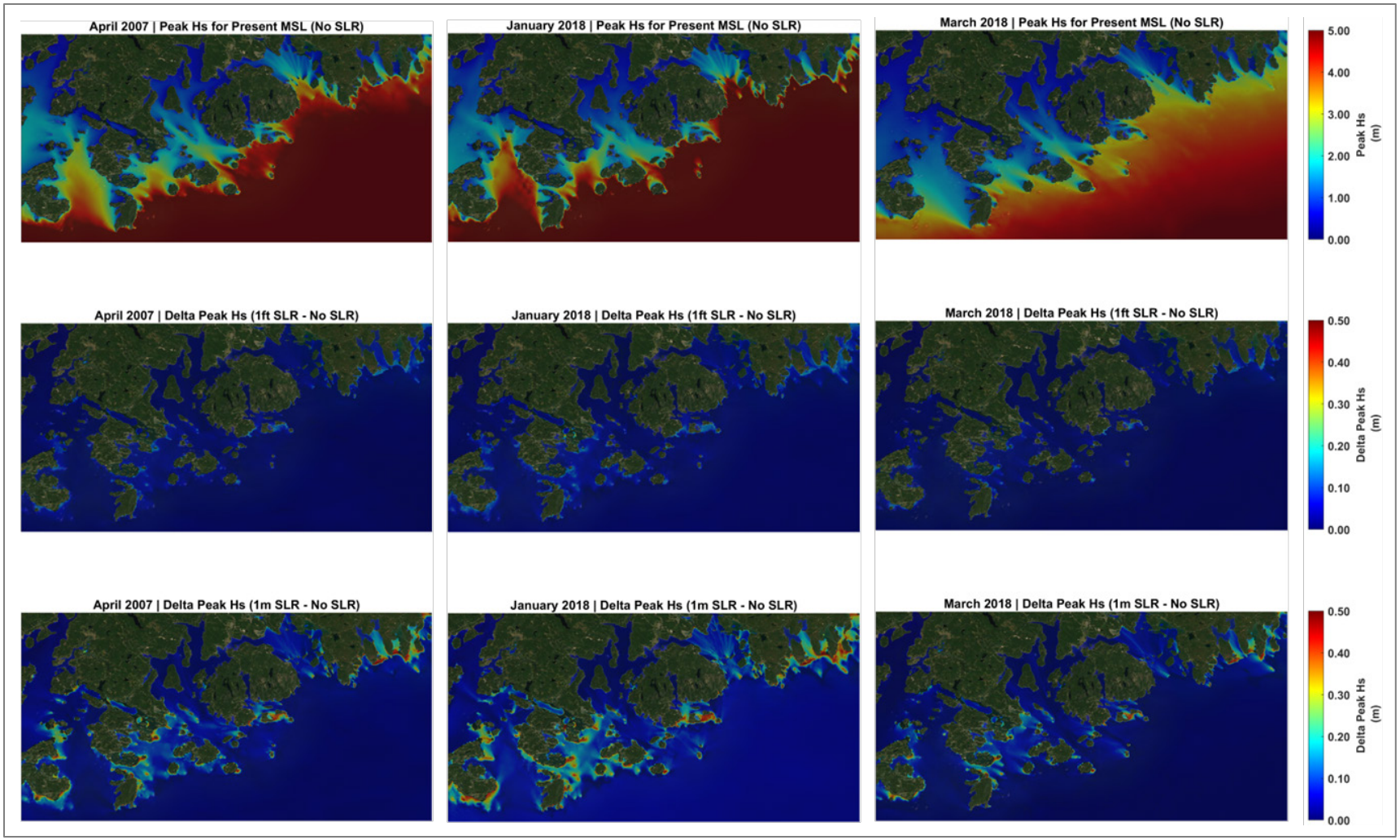


Figure 38. Advanced circulation-simulating waves in the nearshore (ADCIRC-SWAN) results of the April 2007 (left), January 2018 (center), and March 2018 (right) nor'easters at Acadia National Park; peak significant wave height (Hs) from the simulation using 2020 mean sea level (top), change in peak Hs when 1 ft (0.3048m) of sea level rise is simulated (middle), and change in peak Hs when 1 m of sea level rise is simulated (bottom).

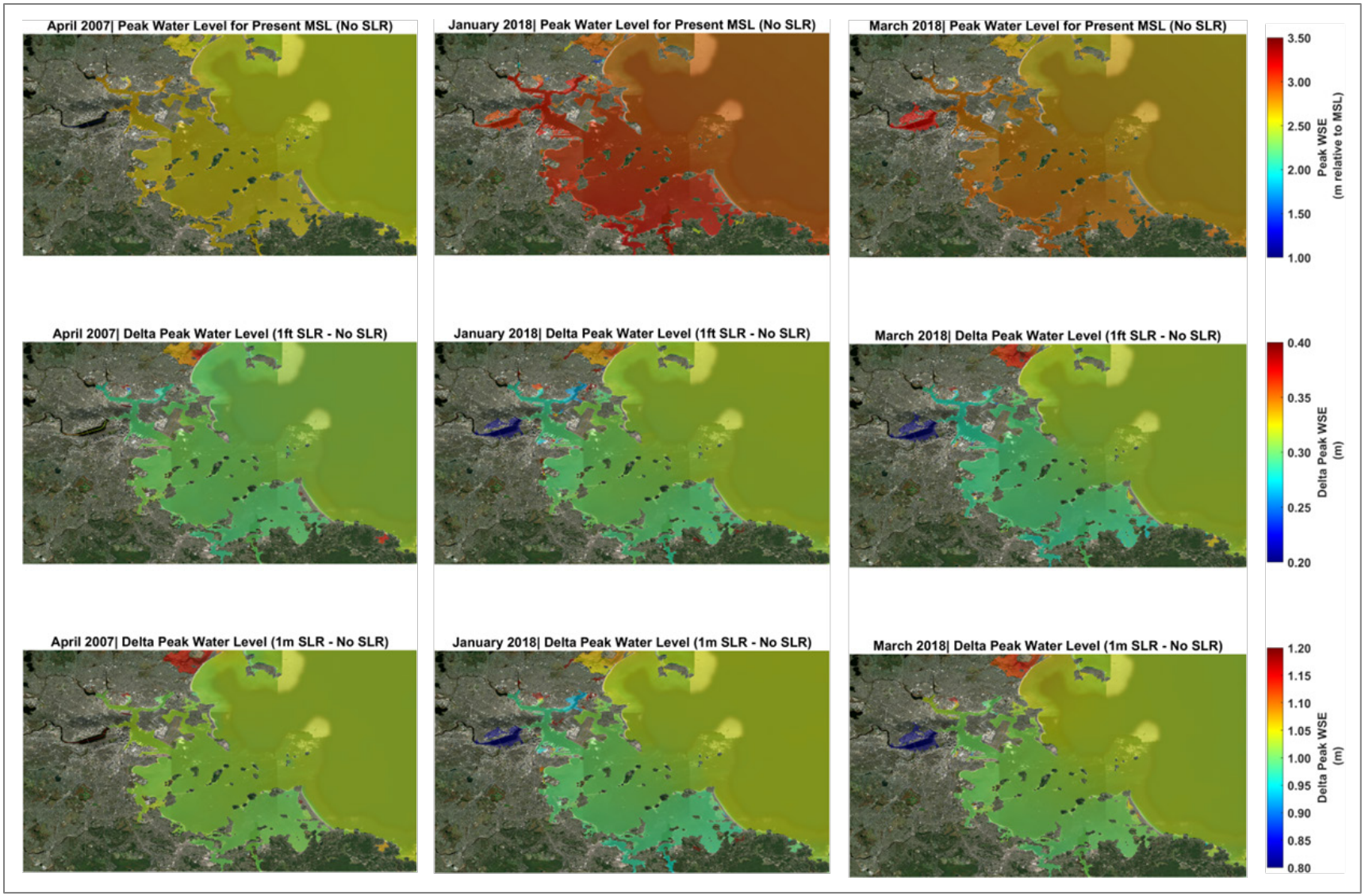


Figure 39. Advanced circulation-simulating waves in the nearshore (ADCIRC-SWAN) results of the March 2018 nor'easter at the National Parks of Boston; peak water levels from the simulation using 2020 mean sea level (top), change in peak water levels when 1 ft (0.3048m) of sea level rise is simulated (middle), and change in peak water levels when 1 m of sea level rise simulated (bottom).

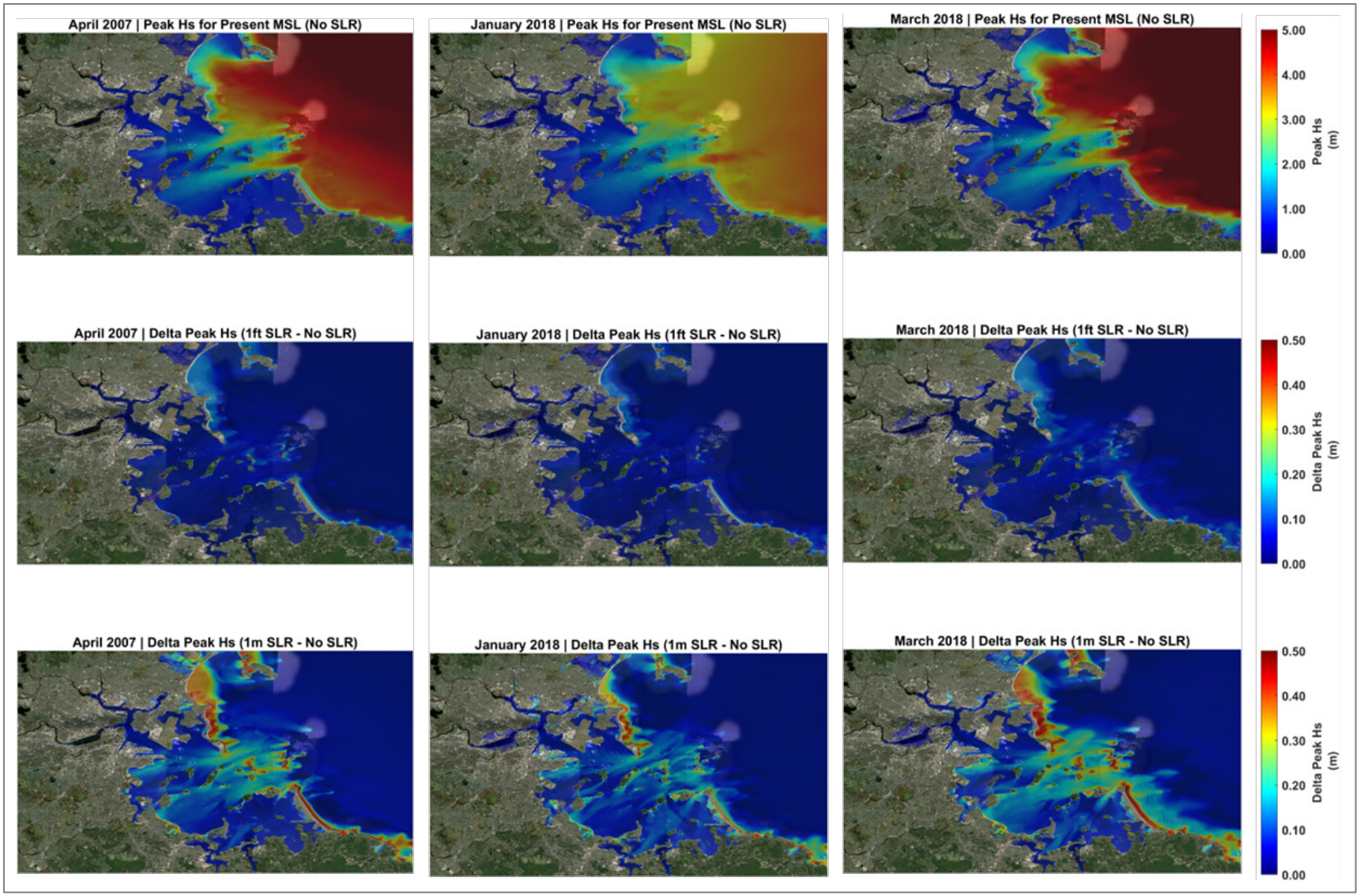


Figure 40. Advanced circulation-simulating waves in the nearshore (ADCIRC-SWAN) results of the March 2018 nor'easter at the National Parks of Boston; peak significant wave height (Hs) from the simulation using 2020 mean sea level (top), change in peak Hs when 1 ft (0.3048m) of sea level rise is simulated (middle), and change in peak Hs when 1 m of sea level rise is simulated (bottom).

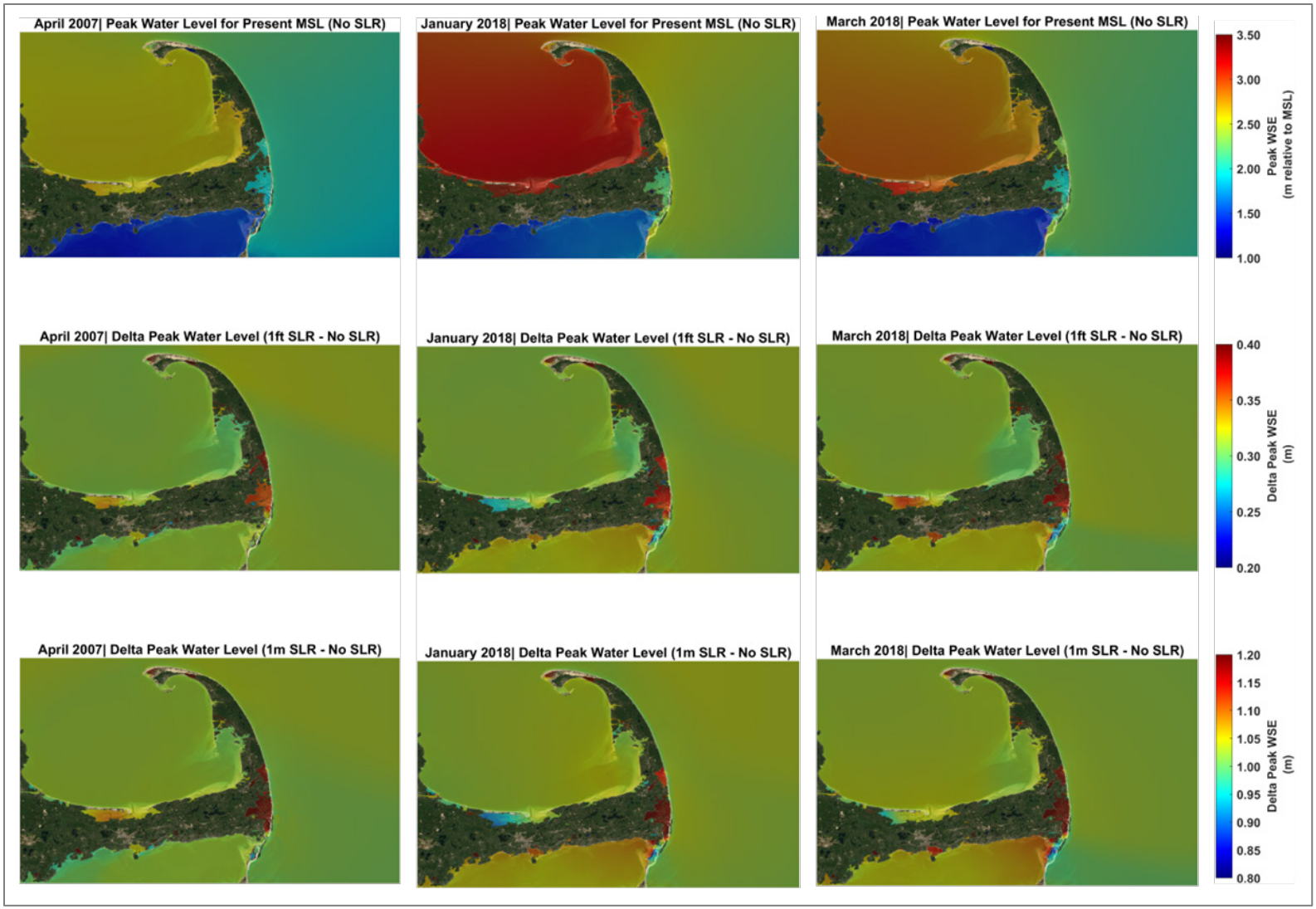


Figure 41. Advanced circulation-simulating waves in the nearshore (ADCIRC-SWAN) results of the April 2007 (left), January 2018 (center), and March 2018 (right) nor'easters at Cape Cod National Seashore; peak water levels from the simulation using 2020 mean sea level (top), change in peak water levels when 1 ft (0.3048m) of sea level rise is simulated (middle), and change in peak water levels when 1 m of sea level rise simulated (bottom).

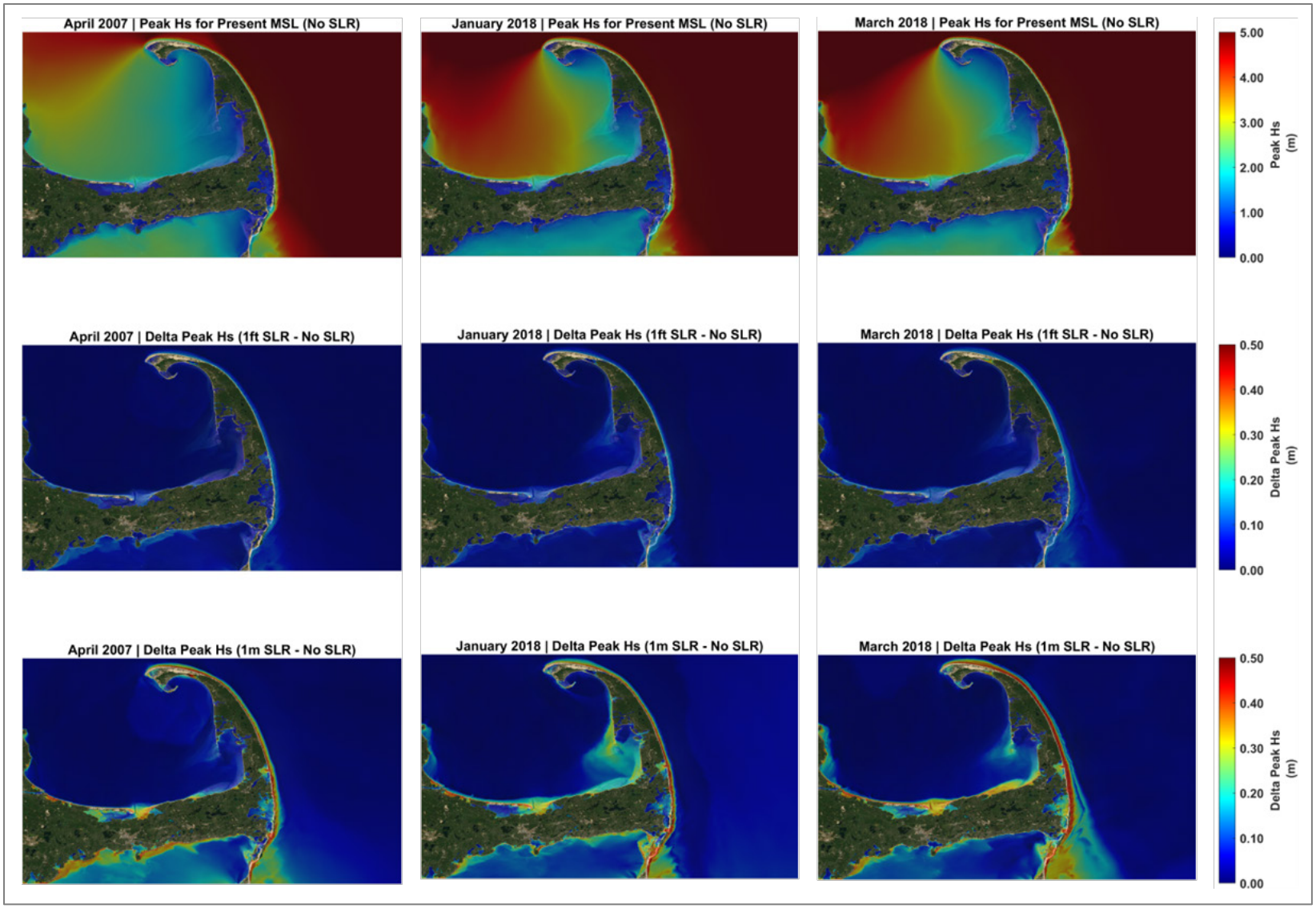


Figure 42. Advanced circulation-simulating waves in the nearshore (ADCIRC-SWAN) results of the March 2018 nor'easter at Cape Cod National Seashore. Peak significant wave height (Hs) from the simulation using 2020 mean sea level (top), change in Hs when 1 ft (0.3048m) of sea level rise is simulated (middle), and change in peak Hs when 1 m of sea level rise is simulated (bottom).

The water level figure presents each storm in separate columns, and within each column, the top panel presents the peak water level from the baseline (MSL of 2020) simulation. The middle panel maps show the change in peak water level relative to the baseline from the simulation that includes 1 ft of SLR, and the bottom panel maps show the change in peak water level relative to the baseline from the simulation that includes 1 m of SLR. The peak water level is plotted relative to the present MSL, and each change map uses a narrow scale to highlight the simulated level of change.

The results of significant wave height are presented in a similar manner, with three plots per storm and all three storms in a single figure. The top plot presents the peak significant wave height from the baseline simulation (MSL of 2020), the middle plot presents the change in peak significant wave height relative to the baseline from the simulation that includes 1 ft of SLR, and the bottom figure plot shows the change in significant wave height relative to the baseline from the simulation that includes 1m of SLR.

The summary of peak water level results and peak significant wave height results are presented in Figure 37 and Figure 38 for ACAD, in Figure 39 and Figure 40 for BOHA and BOST, and in Figure 41 and Figure 42 for CACO.

The highest water level is not always associated with the storm, or portion of the storm, that produces the greatest surge, as the peak water level is a function of the astronomical tides and wind driven effects. This was observed in all three storms simulated. The January 2018 nor'easter had the highest peak at all three parks. However, based on the data analysis at tide gauges (Figure 18–Figure 23), the March 2018 storm produced the largest surge (increase over the tidal water level). While the details of peak water level depend on location, storm severity, and tides, a few general trends are noted. At each park, the peak water level is relatively consistent for a broad region offshore of the coast, with little variability as a function of distance from the shore; at CACO, there is gradual variability offshore of the coast due to geometry and tidal variability in the region. However, coastal embayments tend to have water levels that exceed offshore peaks. Additionally, regions exposed to high waves experience a localized wave setup that increases the water level at the coastline, which will be explored further in the following section (*Analysis of Impact of Waves and SLR*). The change in peak water level can be greater or less than the applied SLR, and there is more variability at the coast. The relative change in total water depth is more significant in shallower regions, leading to a greater impact of the wave-driven setup on coastal water levels. Moreover, changes in total water depth affect the current speeds. The change in peak water levels increases with higher SLR, meaning the deviation from the applied SLR (e.g., 1 ft or 1m) is more significant for higher SLR levels.

The peak significant wave at each park is influenced by the fetch, wind speed and direction, as well as the water depth, with the latter being a limiting factor, particularly in shallow waters. This is evident in the attenuation of peak significant wave height from offshore regions to the coast. The change in peak significant wave height is primarily determined by the change in water depth in the shallow regions, where deeper water allows for larger waves. Therefore, the degree of change in peak significant wave height at a given point increases with higher SLR levels, as expected. Additionally, SLR increases flooded regions, extending the regions affected by waves.

We analyzed the time-varying nature of water levels and significant wave heights for each storm at a set of query points that span the three parks, as shown in Figure 43. The points analyzed here are primarily located outside of the surf zone, as a detailed examination of the surf zone and coastal embayments is provided in subsequent sections. The time series of baseline (2020 MSL) water level and the change in water level for the 1 ft SLR and 1m SLR at the query points are shown in Figure 44 for each park for the January 2018 nor'easter. Similarly, we investigated the baseline and change in significant wave height at these points, as shown in Figure 45. These figures present the time series of all points to examine the trends collectively.

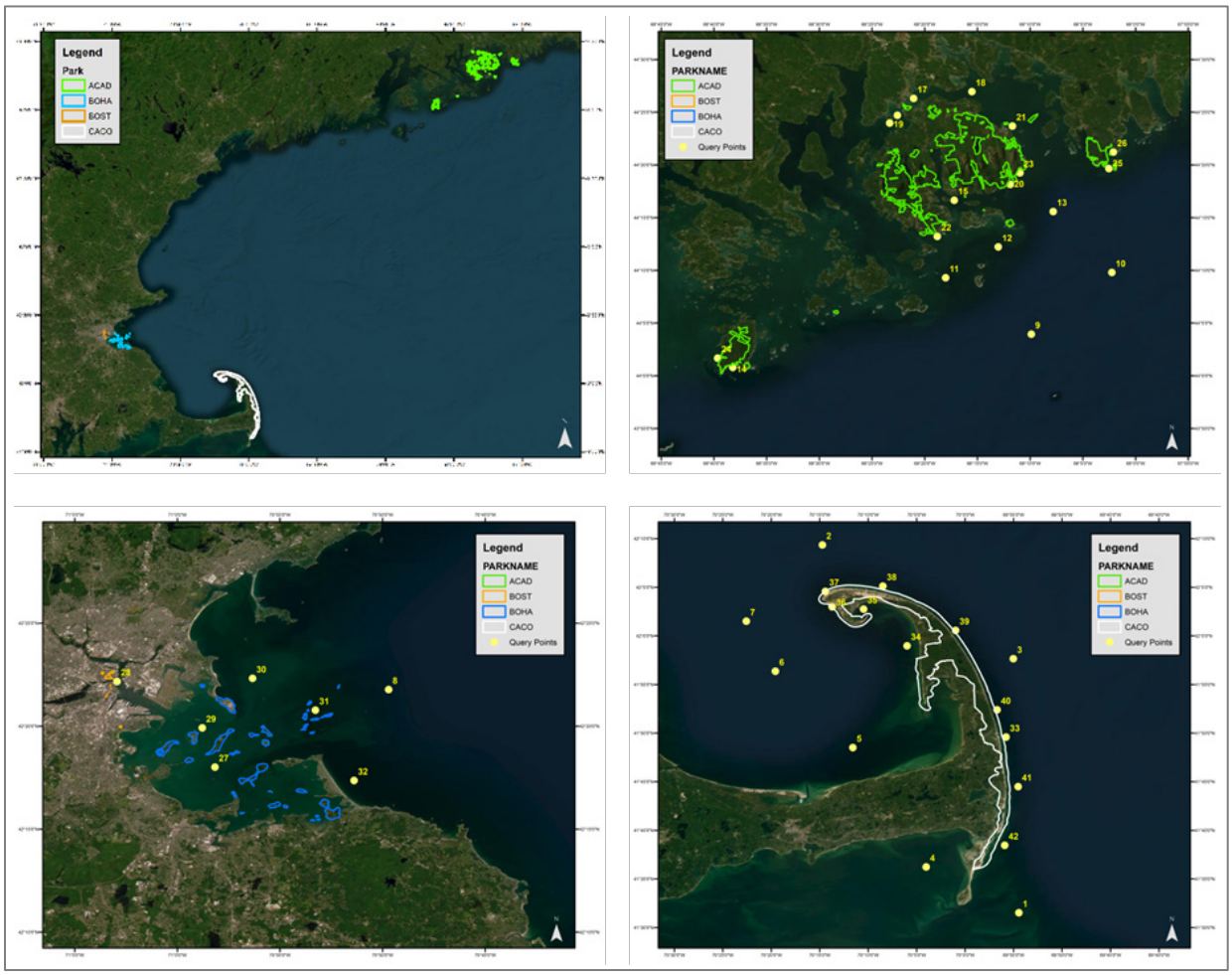


Figure 43. Maps of the study areas and analysis query points; all parks within the study area (upper left), the National Parks of Boston region showing query points (bottom left), Acadia National Park region showing query points (upper right) and Cape Cod National Seashore region showing query points (bottom right).

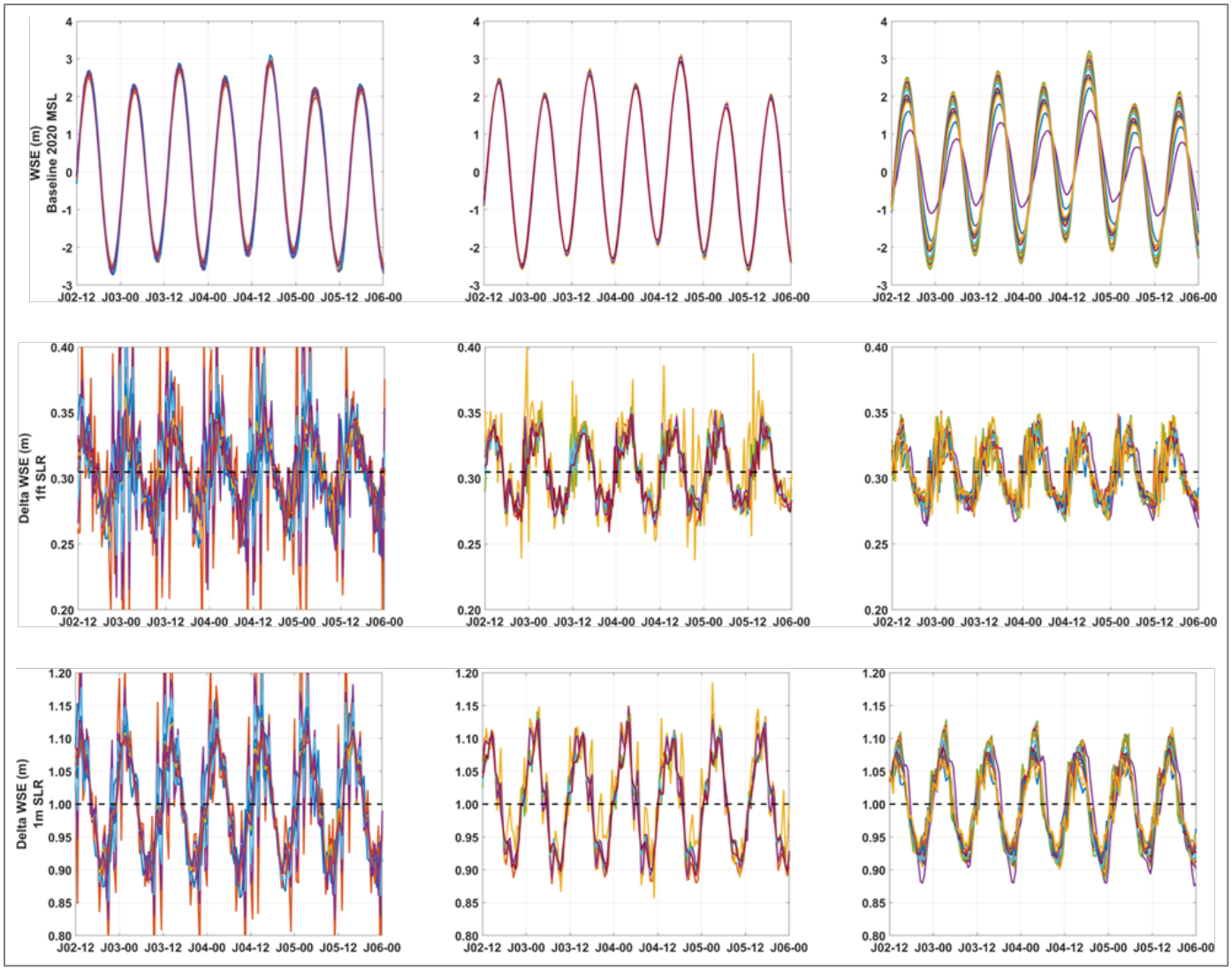


Figure 44. Water level summary for January 2018 nor'easter at Acadia National Park (left), the National Parks of Boston (middle), and Cape Cod National Seashore (right). Top plot shows time series of water level from the 2020 mean sea level baseline simulation (top), the middle plot shows the change from baseline from the simulation with 1 ft sea level rise and the bottom plot shows the change from baseline from the simulation with 1 m sea level rise. Time is UTC.

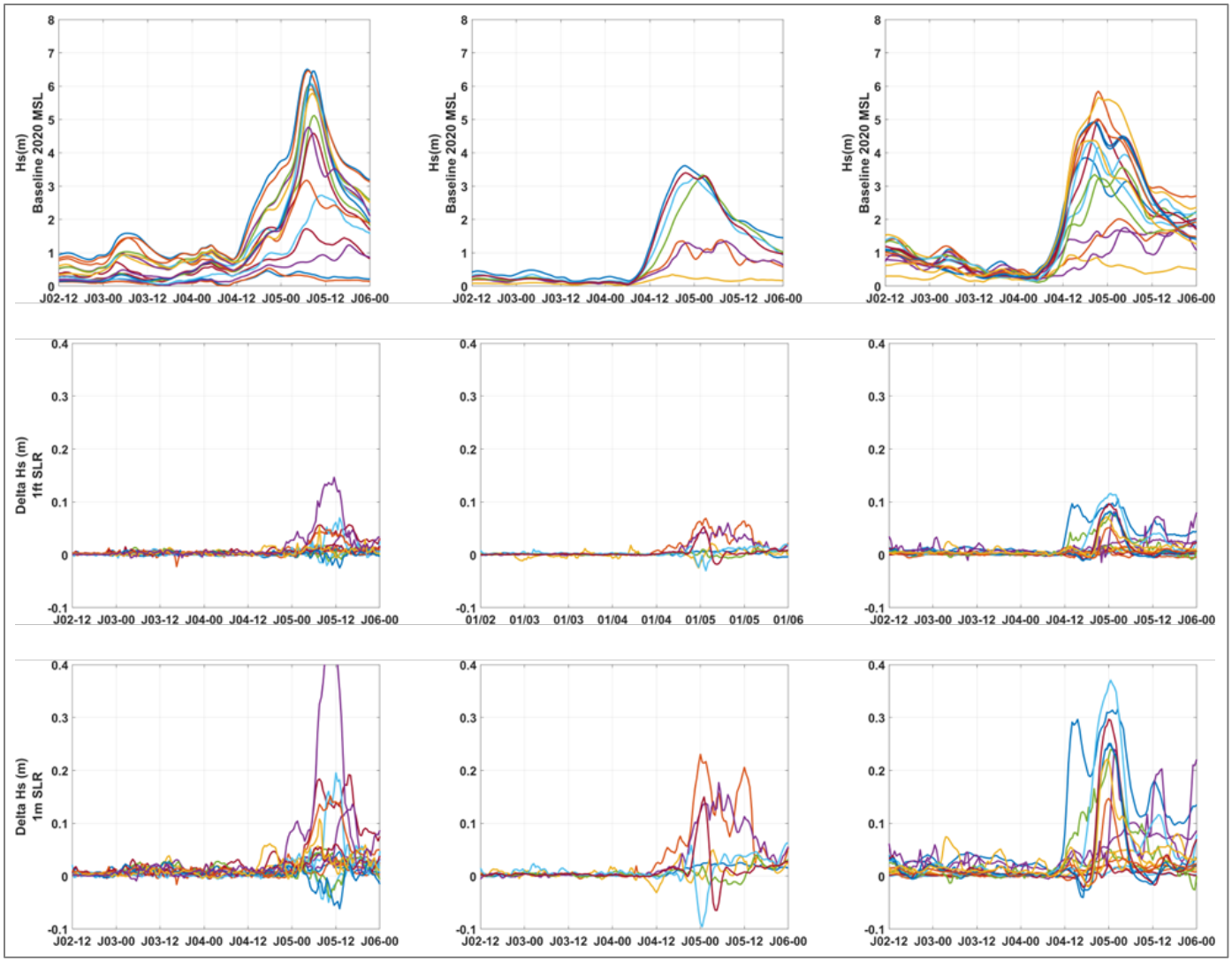


Figure 45. Significant wave height summary for April 2007 nor'easter (left), January 2018 nor'easter (center) and March 2018 nor'easter (right) at Acadia National Park; top plot shows time series of significant wave height (Hs) from the 2020 mean sea level baseline simulation (top), the middle plot shows the change from baseline from the simulation with 1 ft sea level rise and the bottom plot shows the change from baseline from the simulation with 1 m sea level rise. Time is UTC.

Figure 44 shows that the changes in water levels are not constant and vary periodically with time, likely related to the tidal period. The changes oscillate from values greater than the applied SLR to less than the applied SLR, with the peaks out of phase with the water level peaks. The degree of change is proportional to the amount of SLR applied, as evidenced by a greater amplitude of the signal for the 1m SLR relative to that of 1 ft of SLR (~+/- 0.08 m versus +/- 0.03 m). Additionally, although there is considerable noise at some of the points in ACAD, the average trends in change are similar at each park for both analyzed SLR increments.

Figure 45 shows that the change in significant wave height is not constant and varies with the baseline wave height. At some locations, there may be a small periodic signal as the wave height changes in response to the total water depth that is influenced by tides. During relatively calm periods, the change is small (<0.02m). The degree of change is proportional to the amount of SLR applied, although non-negligible change is limited to shallower sites and is a function of the change in water depth, as further explored in the following section (*Analysis of Impact of Waves and SLR*).

The peak water level footprint provides an indication of the extent of flooding, and this data was used to calculate inundation depths as the difference between the peak water level and the bottom level. The ADCIRC model mesh resolution allows the identification of areas susceptible to overland flooding, but a more detailed analysis is required to better understand the flooding pathways in these areas. By comparing the inundation footprints for various MSL and storm conditions, potential future vulnerabilities can be identified.

Figure 46 through Figure 49 present inundation plots of different areas local to the study parks. Figure 46 shows the east coast of Mount Dessert Island at ACAD. This figure indicates that regardless of storm or MSL condition, there is no inundation over land in this region with the exception of Sand Beach when considering 1 m of LSR. Figure 47 shows a subset of Boston Harbor Islands, revealing that there are some lower lying areas may be prone to flooding at any storm. The addition of SLR and the severity of the storm does not significantly alter the impacted footprint, but it does alter the flood depth. Figure 48 and Figure 49 show the Provincetown-Truro region and a region of Eastham, respectively. These figures indicate that this region has various pathways for coastal inundation, and the extent of inundation is sensitive to storm severity and MSL condition.

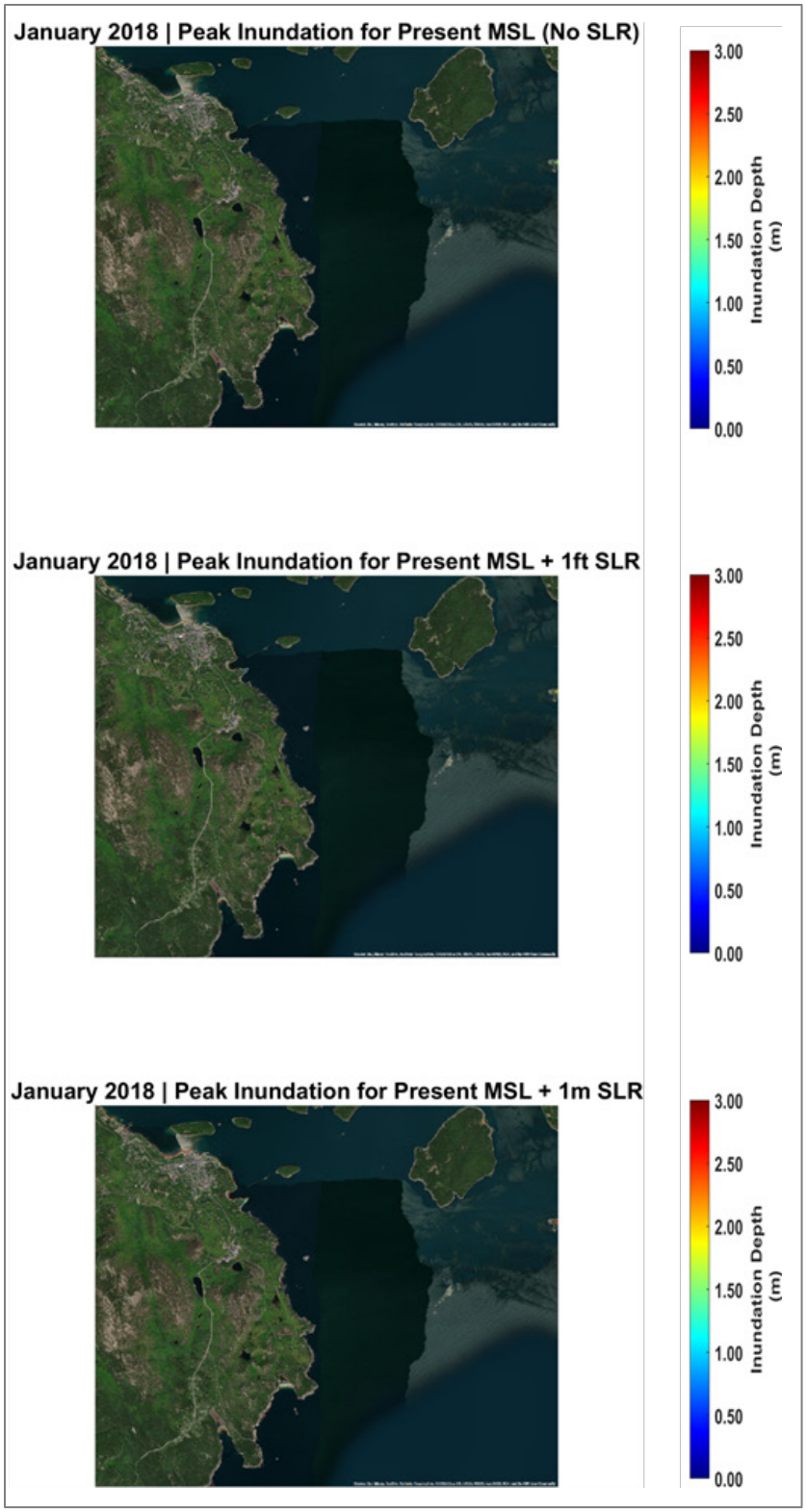


Figure 46. Inundation over land for January 2018 nor'easter at Acadia National Park; top plot shows inundation for the 2020 mean sea level baseline simulation (top), the middle plot shows the change from baseline from the simulation with 1 ft sea level rise and the bottom plot shows the change from baseline from the simulation with 1 m sea level rise.

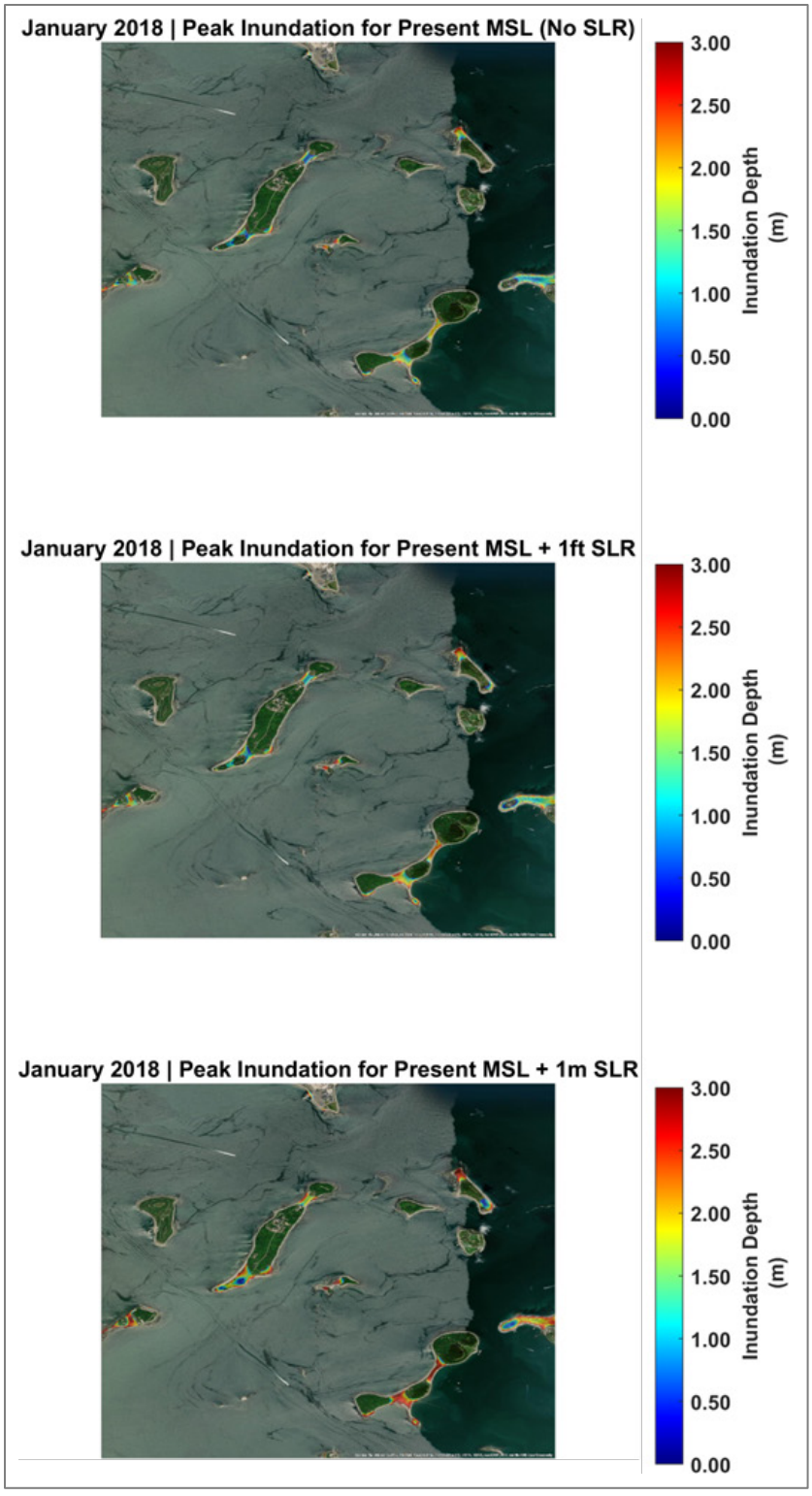


Figure 47. Inundation over land for the January 2018 nor'easter at the National Parks of Boston. Top plot shows inundation for the 2020 mean sea level baseline simulation (top), the middle plot shows the change from baseline from the simulation with 1 ft sea level rise and the bottom plot shows the change from baseline from the simulation with 1 m sea level rise.

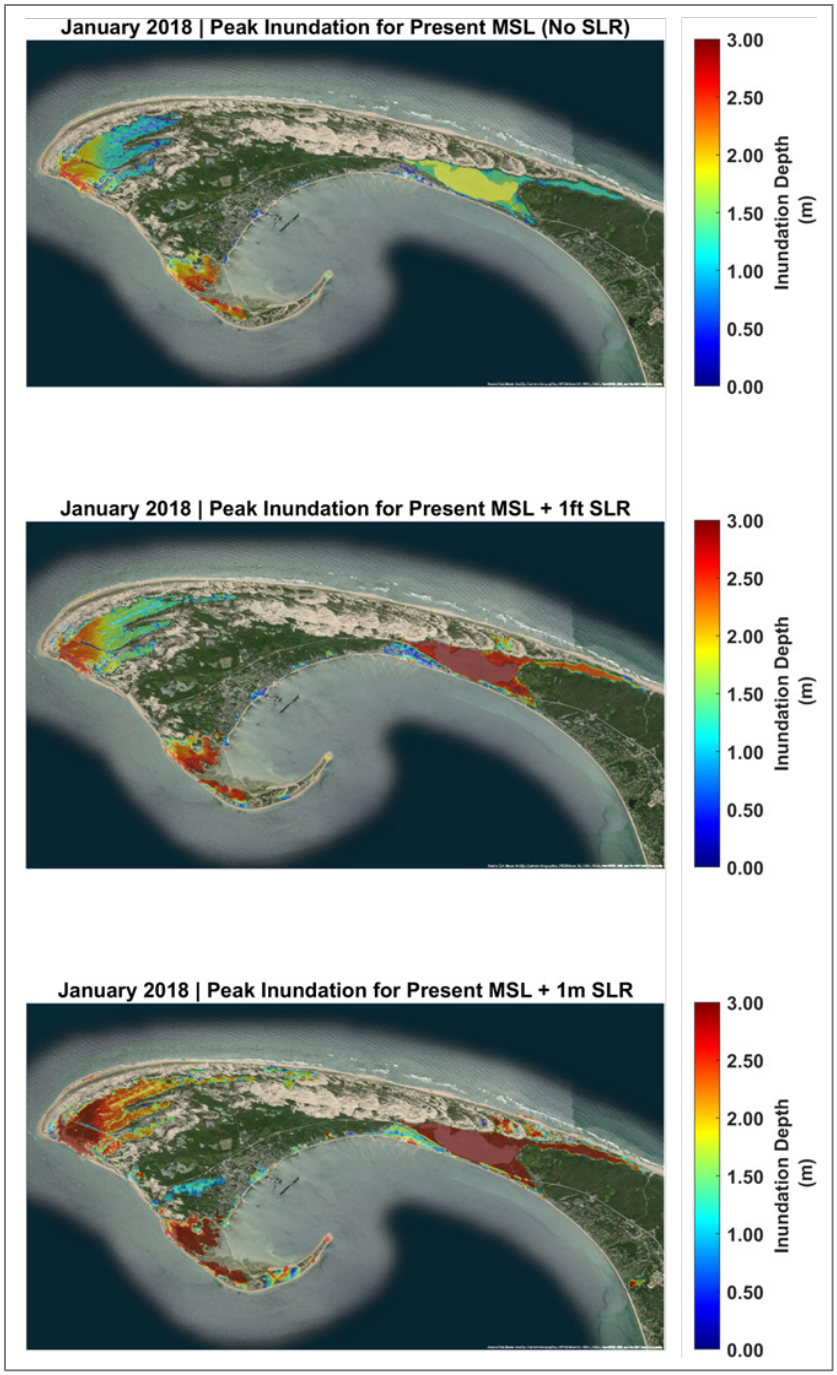


Figure 48. Inundation over land for the January 2018 nor'easter at Cape Cod National Seashore in the region of Provincetown and Truro. Top plot shows inundation for the 2020 mean sea level baseline simulation (top), the middle plot shows the change from baseline from the simulation with 1 ft sea level rise and the bottom plot shows the change from baseline from the simulation with 1 m sea level rise.

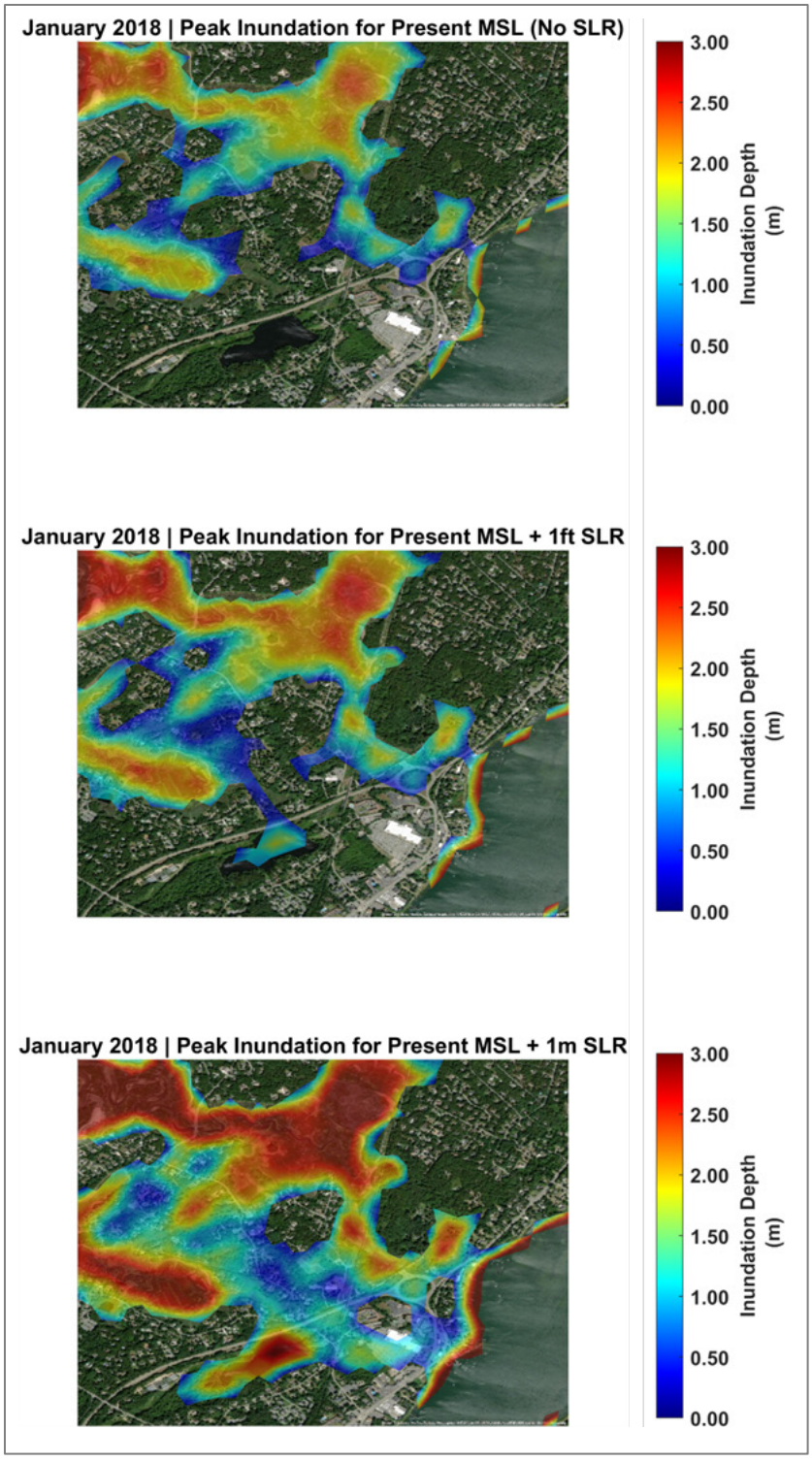


Figure 49. Inundation over land for the January 2018 nor'easter at Cape Cod National Seashore, Eastham region. Top plot shows inundation for the 2020 mean sea level baseline simulation (top), the middle plot shows the change from baseline from the simulation with 1ft sea level rise and the bottom plot shows the change from baseline from the simulation with 1 m sea level rise.

Results of Analysis of Impact of Waves and SLR (CACO East Coast)

The January 2018 nor'easter simulations included scenarios with and without SLR and with and without wave coupling. The results were analyzed in terms of coastal storm surge, inundation, and wave height profiles along a representative transect in the study area. Figure 50 compares peak simulated water levels from simulations with wave coupling with and without 1m of SLR. The scales in this figure are offset by 1m to highlight areas where the change is different from the applied 1m of SLR. The results show that changes in peak water level with the addition of 1m SLR are close to 1m along the open coast, but the change is more than 1m within the embayment. Furthermore, the footprint of inundation is extended with the addition of 1m SLR.

Figure 51 presents a comparison of the peak water levels with 1m of SLR from results obtained with and without wave coupling. Both maps use the same scale, as they both include the 1m of SLR. As can be seen in this figure, the inclusion of wave coupling results in increased water levels along the coast as well as within the Nauset embayment. The white circles outline areas that to the simulation shows will become flooded when wave coupling is included, compared to being dry without wave coupling.

The difference in water level between the scenarios with and without wave coupling is shown in Figure 52. In this figure, a transect is shown extending from the shoreline to a point offshore with relatively deep water. The peak water level and significant wave height are plotted along this transect in Figure 54 for the simulations with wave coupling, both with and without 1m of SLR. This figure illustrates that at the peak of the storm, the water level inundated most of the beach and reached the dune. Due to the steep topography of the dune, the water elevation with and without SLR is terminated at approximately the same location. However, the simulation with SLR shows increased water level and wave height due to the increased total water depth.

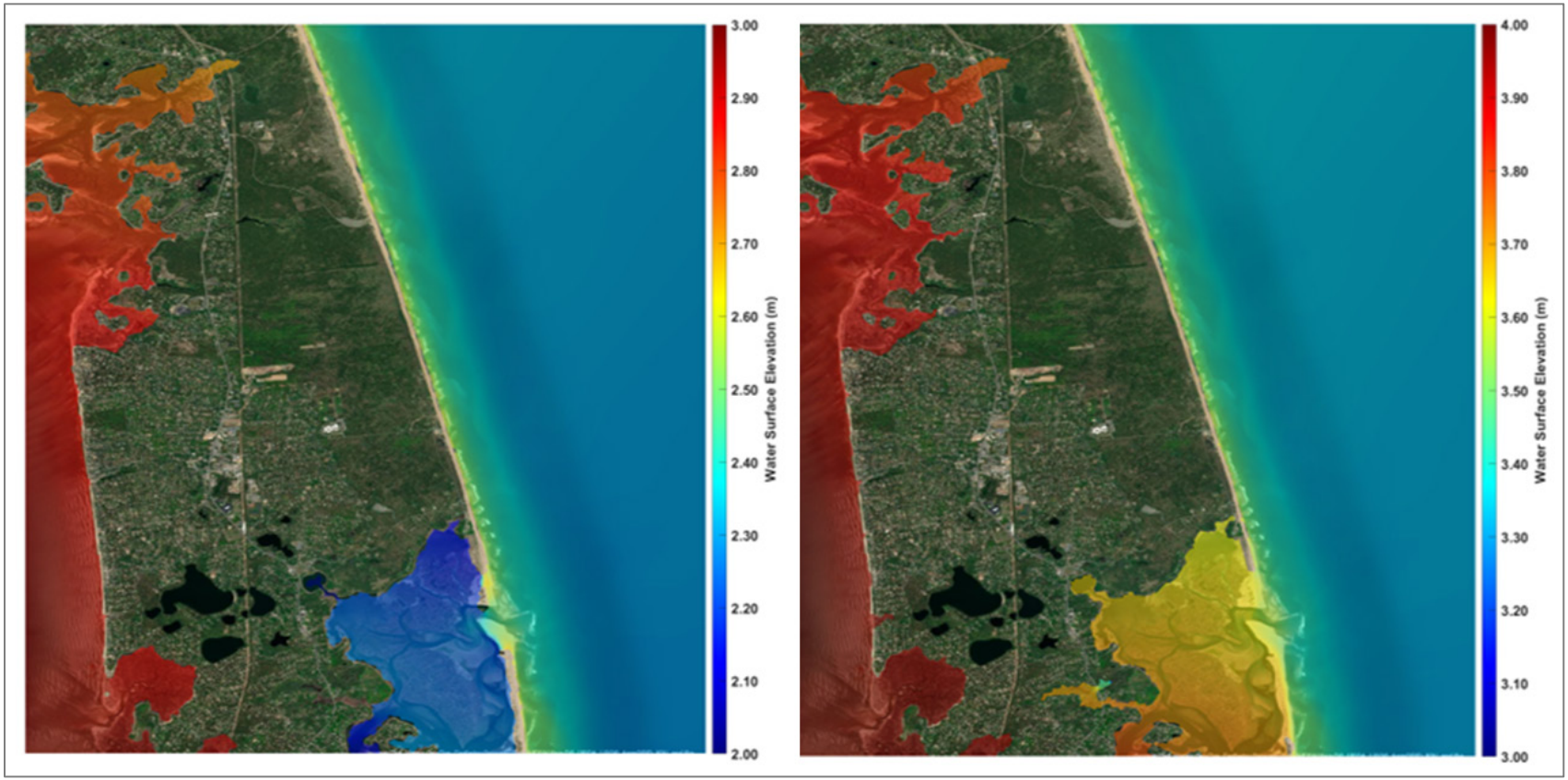


Figure 50. Comparison of peak water level without sea level rise(left) and with 1 m of sea level rise (right) from simulations of the January 2018 nor'easter along the central east coast of Cape Cod. White outlined areas illustrate areas that have increased inundation over land with 1 m sea level rise.

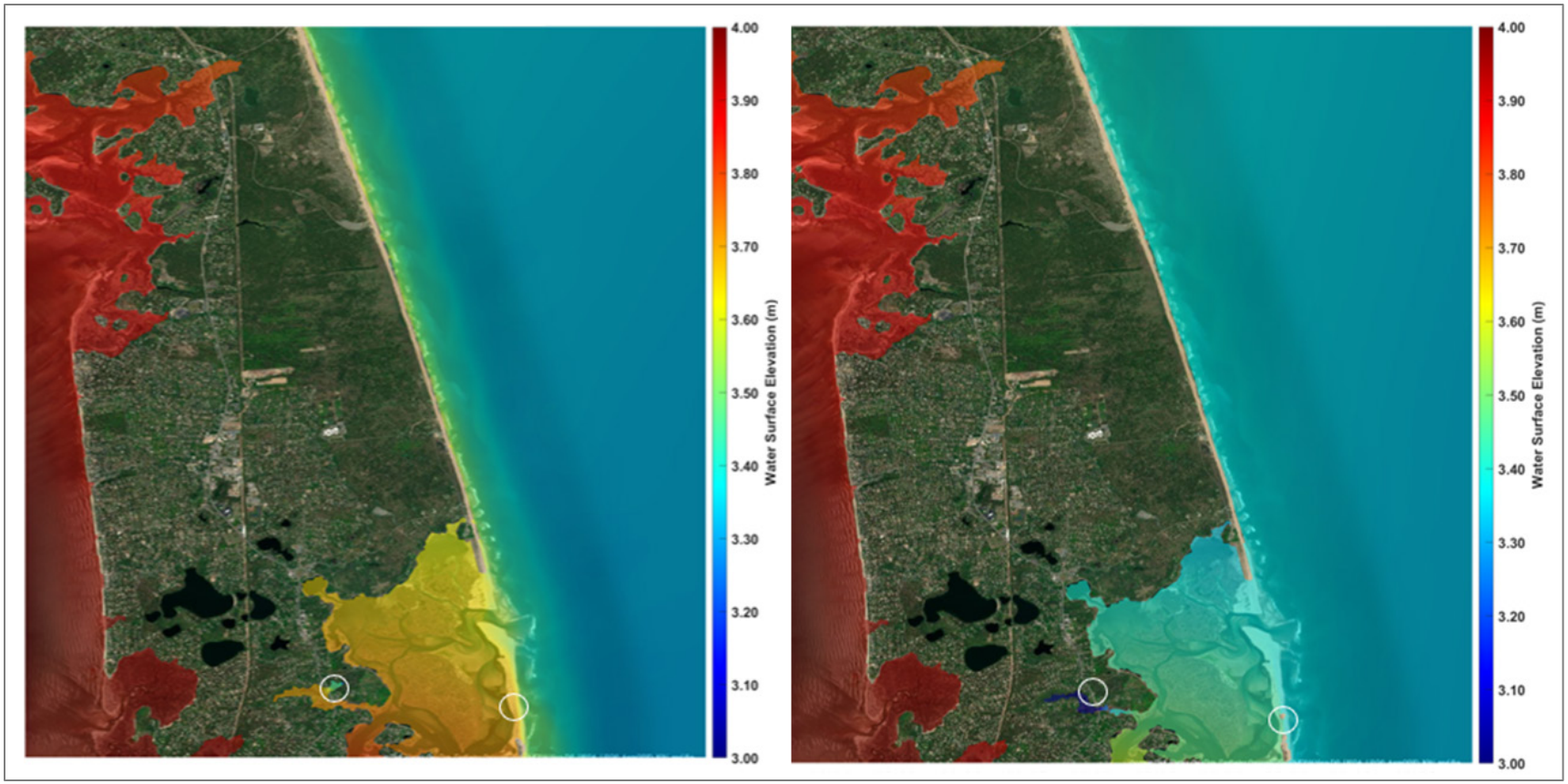


Figure 51. Comparison of peak water level from simulations of the January 2018 nor'easter with 1m sea level rise with wave coupling (right) and without wave coupling (left) along the central east coast of Cape Cod. White outlined areas illustrate examples of areas that have increased inundation with the use of wave coupling.

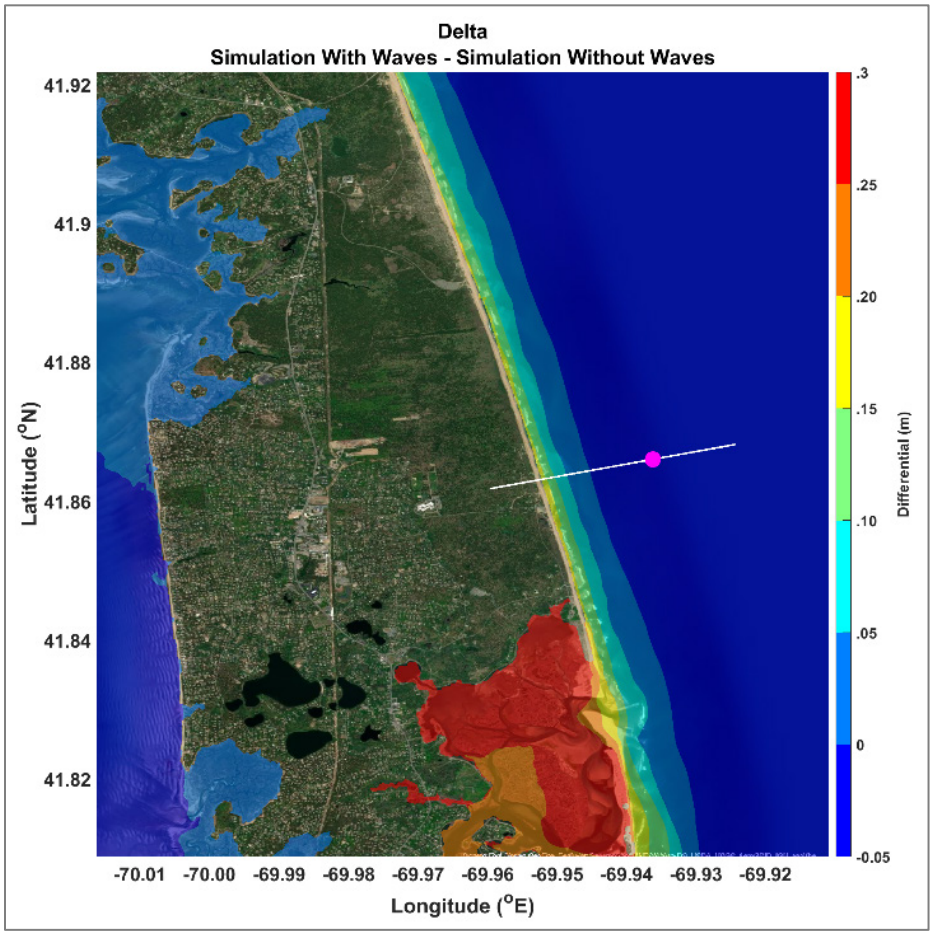


Figure 52. The difference in water elevation between the simulations of the January 2018 nor'easter with and without wave coupling along the central east coast of the Cape Cod National Seashore. The white line extending perpendicular to the shore is a transect for which more in-depth analysis was performed.

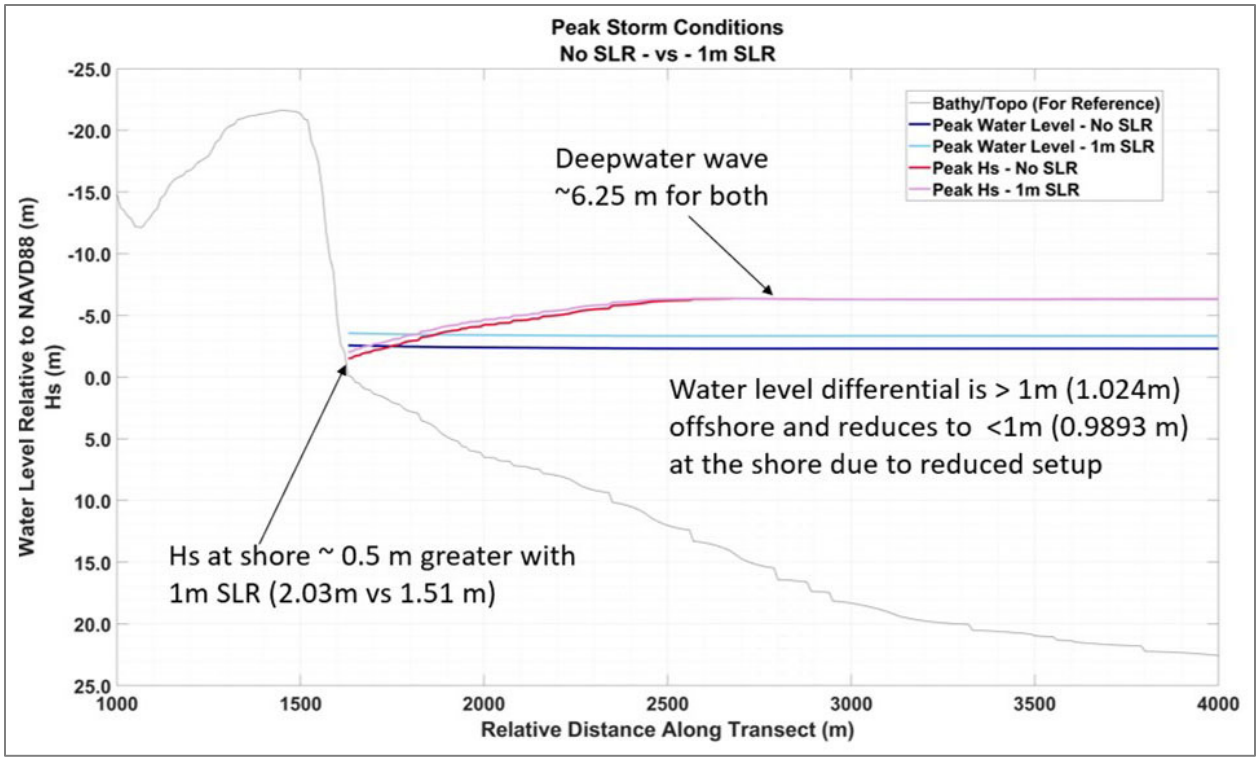


Figure 53. The peak water elevation and peak significant wave height along the central east coast of the Cape Cod National Seashore (the transect shown in Figure 52) from simulations of the January 2018 nor'easter with and without 1m of sea level rise. The bottom elevation is depicted by the grey line.

Figure 54 shows the difference in peak water level along this transect in the simulations with and without waves along this transect for the case without SLR and with 1m of SLR. The water elevation difference increases at the shore, where the wave-generated setup contributes to the total water level in the simulations with waves. The difference is up to 21 cm for the no SLR case and 18 cm for the case with SLR. This difference is approximately 30% of the total surge in this location, indicating that the wave-generated setup plays a significant role in the total water level. Notably, the relative contribution of waves is slightly reduced with SLR, likely due to reduced radiation stress and greater total water depth resulting from the addition of SLR.

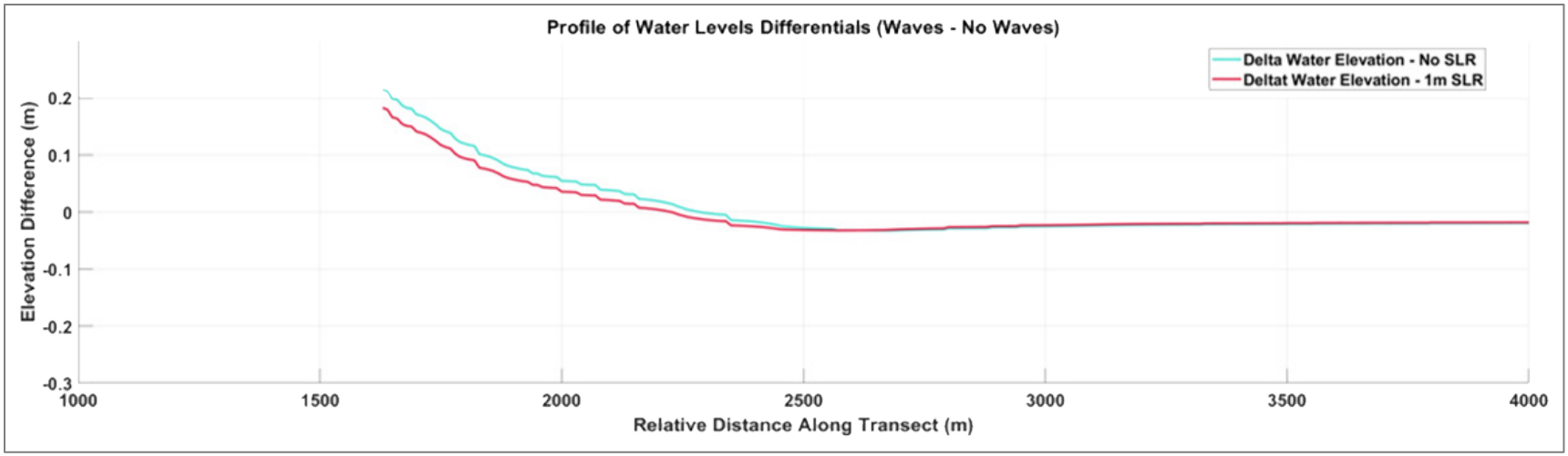


Figure 54. The difference in peak water elevation in the simulations with and without waves from simulations of the January 2018 nor'easter along a transect in central east Cape Cod (shown in Figure 52) for the cases without and with 1 m of sea level rise.

Results of Analysis of Impact of Shoreline Configuration (Pleasant Bay)

The maximum water elevations from the simulations of each scenario (shoreline configuration) during the storm period with no wind forcing (tides only) are presented in Figure 55, with wind forcing in Figure 56, and the calculated surge is shown in Figure 57.

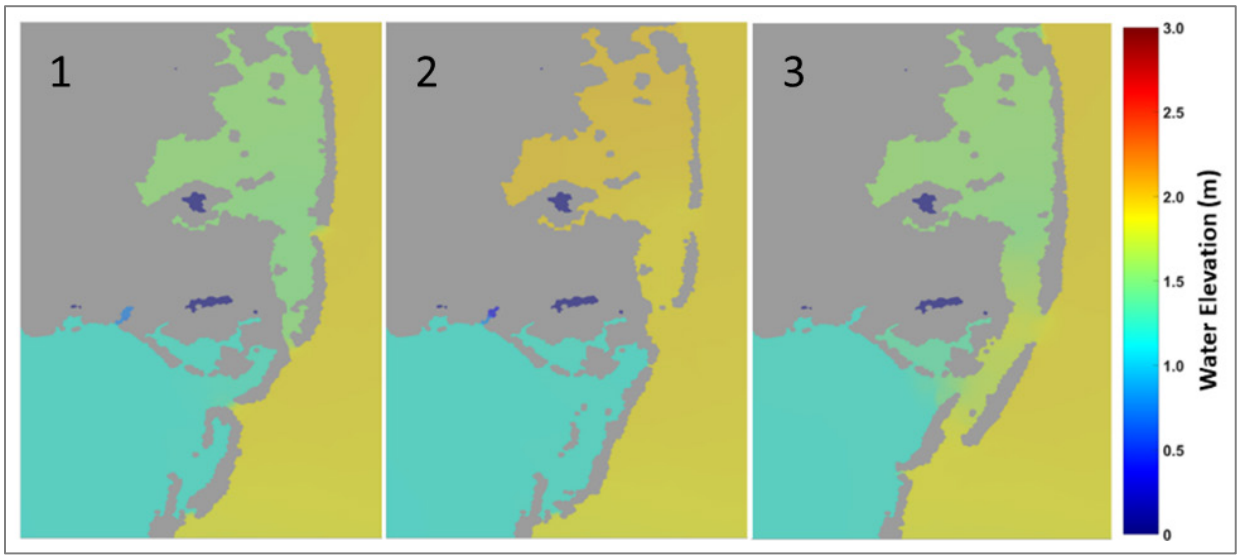


Figure 55. Maximum water elevation for simulation with tides only forcing (no wind) for shoreline configuration 1 (left), 2 (middle) and 3 (right) of the Pleasant Bay region of Cape Cod National Seashore. Water elevation is relative to the North American Vertical Datum of 1988.

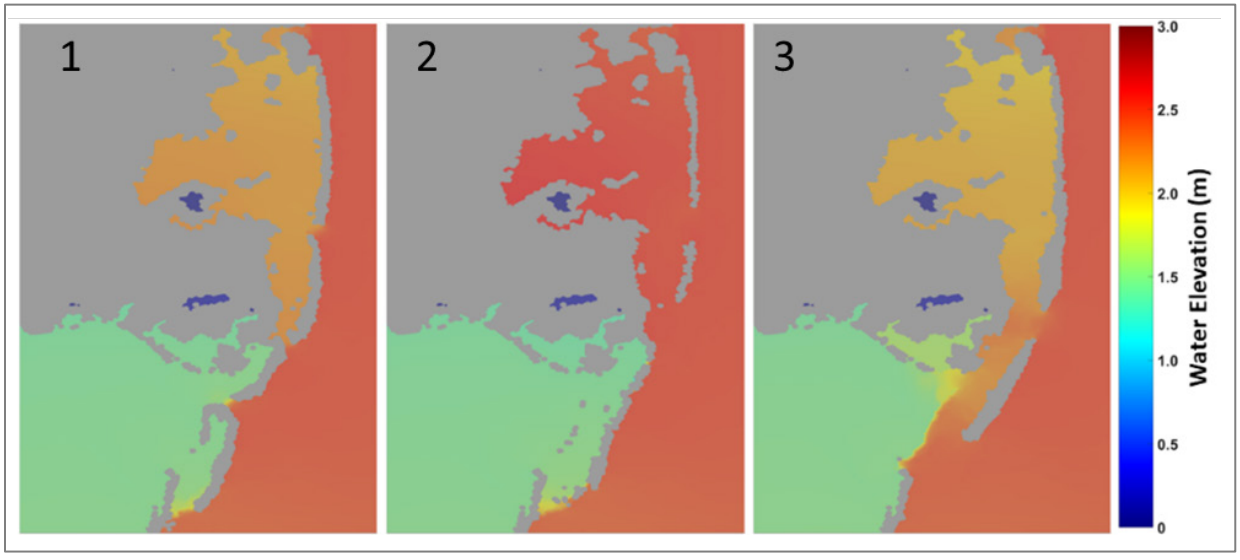


Figure 56. Water elevation at storm peak from simulation with tides and wind forcing based on the January 2018 nor'easter for shoreline configuration 1 (left), 2 (middle) and 3 (right) of the Pleasant Bay region of Cape Cod National Seashore. Water elevation is relative to North American Vertical Datum of 1988.

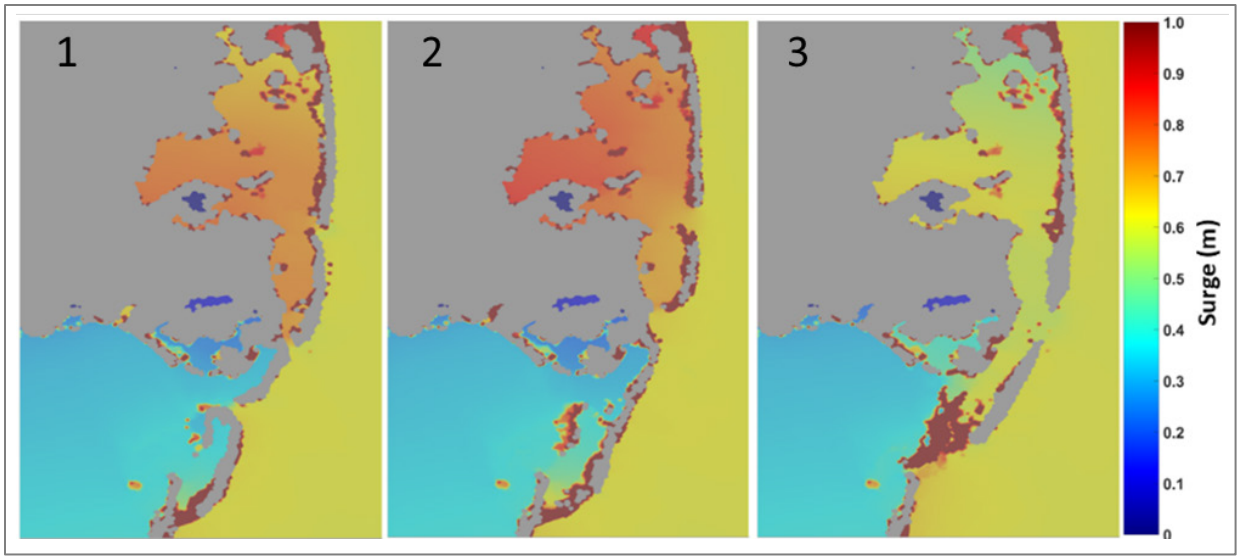


Figure 57. Maximum surge for shoreline configuration 1 (left), 2 (middle) and 3 (right) of Pleasant Bay region of Cape Cod National Seashore.

Figure 55 shows the spatial variability in the maximum water level across the domain from tidal water elevations. There is a notable difference in the maximum tidal water elevation on the Atlantic Ocean side (~ 1.9 m) versus Nantucket Sound (~1.2 m). This figure also shows that the maximum water level within the embayment varies depending on configuration. The maximum water level in the Pleasant Bay Region for Configurations 1 and 3 are similar (~1.55–1.58 m), whereas it is greater for Configuration 2 (~ 1.9 m). While maximum water elevations are similar in Pleasant Bay for Configuration 1 and 3, there is more variability between these in closer proximity to the inlets where the shoreline differs between the configurations. The maximum water elevations in the simulations including wind forcing (Figure 56) show similar trends as the tides only results, however with overall higher water elevations and more variability between the results for Configuration 1 and 3.

The maximum surge (Figure 57) shows that there is a difference in the peak surge on the Atlantic Ocean side (~ 0.61 m) compared to the Nantucket Sound side (~0.35 m). The figure also shows the difference in the surge within the embayment, which is more prominent than the difference in maximum water level due to the smaller range of surge values. Within the embayment, Configuration 2 typically has the largest surge, and Configuration 3 typically has the smallest surge, though there are site specific differences in trends, mainly local to the inlets.

The water level and surge results were queried at a set of points across the domain to evaluate the differences between results for the different scenarios. The locations of the query points are shown in Figure 58. Time series of and surge and total water level from the wind forced simulations at select query points for each configuration are presented in Figure 59. The time series show that outside the embayment, there are negligible differences in total water elevation between the three configurations, while there are significant differences in the water elevations within the embayment. Configuration 2 has the largest tide range and less phase difference relative to the offshore tides, indicating that the high tide occurs slightly earlier for Configuration 2. The time series of surge shows that

Configuration 2 also has the highest surge within the embayment and that the surge occurs slightly ahead of the other configurations. The peak surge for Configurations 1 and 3 coincides, and Configuration 3 has the smallest peak surge. After the peak of the storm, all configurations show a negative storm surge, and small differences between the configurations persist for multiple tidal cycles.

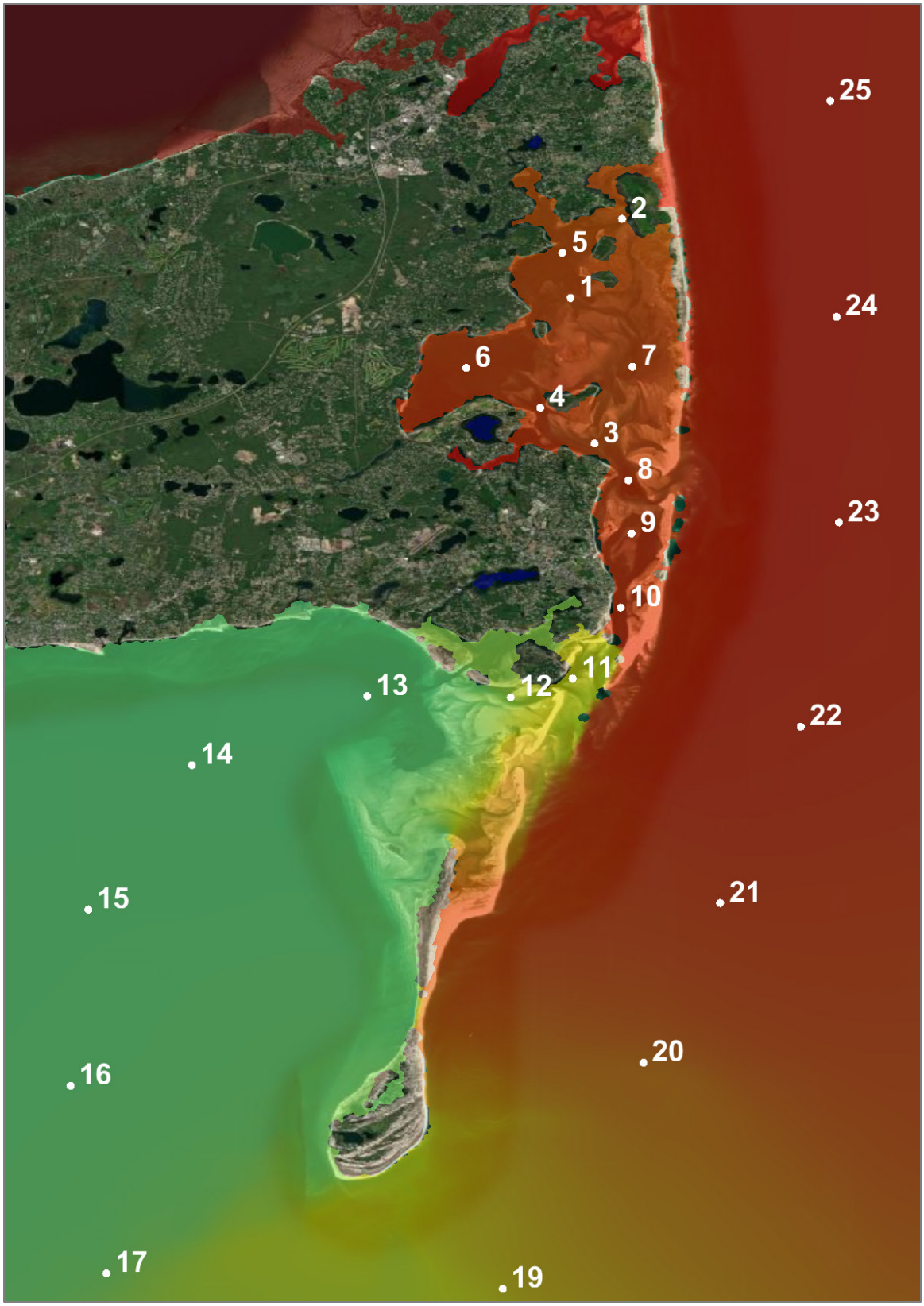


Figure 58. Query point locations in the Pleasant Bay region located in southeastern Cape Cod overlaid on maximum water elevation from Configuration 3.

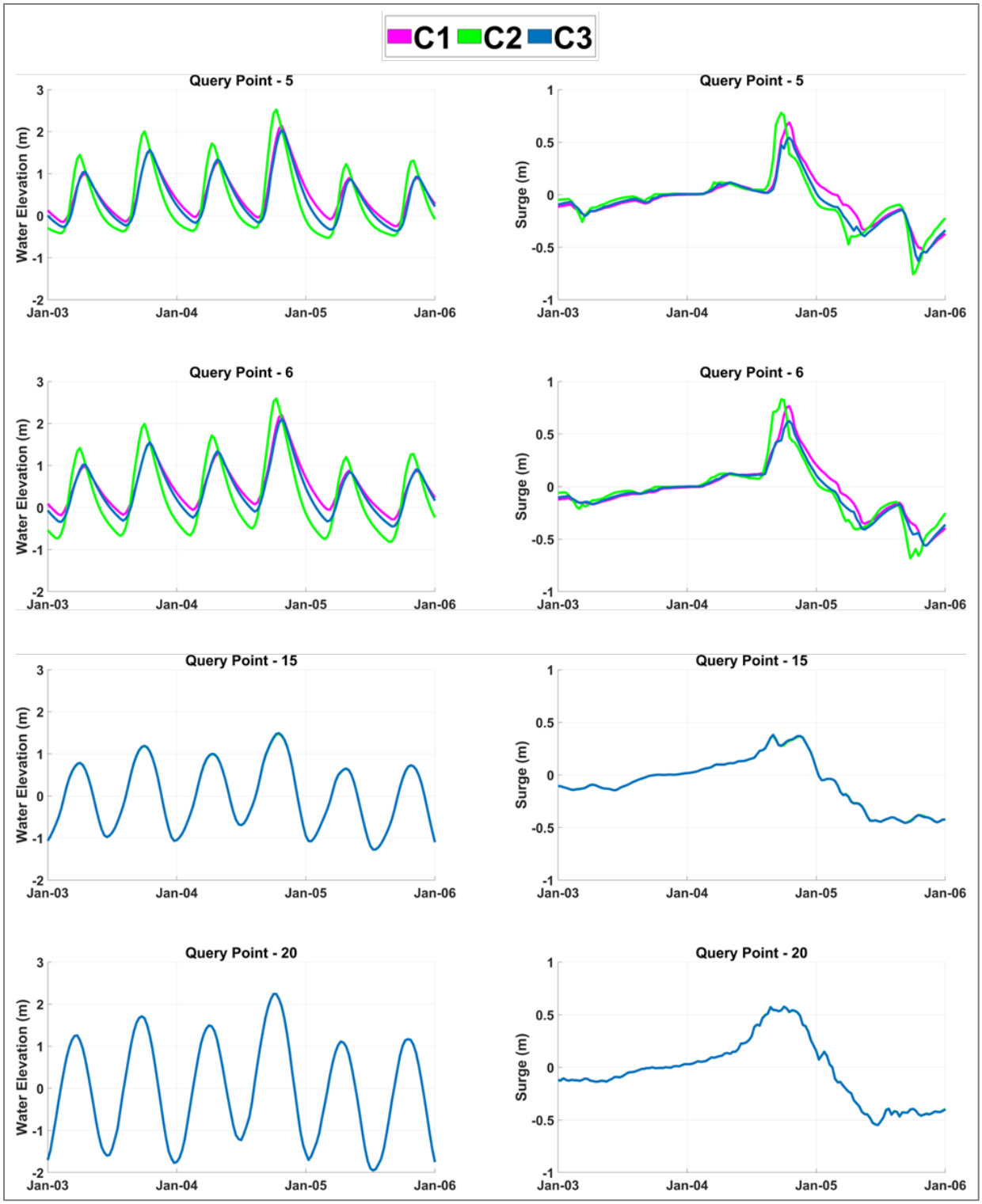


Figure 59. Time series of water elevation and storm surge from simulations of the January 2018 nor'easter at query points 5, 6, 15 and 20 all located in the Pleasant Bay region in southeastern Cape Cod from simulations of each of the three shoreline configurations. Colors for configuration 1 (C1), configuration 2 (C2) and configuration 3 (C3) are shown in legend at top of plot. Time is UTC.

The maximum water level and maximum surge for each configuration at every query point are shown in Figure 60. At the locations deep within the embayment farther from the inlets (locations 1–8), Configuration 2 shows the highest peak water elevations of 2.48–2.55 m, whereas the water elevations for Configuration 1 range from 2.10–2.20 m and Configuration 3 from 1.99 m to 2.11 m. The peak surges are similar for Configuration 1 and 2, but consistently lower for Configuration 3. There is a more significant difference in total water level than surge due to the increase in tide range and surge for Configuration 2. Overall, within the embayment across the scenarios, the peak surge ranges from 0.50 m to 0.83 m, location dependent. In Little Pleasant Bay (Location 5) and Pleasant Bay (Location 6), the difference between peak surge for Configuration 1 and Configuration 2 is 0.23 m and 0.21 m, respectively.

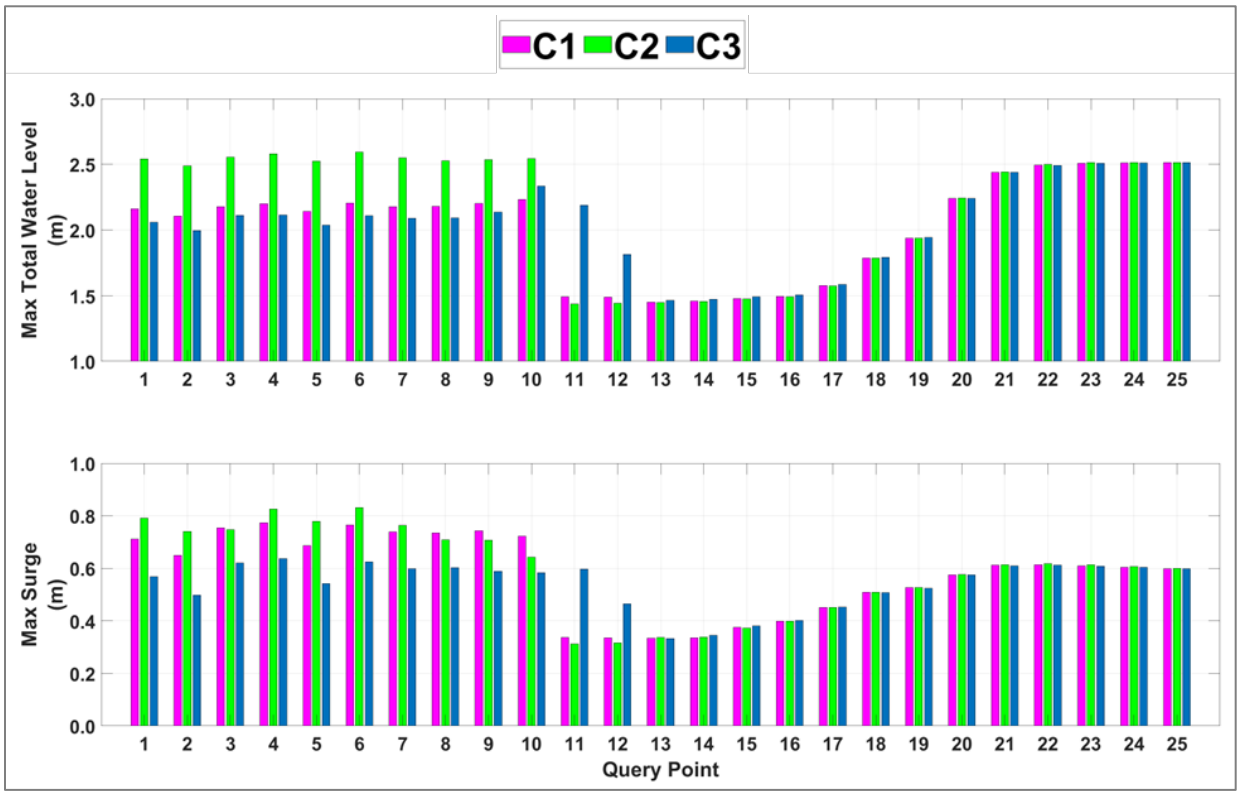


Figure 60. Maximum water level (top) and maximum surge (bottom) at the 25 query points all located in the Pleasant Bay region in southeastern Cape Cod from simulations of the January 2018 nor'easter for three different shoreline configurations: Configuration 1 (C1) shown in pink, Configuration 2 (C2) shown in green (yellow) and Configuration 3 (C3) shown in blue.

Results of 3D Visualizations and Engagement

The visualizations produced in the project were developed in consultation with representatives of Acadia National Park, Boston Harbor Island National Recreation Area, and Cape Cod National Seashore. These visualizations were created to provide a clear understanding of the potential impacts of storms and sea-level rise and to aid in the development of adaptation plans. The visualizations were tailored to the needs and perspectives of each park, with multiple iterations made to ensure they were oriented in ways that park managers and visitors were accustomed to. Visualization sites, such

as the Charlestown Navy Yard (BOST), were added to the project, which can be used to evaluate future adaptation plans. All visualizations produced in this project were made available to parks for incorporation into interpretive materials and other educational resources.

Base Visualizations

Figure 61, Figure 62, and Figure 63 illustrate some of the visualization infrastructure created for the sites that were subsequently connected to ADCIRC outputs. The visualizations depicting storm impacts are included in the site-specific results that follow.

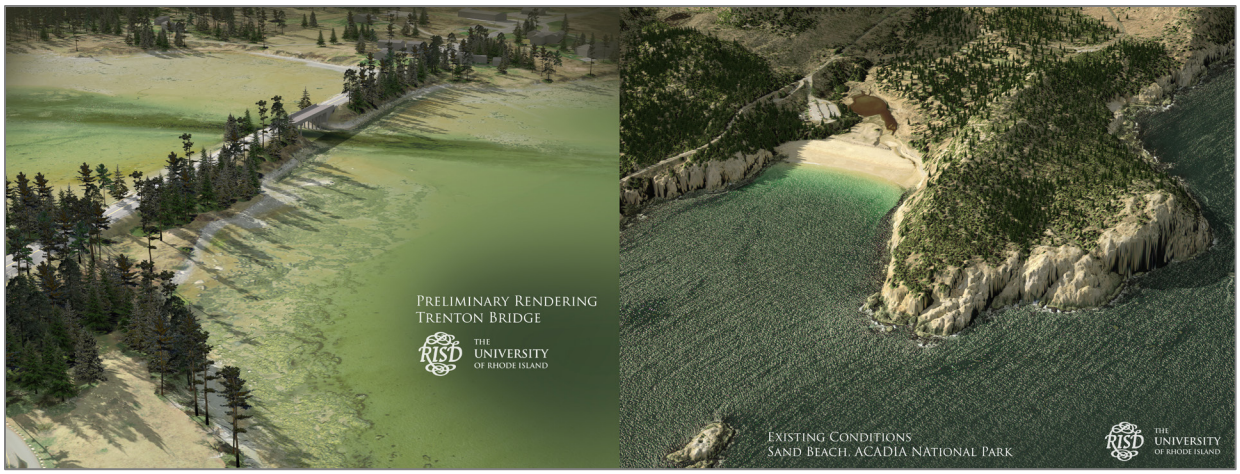


Figure 61. Overview of existing conditions, Trenton Bridge, left, and Sand Beach, right, Acadia National Park.



Figure 62. Existing conditions at Georges Island, Boston Harbor Islands National Recreation Area.



Figure 63. Existing conditions at Race Point Light and Herring Cove Beach (showing relocated Herring Cove Bathhouse, Cape Cod National Seashore.

Engagement

Throughout the project, engagement with the parks staff and affiliates was ongoing through meetings and shared content, resulting in the development of interpretive products. The modeling studies were presented at various seminars and conferences. The primary outcome of this engagement is a set of visualizations and materials for an interpretive film (Video (U.S. National Park Service) (nps.gov)), a

snapshot of which is shown in Figure 64. The film has been used by the parks for educational and outreach purposes, providing visitors with a better understanding of the potential impacts of climate change on the parks, as well as the measures being taken to adapt to these impacts. Three versions of this film have been created to cater to the location and priorities of other national parks. A longer 14-minute version specific to CACO is being shown in their Visitor Center. A shorter CACO version is available on their website and a more general short version is available on ACAD's websites ((Nor'easters - Acadia National Park (U.S. National Park Service) (nps.gov)).



Figure 64. Title frame from the interpretation video (top) and a snapshot of video footage from the interpretation video showing URI student Deb Crowley speaking with National Park service project manager Amanda Babson (bottom).

Results Summary by Park

Peak water levels and thresholds for flooding vary across the parks and within the parks due to the differences in topography, tide range, and storm characteristics. ACAD, BOHA, and BOST have

relatively low peak water level variability, and variability is higher at CACO due to the variability of the tide range across this park and the geometry of the shoreline. Table 9 provides a summary of peak water levels for the three parks, including three separate regions of CACO (Cape Cod Bay, Northeast Atlantic Coast, and Southeast Atlantic Coast). For reference, the local MHHW is also provided for each region, obtained from local tide gauges at Boston and Bar Harbor and NOAA's online vertical datum tool VDATUM (NOAA 2022a) at the three regions in Cape Cod. Water levels over MHHW do not necessarily result in flooding, as the potential for flooding is site specific and depends on coastal topography. The following subsections provide a general summary with site-specific results for each park.

Table 9. Summary of peak water levels at the query points across the different park regions in Region 1.

		Peak Water Level at Time Series Points meters above MSL[1]				
Storm	MSL Condition	ACAD[2] MHHW[3] 1.74	BOHA[4] MHHW 1.55	CACO[5] Cape Cod Bay MHHW 1.54	CACO Northeast Atlantic MHHW 1.35	CACO Southeast Atlantic MHHW 1.15
April 2007	2020	2.59	2.71	2.60	2.32	2.06
April 2007	2020 +1 ft SLR	2.90	3.00	2.91	2.64	2.37
April 2007	2020 +1m SLR	3.62	3.74	3.63	3.36	3.08
January 2018	2020	3.10	3.12	3.21	2.73	2.45
January 2018	2020 +1 ft SLR	3.41	3.41	3.53	3.04	2.77
January 2018	2020 +1m SLR	4.13	4.11	4.25	3.76	3.49
March 2018	2020	2.65	2.88	2.87	2.51	2.29
March 2018	2020 +1 ft SLR	2.96	3.17	3.18	2.83	2.60
March 2018	2020 +1m SLR	3.68	3.89	3.91	3.54	3.32

[1]MSL = Mean sea level

[2]ACAD = Acadia National Park

[3]MHHW = Mean higher high water

[4]BOHA = Boston Harbor Islands National Recreation Area

[5]CACO = Cape Cod National Seashore

Acadia National Park

ACAD encompasses an area approximately 66 km from Isle Au Haut to the Schoodic Peninsula, including partial and entire islands and peninsulas of the coastal terrain in this region. The park boundaries are aligned with the shoreline in some places, but a significant portion is inland on Mount Dessert Island. Although a detailed shoreline analysis was not performed, satellite imagery indicates that a large portion of the shoreline consists of rocky cliffs. For reference, the ADCIRC mesh elevations are shown in Figure 65 to demonstrate the steep topography of the region. The ADCIRC mesh only covers inland areas up to approximately 10m above MSL, and regions not contoured are above 10m elevation. Orange areas designate regions 5m above MSL, and the transition from blue

(locations with bottom elevation at or below MSL) to orange is sharp in most locations, demonstrating the steep topography in this region.

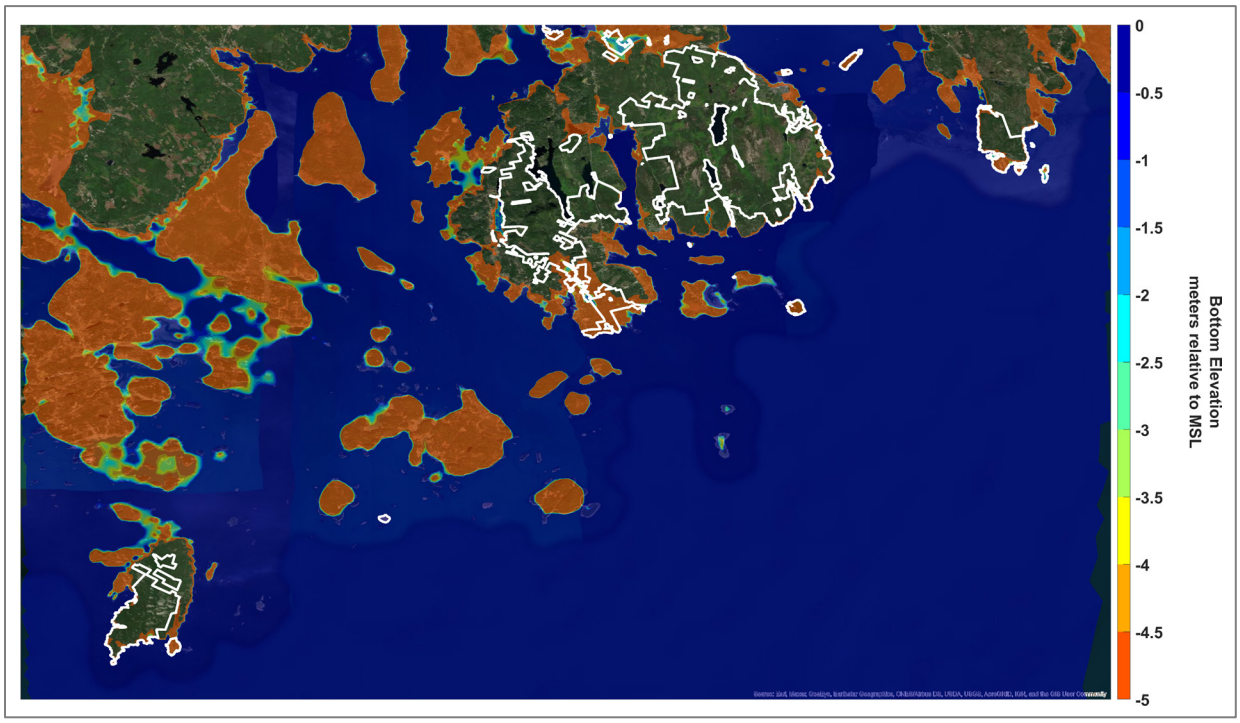


Figure 65. Map of bottom elevations at Acadia National Park.

The tide range in this region, as delineated by the difference between MHHW and MLLW, is 3.44 m. Analysis of storm surges at the NOAA gauge at Bar Harbor reveals that the top 50 surges recorded range from approximately 0.8 m to just under 1.5 m, with the most extreme surge on record resulting from an extratropical (nor'easter) storm. The analysis also indicates that extreme storm surges are not always associated with peak water levels, and smaller storm surges combined with a spring tide can produce high water levels. The large tide range has provided some level of protection from extreme water levels during storms that occur during neap tides. However, higher peak water levels may occur if an extreme storm combines with a spring tide. SLR will further increase peak water levels during storms.

Based on our storm surge results with SLR, there appears to be a low risk of widespread inundation in the ACAD region due to the steep topography of the region. However, we have identified one location that may be vulnerable to flooding from peak surges and SLR – specifically, the Trenton Bridge where it connects to Mount Desert Island via Bar Harbor Road. While the northern extent of Mount Desert Island is protected from the open ocean by the island and coastal morphology, the area has relatively low elevation and could experience flooding during extreme water levels caused by storm surge, particularly with SLR. Such flooding could potentially cut off Mount Desert Island from the mainland where Trenton Bridge provides access. Figure 66 shows high resolution ground elevations from the USGS 2021 Midcoast Maine data set (OCM 2023) in this region. As summarized

in Table 9, multiple scenarios may result in peak water elevations exceeding 3.0 m (relative to MSL), leading to flooding of the roadway through the low elevation pathways. Visualizations of inundation from the January 2018 nor'easter for the existing MSL and with 1m of SLR are shown in Figure 67.

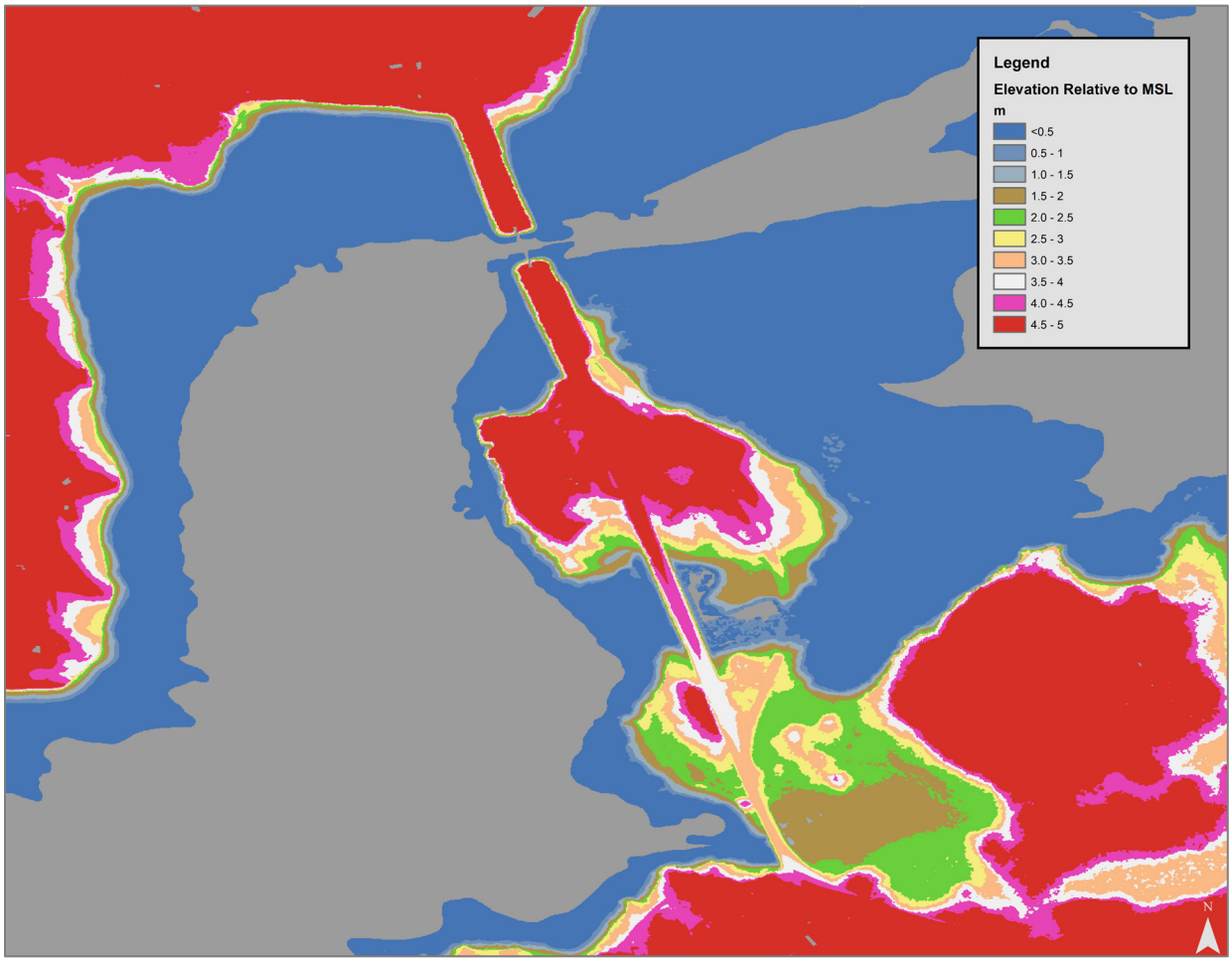


Figure 66. High resolution ground elevations relative to mean sea level at Trenton Bridge and Northern Mount Desert Island, Acadia National Park.

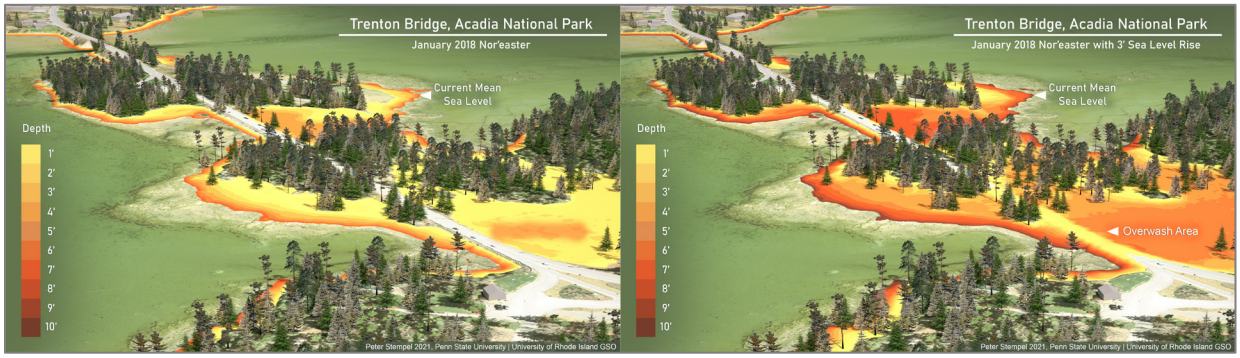


Figure 67. Trenton Bridge illustrating the January 2018 nor'easter under different sea level conditions. Trenton Bridge, the primary access to Mount Desert Island is cut off in the 1 m sea level rise scenario.

Another example of the impact of 1m of SLR is demonstrated with a composite of the storm surge inundation extent at Sand Beach, presented in Figure 68. This figure shows the extent of inundation from the total water level for mean tide level, mean high water, surge from the January 2018 nor'easter without SLR and surge from the January 2018 nor'easter with 1m of SLR. The delineated extents do not capture wave runup that may inundate areas further inland for each of these conditions.

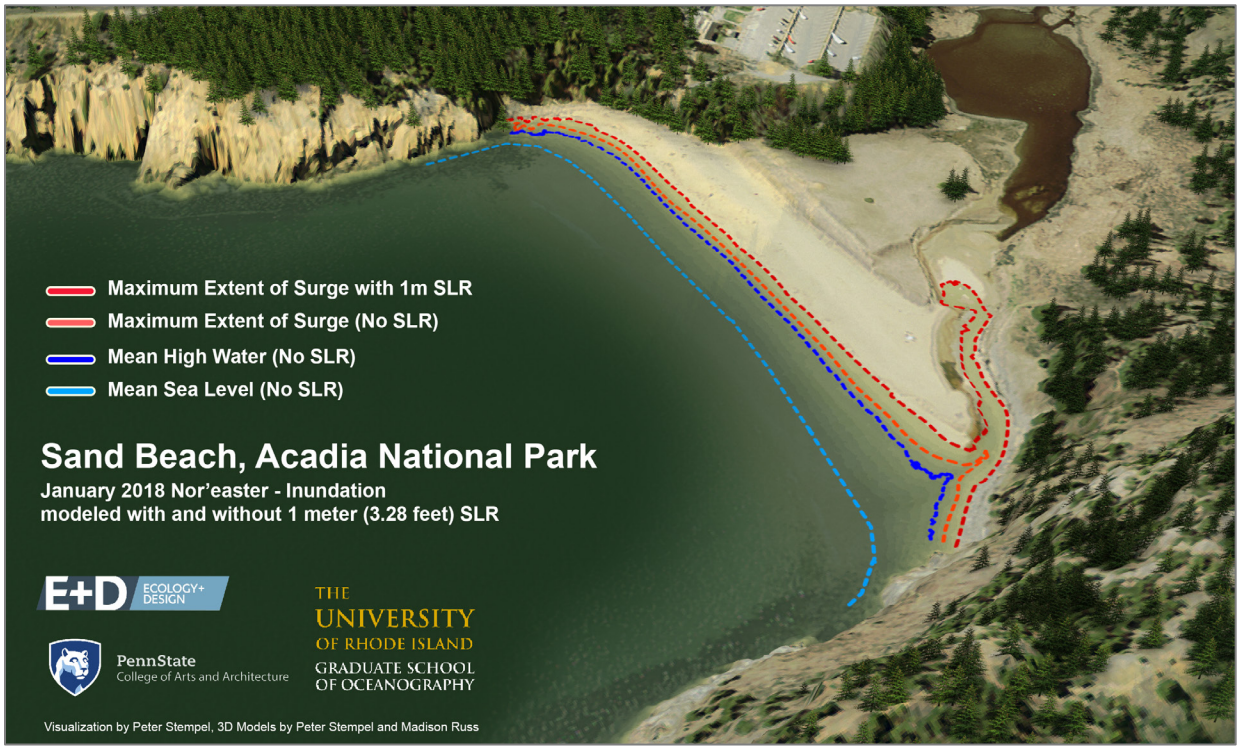


Figure 68. Composite visualization showing the extent of surge in relation to mean high water and mean sea level at Sand Beach, Acadia National Park from simulations of the January 2018 nor'easter with and without 1m of sea level rise. The composite was chosen because the high tidal range makes it difficult to distinguish variations in surge extents.

Nor'easters produce some of the largest waves in this region, and the steep bathymetry and topography result in high wave energy at the coast. The proximity of the exposed steep shoreline to deep water allows large waves to reach the coast without significant attenuation. Coastal regions with more gradual topography are also prone to increased wave impacts during storms due to the large incident wave and storm surge. NPS staff have reported storm impacts, such as dislocated vessel moorings and wave overwash on the roads on Schoodic peninsula. The modeling results are consistent with these observations, indicating that coastal flooding is not widespread in this area, but coastal waves are extreme, which can contribute to overwash of rocks and debris.

The waves that reach the coast via sharp changes in bathymetry from deep to shallow are not expected to undergo significant changes with SLR as they are more likely dominated by deep water conditions. However, the vertical extent that they interact with the coast will be higher due to

elevated water levels. Wave runup, overtopping, and interactions with structures are not explicitly modeled or visualized, as these processes are beyond the capability of the ADCIRC modeling system and the scope of the present study. Nevertheless, some points can be speculated based on the conditions modeled that influence these factors. The potential for overwash in areas with wave runup along the coastline is expected to increase with SLR since the increase in water level will slightly diminish wave attenuation in the approach, allowing for the further inland extent of wave action. Coastal structures, such as access to Thunder Hole or exposed sections of the Park Loop Road, are expected to be exposed to greater forces and more potential for damage due to larger wave heights in the shallower shore adjacent regions.

Lastly, an area of concern that emerged through the modeling, visualization, and engagement process is the effect of SLR on access to Bass Harbor Marsh. This area is of significant cultural importance because it is a site for gathering sweetgrass as a traditional craft material for members of the Wabanaki Nation. These concerns have been noted for inclusion in subsequent work that can focus more specifically on these issues by developing additional visualization materials for these sites.

Boston Harbor Islands and Boston National Historic Park

The park boundaries of BOHA & BOST consist of multiple separate islands and shore adjacent parcels at the entrance and within Boston Harbor. The extent of the parks spans approximately 18 km, measured in a northwest to southeast shore parallel line. Most of the park boundaries are aligned with the shoreline. BOHA consists of 30 islands and 4 peninsulas, and some islands have rocky bluffs and armored shorelines that may have steep or gradual surrounding bathymetry. The coastal unit of BOST is the Charlestown Navy Yard, which is lined with bulkheads along its shore aligned boundaries.

The tide range in this region, delineated by the difference between MHHW and MLLW, is 3.131 m. An analysis of storm surges at the NOAA gauge in Boston shows that the top 50 surges range from approximately 1 m to 2 m, with the most extreme surge on record occurring during extratropical (nor'easter) storms. The peak surges have not always been coincident with spring tides, and higher peak water levels may occur if an extreme storm combines with a spring tide, which will worsen with SLR.

Our modeling results show that the potential for inundation over land is primarily limited to the low points of BOHA. Visualizations of the impacts from the March 2018 nor'easter for the present MSL and with 1m of SLR local to Georges Island are shown in Figure 69. This figure illustrates that with present conditions the inundation is limited to areas local to the beach shoreline, however with 1m of SLR will extend to further upland regions of developed land.



Figure 69. Visualization of flood depths from simulations of the March 2018 nor'easter without sea level rise (left,) and with 1m of sea level rise (right) at Georges Island, Boston Harbor Islands National Recreation Area.

Although most low points are spatially limited and adjacent to higher terrain, the extent of inundation does not increase significantly landward with SLR but instead deepens in the locations that flood during storms at the current sea level. The ADCIRC mesh elevations of the region shown in Figure 70 illustrate that these low-lying areas (blue-green-yellow) are limited and are often behind narrow, higher-elevation armoring that is not captured in the ADCIRC mesh. However, much of the shoreline armoring is historic and the condition varies; our review of satellite imagery reveals that armoring has been compromised in some locations, as shown in Figure 71 for Lovells Island and Georges Island. The integrity of the armoring is critical to the coastal protection service it offers, and changes in the armoring could result in alterations to the potential for flooding.

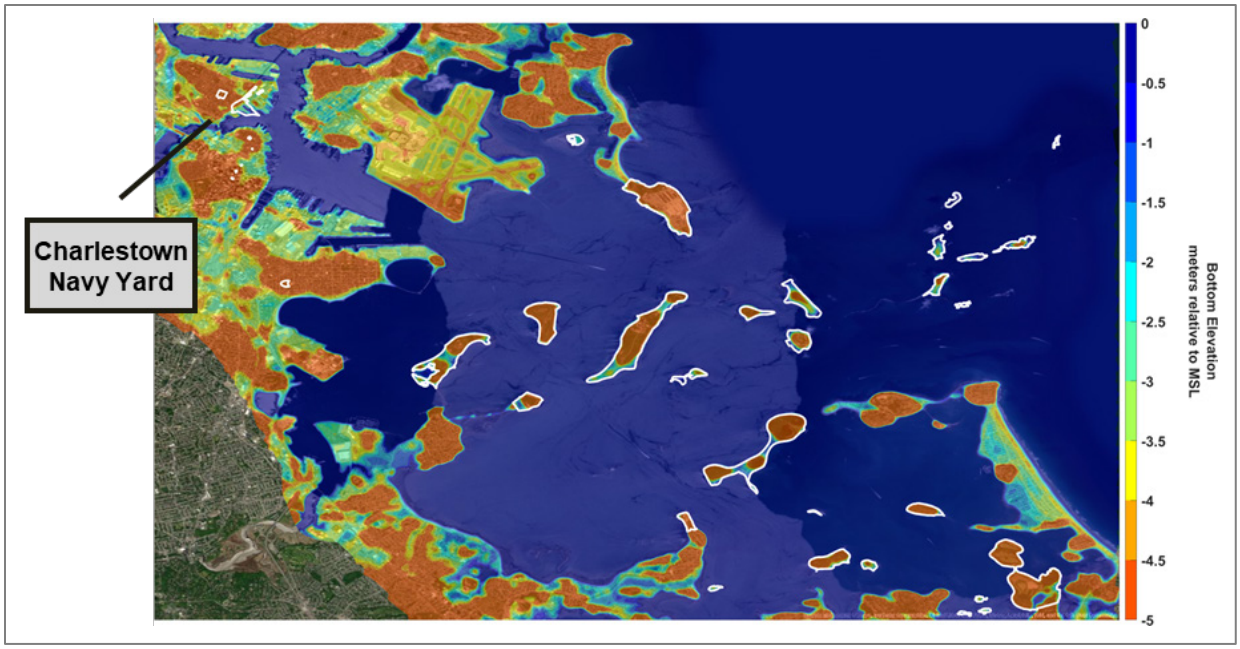


Figure 70. Map of bottom elevations at the National Parks of Boston, MA.



Figure 71. Satellite images of Lovells Island (top left) and Georges Island (bottom left), Boston Harbor Islands National Recreation Area, from the Massachusetts GIS 2021 Aerial Imagery. Right hand side shows zoomed in view of areas outlined in red box showing locations of failed shoreline armoring.

The impact from waves is most significant at the outer harbor islands, where there is little attenuation of the deepwater waves due to steep bathymetry. The geometry and bathymetry of the inner harbor attenuate storm waves. The modeling results show that some of the islands with a relatively shallow approach may experience moderate changes in the waves at the coast due to SLR since the waves in these regions are limited by water depth, and the additional depth from SLR allows for larger waves. Examples of this can be seen in Figure 37, particularly in the offshore regions of Deer Island and Lovells Island. NPS park managers expressed concerns regarding the repair and ongoing management of historic revetments and sea walls surrounding Georges Island.

NPS staff expressed interest in understanding the impacts of nor'easters with SLR at the Charlestown Navy Yard, located on the coastal portion of Boston National Historical Park. A map of high-resolution elevation data in this region is provided in Figure 72, although some small features, such as bulkheads may not be captured entirely.

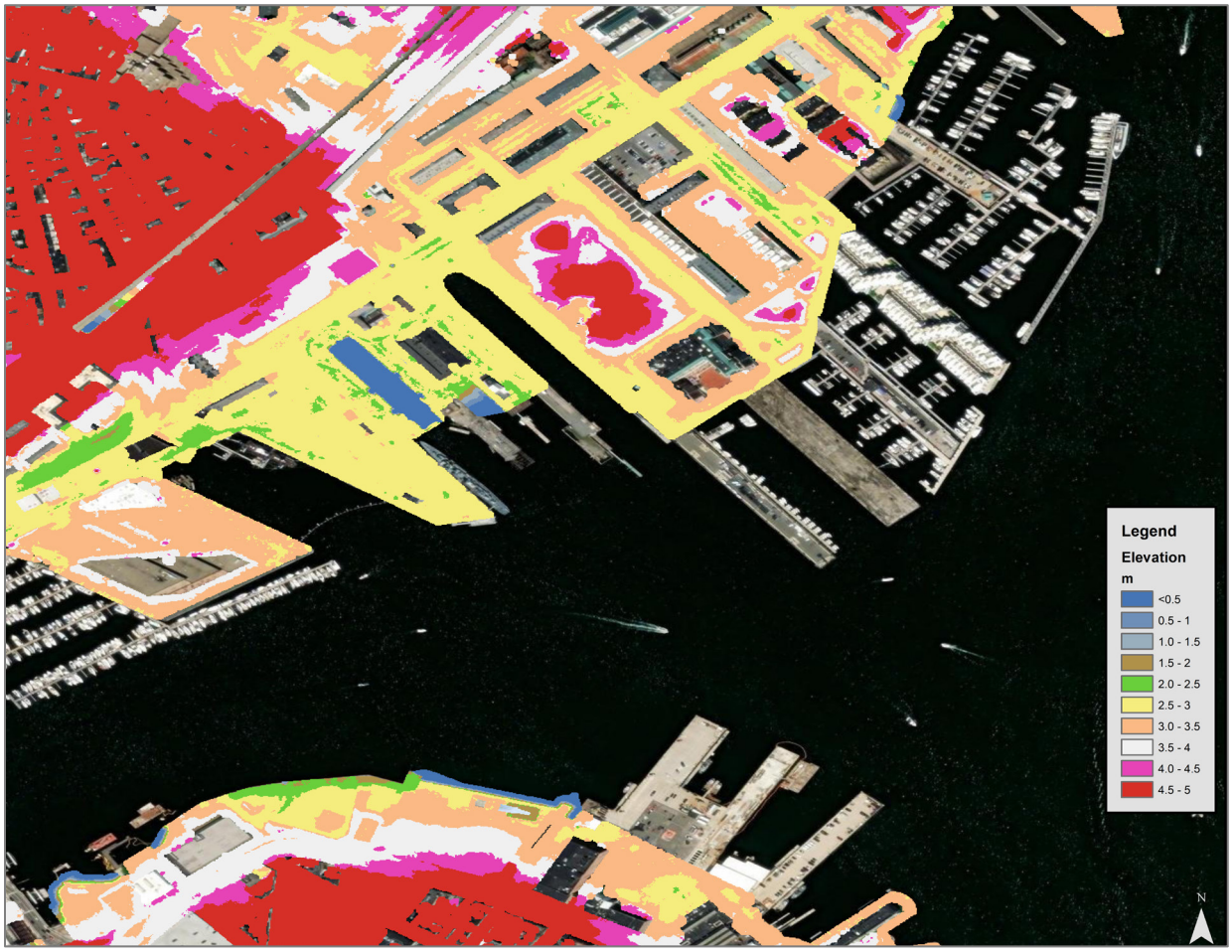


Figure 72. High resolution bottom elevations relative to mean sea level (elevation positive) in the region of the Charlestown Navy Yard, Boston National Historical Park.

Referring to the summary of peak water levels local in this region, as summarized in Table 9, peak water levels from the scenarios modeled range from 2.7-4.1m above MSL. Comparing these to the high-resolution elevation data, coastal flooding would be expected in this region unless storm protection structures are elevated to provide protection from these elevated levels. SLR will exacerbate the storm impacts as shown in the visualization from the March 2018 nor'easter with 1 m of SLR shown in Figure 73. This figure shows that inundation may be extensive in this region due to the low-lying land.

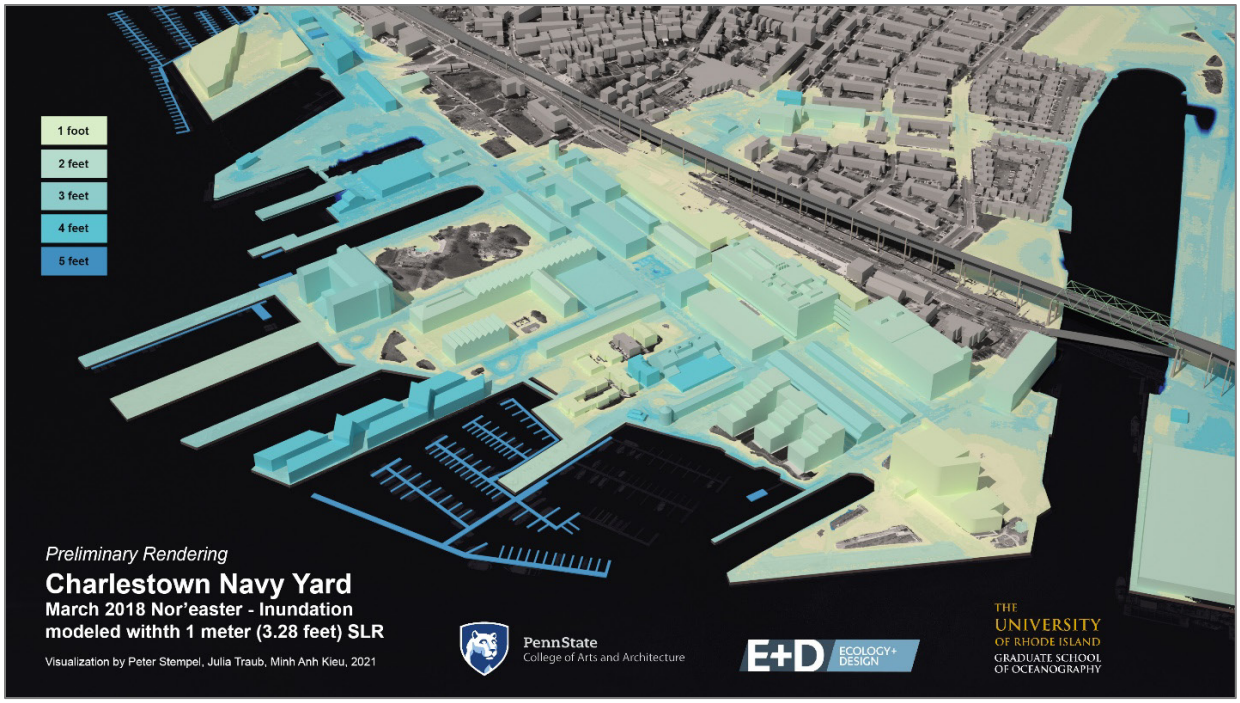


Figure 73. Visualization of Charlestown Navy Yard during the March 2018 nor'easter with 1 m sea level rise.

Cape Cod National Seashore

The park boundaries of CACO follow the outer eastern shoreline of Cape Cod and include the hook at Provincetown, spanning an extent of approximately 100 km. While most of the park's shoreline is contiguous with the mainland, there are small barrier islands near the two coastal embayments (Nauset and Pleasant Bay) along the southeastern coast. The northern hook also includes a coastal harbor (Hatches Harbor) that is connected through a non-stationary inlet on the western coast of Provincetown. The shoreline along Provincetown Harbor also includes a connection to marsh and embayment, which is connected through the Provincetown Long Point Dike. The western shore of the park also includes marsh and natural beaches along Wellfleet, including Wellfleet harbor.

The tide range in this region is variable. Along the open coastlines (not in embayments), it ranges from 3.16–3.35 m between MLLW and MHHW. The tide range is greatest in Cape Cod Bay and decreases along the east coast, from the northeast to southeast. Observed records of long-term water level and astronomical tide predictions from NOAA or other sources are not available at this location and therefore a long-term record of storm surge is not available. However, it is expected that most of the open coastline of the park will experience a similar surge as observed at the Boston tide gauge (1–2 m). Our modeling results show that the storm surge within the coastal embayments can exceed the surge on the open coast.

The ADCIRC mesh elevations of the region are shown for reference in Figure 74. It shows many different areas of low elevation, as evident in the blues, greens, and yellow areas. One area with a relatively large fraction of low elevation is the northern Provincetown/Truro region. This is the

thinnest part of the peninsula and is subject to flooding from both the Atlantic Ocean side and Cape Cod Bay. Within this region, there is low-lying land adjacent to Route 6 in front of East Harbor. Note that Route 6 disrupts tidal exchange with East Harbor; the tide gate was enlarged to allow limited tidal exchange but is not resolved by the model. The ADCIRC modeling of some scenarios, particularly those with SLR, shows flooding that crosses the entire peninsula in this region. While some of this is outside the park boundaries, these regions include the only paved roads from different park parking lots that lead outside this area. The ADCIRC modeling shows the road as flooded, but this should be further investigated as the model resolution may not capture small or sharp changes in elevation well, such as the narrow-elevated roadway.

A map of high-resolution elevation data in this region is provided in Figure 75. Referring to the summary of peak water levels local in this region, as summarized in Table 9, peak water levels from the scenarios modeled range from 2.6–4.25 m above MSL. Comparing these to the high-resolution elevation data, coastal flooding could be a threat in this area.



Figure 74. Map of bottom elevations in the Cape Cod, MA region.

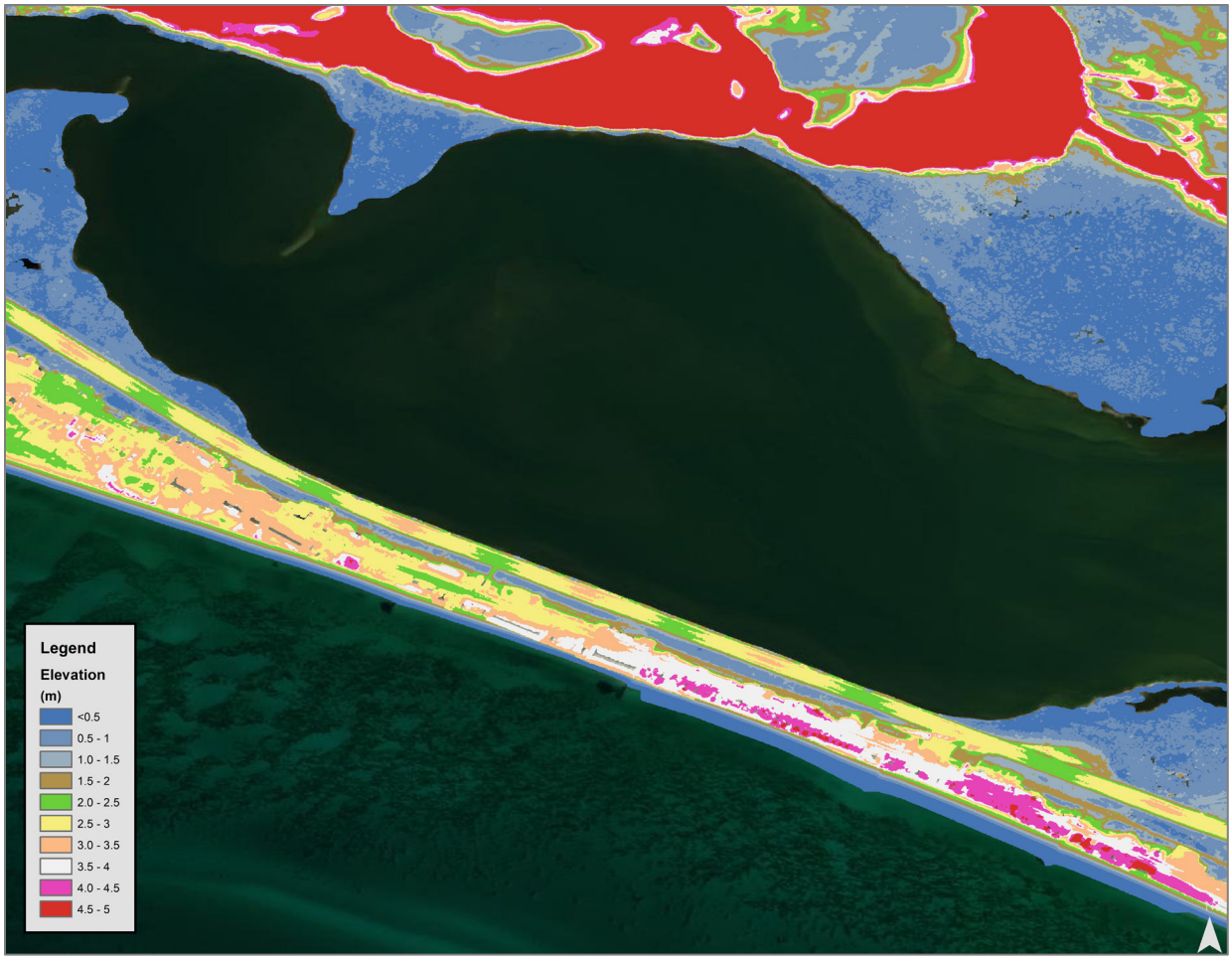


Figure 75. Map of bottom elevations relative to mean sea level (elevation positive) in the Cape Cod, MA region near East Harbor.

Other regions of the bay side are vulnerable to flooding as well. The visualization of the storm impacts in the Wood End–Long Point region of Provincetown from the March 2018 nor'easter for present MSL is provided in Figure 76 showing that the marsh would be almost completed inundated at the peak of that storm without SLR. Figure 77 shows a visualization of Wellfleet Harbor from the January 2018 nor'easter with 1 m of SLR, showing extensive inundation in developed area.

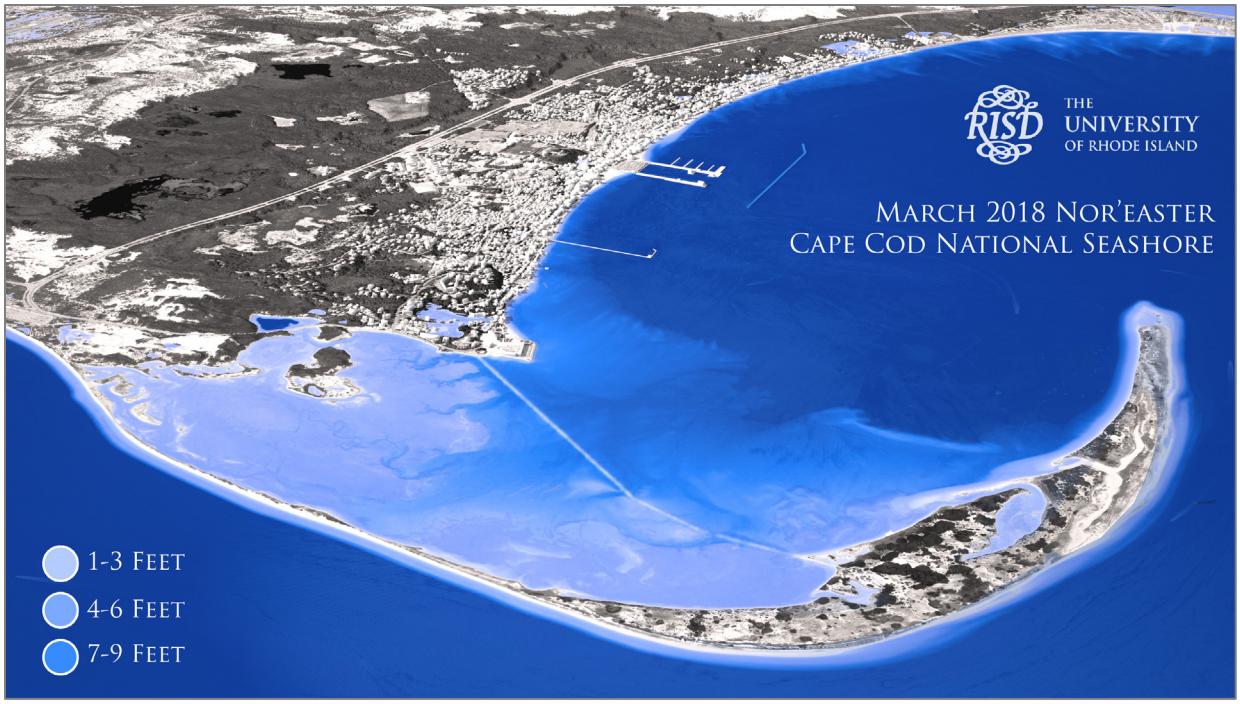


Figure 76. Visualization of the March 2018 nor'easter at Provincetown–Wood End, MA, showing the Long Point Dike.

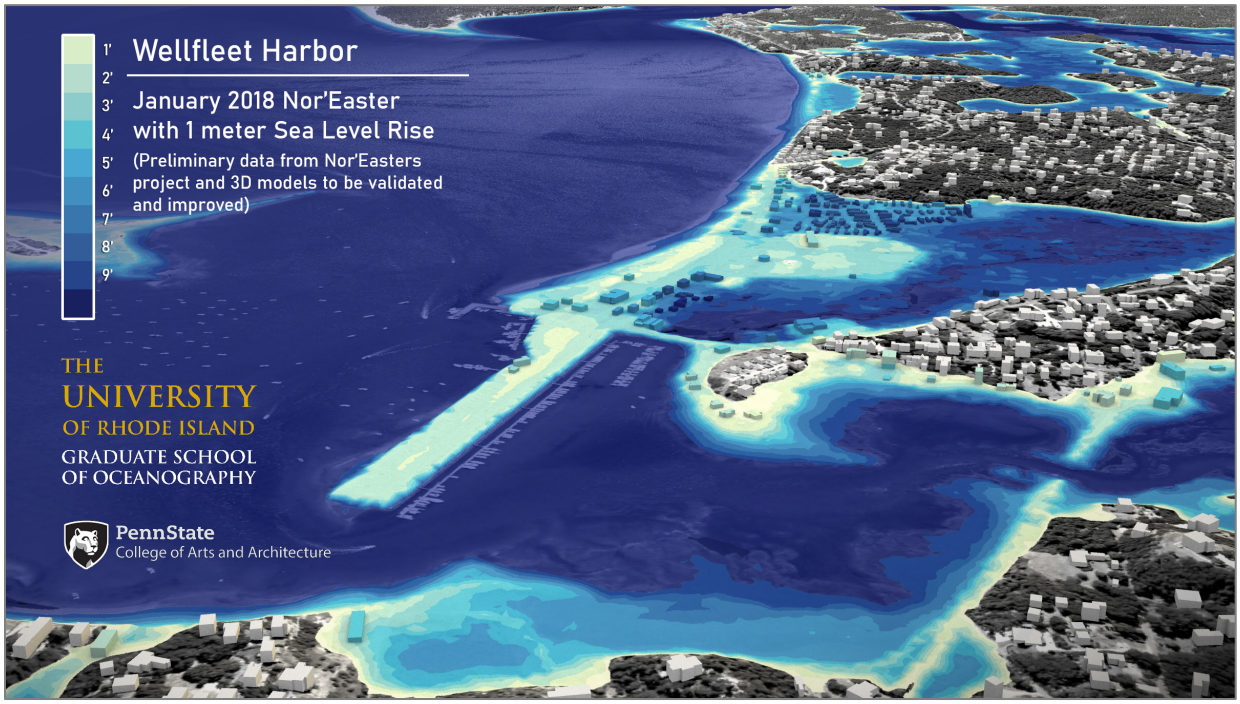


Figure 77. Visualization of Wellfleet Harbor, MA, during the January 2018 nor'easter including 1 m of sea level rise.

Other potential vulnerabilities to RT6 throughout the Cape were identified, especially under conditions of SLR. Figure 78 provides a visualization of the March 2018 nor'easter with 1m of SLR in the Eastham MA region at large and Figure 79 presents visualizations zoomed in on the Orleans Circle from the January 2018 nor'easter for both present MSL and with 1m of SLR. These figures show that vulnerable regions extend beyond the marsh to developed regions. These vulnerabilities similarly require further investigation.



Figure 78. Visualization of Eastham, MA, looking from First Encounter Beach across Nauset Marsh towards Coast Guard Beach and Orleans Circle depicting the March 2018 nor'easter with 1 m sea level rise.

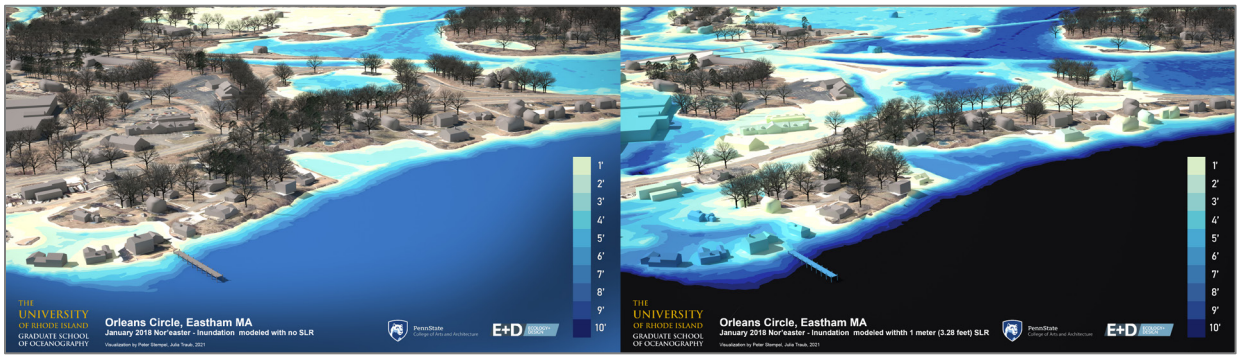


Figure 79. Visualization of Orleans Circle, MA, January 2018 nor'easter (left) and the January 2018 nor'easter with 1 m sea level rise (right).

Our modeling analysis shows that coastlines, such as the east coast of CACO, are exposed to high wave energy and experience additional surge due to wave setup. This additional surge is proportional

to the wave heights, which increase with SLR, as waves with SLR are larger due to the greater water column depth. The wave heights on the eastern coast of CACO are already extreme, and SLR will allow higher wave heights in the shallow regions that are depth limited, as well as a further inland extent of wave activity. However, in areas where waves reach the steep dunes and bluffs, the extent will be the same, but the vertical extent of interaction will be greater.

CACO has shown leadership in managing structures and infrastructure in locations such as Herring Cove Beach by elevating, redesigning, and moving landward a bathhouse and parking lot. Figure 80 and Figure 81 present visualizations in this region of the peak inundation from the January 2018 nor'easter for present MSL and with 1m of SLR. Figure 80 shows 3D visualizations of the bathhouse and parking lot in the new locations. Figure 81 communicates impacts on other park resources and infrastructure, including Race Point Light and Hatches Harbor. These figures show that 1 m SLR will extend the inundated areas beyond the beach and marsh to developed regions.

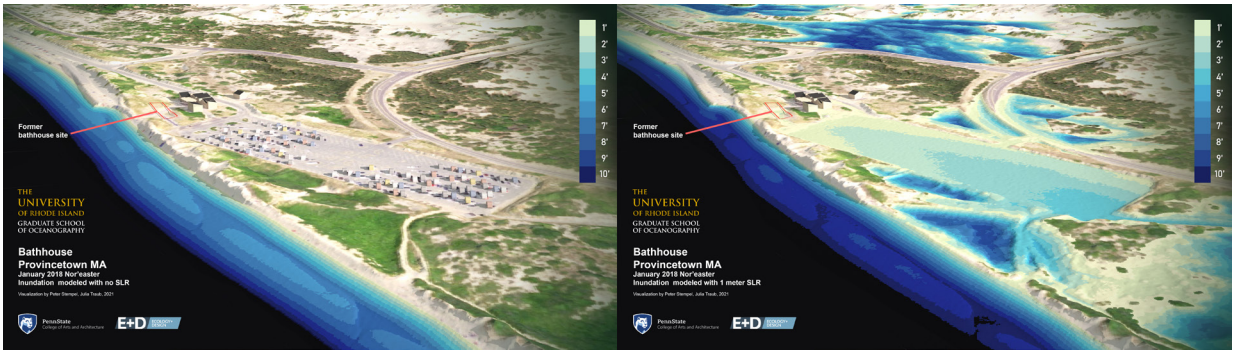


Figure 80. Herring Cove Beach, Provincetown, MA, shown with January 2018 nor'easter (left), and the January 2018 nor'easter with a 1 m sea level rise (right).

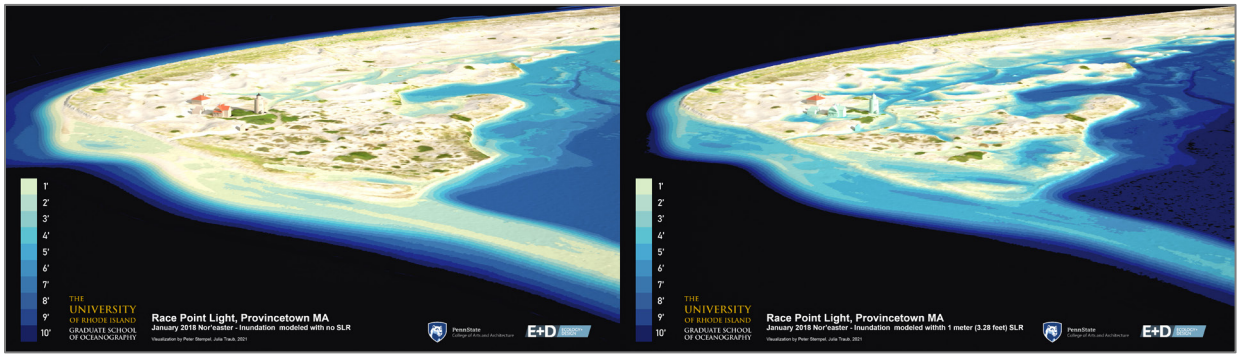


Figure 81. Race Point Light, Provincetown, MA, shown with January 2018 nor'easter (left), and the January 2018 nor'easter with 1 m sea level rise.

Conclusions

This study examined the hazards from nor'easters and SLR at four parks across New England by combining literature review, data analysis, and numerical modeling. Throughout this process, we conducted various activities aiming at addressing the research questions outlined in the introduction. Our findings and conclusions in response to these questions are summarized below.

1. What coastal impacts have been observed local to the parks during nor'easters?

Nor'easters profoundly impact coastal areas, resulting in high winds, storm surges, large waves, and beach erosion. Historical data from New England show that storm surges, combined with tides, produced total water levels that caused coastal inundation over land. Storm surges of up to 2 m have been observed locally at the New England parks from nor'easters.

The slow-moving nature of nor'easters which can last over a tidal cycle, combined with strong winds, leads to larger than average waves. Elevated water levels from storm surges allow waves to reach further inland on the natural shoreline with gradually changing bathymetry/topography, though this study did not model those changes. Additionally, waves contribute to elevated water levels at the coast due to wave setup, with the magnitude of setup increasing with increased wave heights. These wave-related processes result in additional erosion and damage to structures exposed to their forces.

2. What is the range of SLR expected at the parks from 2020–2100?

There is a significant amount of uncertainty surrounding SLR projections, both in terms of what will happen in the future and our ability to predict the corresponding SLR at a regional scale. Based on our analysis of the 2022 interagency report (Sweet et al. 2022), the following findings are specific to the study area. The spatial variability across the northeast is small, it is approximately 0.02 m (0.07 ft) in the year 2050 and 0.05 m (0.16 ft) in the year 2100 relative to 2020 for the expected values from the intermediate scenario. Considering Boston as a proxy for the region, the projected MSL by 2050 relative to 2020 ranges from 0.13–0.48 m (0.43–1.58 ft) while the expected value for the intermediate scenario is 0.28 m (0.919 ft). Similarly, the projected MSL by 2100 relative to 2020 ranges from 0.20–2.08 m (0.66–7.15 ft) while the expected value for the intermediate scenario is 0.72 m (2.36 ft). It is notable that the rate of SLR between 2020–2050 based on the expected value for the intermediate scenario is approximately 3–4 times greater than the SLR rate that was experienced over the period of 1980–2020, where approximately 0.10 m (0.316 ft) of SLR had occurred. These projections emphasize the importance of addressing SLR as a major threat to coastal regions, including the parks in the study area, and the need for adaptive measures to mitigate its potential impacts.

3. What is the effect of SLR on nor'easter impacts at the parks?

We used numerical modeling to investigate the impacts of three nor'easters that caused extreme storm surge and waves. We simulated each event four ways, (1) as it occurred for model validation, (2) with a baseline MSL reflecting 2020, (3) with 1ft of SLR and (4) with 1m of SLR. The effect of SLR on nor'easter impacts varied across the parks and within the parks with different shoreline features. The key findings are presented below.

The inclusion of SLR resulted in changes in the peak water levels experienced during the storms. However, these changes were not equal to the applied SLR. The deviation from the applied SLR varied in space and time due to nonlinear effects. The magnitude of the deviation increased as the SLR increased, and the patterns of peak water level changes were consistent across all parks. These results demonstrate a substantial improvement in accurately representing the physical processes responsible for water level changes, as compared to additive approaches used in other studies, where the SLR increment is added to the water level.

The rise in peak water levels caused by SLR can increase overland inundation. Shorelines with low grades are more susceptible to overland inundation than steep or high-grade shorelines. The shoreline characteristics at each park are different, but in general, ACAD has a mostly high-grade shoreline, CACO has mostly low-grade shoreline, BOHA has a mix of shoreline and utilizes armoring in many areas, while BOST has man-made bulkheads. BOHA has some low-lying areas that may be vulnerable, but the model results indicate that the impact will be limited spatially. SLR will primarily deepen the areas instead of causing widespread changes to the inundation footprint. Conversely, SLR may lead to more dramatic changes to the flooding footprint at CACO. In addition, much more of CACO geomorphology is likely to change in response to storm impacts. Future modeling will examine the combined effects of storms and SLR on shoreline morphology in specific areas.

The inclusion of SLR alters the nearshore wave environment, allowing for larger waves and a greater inland extent of waves on shores with gradually decreasing bathymetry (increasing topography), most notable at the east coast of CACO and northeast coasts of some BOHA islands. Waves reaching BOST are significantly attenuated compared to those at the outer harbor islands, and the water is deep at the shoreline. Consequently, changes in the waves themselves at this location are not expected. However, the elevated waters resulting from SLR could increase wave impacts such as spray and overtopping, potentially affecting adjacent upland areas. At ACAD, where there is a steep change in bottom grade, the higher water level from SLR will modify where the waves interact with the coast vertically on steep, bluffed shorelines. In areas such as the Schoodic Peninsula, the waves reaching the shore could extend further inland, and overtopping and overwash from coastal waves may occur more frequently and more intensely.

4. What is the role of waves in model simulations of storm surge? How does SLR affect the role of waves in model simulated storm surge at the parks?

Waves generate setup, which is an additional localized rise in the water level caused by the radiation stresses generated by waves. Wave setup is greatest at the shore and decreases with distance offshore, with set down (localized depression) at greater distances. The magnitude of wave setup is directly proportional to the height of the waves, with larger waves producing more setup.

The impact of SLR in terms of elevating the mean sea level results in a deeper nearshore water column and further inland inundation from tides and storm surges. For a given wind or deepwater wave condition, larger waves occur in deeper water. SLR will lead to larger waves in the nearshore region where waves are limited by water depth, extending the region of wave activity further inland. This effect will be more noticeable in CACO than in BOHA, BOST, and ACAD due to its larger natural shoreline and gradually shallowing coast in areas of significant wave activity.

5. What is the effect of shoreline configuration in southeast Cape Cod on the degree of storm surge experienced within coastal embayments behind the barrier beach?

The southeast Cape Cod region has a dynamic barrier beach system that has undergone various morphological changes over time. While modeling geomorphic changes in response to storms for the entire area of multiple parks is beyond the scope of this project, an example analysis of one especially dynamic area is described here. The tide range and amount of storm surge that occurs within the embayments are influenced by the number, width, and depth of inlet openings, as well as the bathymetry within the embayments. To explore this further, we conducted simulations of multiple shoreline configurations with storm conditions representing the January 2018 nor'easter. Our findings indicate that larger opening widths to the Atlantic Ocean (adjacent body of water to the east) increase the storm surge within the coastal embayments, whereas the presence of a hydraulic connection with Nantucket Sound (adjacent body of water to the southwest) reduces the peak storm surge. The differences in peak surge vary by up to 0.24m, which is approximately 20–30% of the total surge. Furthermore, the timing of the peak surge shifts, with the peak occurring approximately one hour later in Pleasant Bay when a connection to Nantucket Sound exists due to the phase difference of the tides in Nantucket Sound versus the Atlantic Ocean. This area requires further investigation to evaluate the response to different storms, including tropical storms, and to determine configurations that amplify storm surge within the embayment.

6. How can we better communicate the impact of nor’easters, SLR, and the combination of nor’easters with SLR?

To effectively convey the impact of nor'easters and SLR, we have developed various communication tools, including maps, diagrams, visualizations, and films. Our work demonstrates the effectiveness of using a combination of modalities when communicating with stakeholders. Each product serves as a "boundary object," providing a shared reference point that facilitates interactions between project team experts, national park managers, and other stakeholders.

Our film has been particularly effective, as it uses personal narratives to make the project work tangible and relatable to a broader audience. We have also employed exhibits and visual aids, which align with best practices for climate communication.

We believe science can have the greatest impact by engaging scientists and audiences in conversation. By providing accessible and meaningful information through various communication tools, we increased awareness of the impact of nor'easters and SLR and helped to facilitate informed decision-making among the National Park stakeholders.

Literature Cited

Aubrey, D. G., and L. Weishar, eds. 2013. Hydrodynamics and sediment dynamics of tidal inlets (Vol. 29). Springer Science & Business Media.

Bernhardt, J. E., and A. T. DeGaetano. 2012. Meteorological factors affecting the speed of movement and related impacts of extratropical cyclones along the US East Coast. Natural Hazards 61:1463–1472.

Booth, J. F., H. E. Rieder, and Y. Kushnir. 2016. Comparing hurricane and extratropical storm surge for the Mid-Atlantic and Northeast Coast of the United States for 1979–2013. Environmental Research Letters 11(9):094004.

Catalano, A. J., and A. J. Broccoli. 2018. Synoptic characteristics of surge-producing extratropical cyclones along the northeast coast of the United States. Journal of Applied Meteorology Climatology 57:171–184.

Cialone, M. A., T. C. Massey, M. E. Anderson, A. S. Grzegorzewski, R. E. Jensen, A. Cialone, D. J. Mark, K. C. Pevey, B. L. Gunkel, T. O. McAlpin, and N. C. Nadal-Caraballo. 2015. North Atlantic Coast Comprehensive Study (NACCS) coastal storm model simulations: Waves and water levels. US Army Engineer Research and Development Center, Coastal and Hydraulics Laboratory.

Colle, B. A., J. F. Booth, and E. K. Chang. 2015. A review of historical and future changes of extratropical cyclones and associated impacts along the US East Coastal Current Climate Change Reports1:125–143.

Danielson, J. J., S. K. Poppenga, D. J. Tyler, M. Palaseanu-Lovejoy, and D. B. Gesch. 2018. Coastal National Elevation Database: US Geological Survey Fact Sheet 2018–3037, 2 p.

Dee, D. P., S. M. Uppala, A. J. Simmons, P. Berrisford, P. Poli, S. Kobayashi, U. Andrae, M. A. Balmaseda, G. Balsamo, D. P. Bauer, and P. Bechtold. 2011. The ERA-Interim reanalysis: Configuration and performance of the data assimilation system. Quarterly Journal of the Royal Meteorological Society 137(656):553–597.

Dolan, R., and R. E. Davis. 1992. An intensity scale for Atlantic coast northeast storms. Journal of Coastal Research pp. 840–853.

Douglas, E. M., P. H. Kirshen, K. Bosma, C. Watson, S. Miller, and K. McArthur. 2016. Simulating the impacts and assessing the vulnerability of the central artery/tunnel system to sea level rise and increased coastal flooding. Journal of Extreme Events 3(04):1650013.

Dupigny-Giroux, L. A. L., E. L, Mecray, M. D. Lemcke-Stampone, G. A. Hodgkins, E. Lentz, K. E. Mills, E. D. Lane, R. Miller, D. Y. Hollinger, W. D. Solecki, and G. A. Wellenius. 2018. Northeast pp. 669–742. US Global Change Research Program.

Giese, G. S., S. T. Mague, and S. S. Rogers. 2009. A geomorphological analysis of Nauset Beach/Pleasant Bay/Chatham Harbor for the purpose of estimating future configurations and conditions. Prepared for the Pleasant Bay Resource Management Alliance.

Hirsch, M. E., A. T. Degaetano, and S. J. Colucci. 2001. An East Coast winter storm climatology. Journal of Climate 14(5):882–899.

Knutson, T., S. J. Camargo, J. C. Chan, K. Emanuel, C. H. Ho, J. Kossin, M. Mohapatra, M. Satoh, M. Sugi, K. Walsh, and L. Wu. 2019. Tropical cyclones and climate change assessment: Part I: Detection and attribution. Bulletin of the American Meteorological Society 100(10):1987–2007.

Luettich, R., and J. Westerink. 2007. A parallel ADvanced CIRCulation model for oceanic coastal and estuarine waters. Available at: http://www.adcirc.org (accessed 18 March 2014).

Massachusetts GIS (MassGIS). 2024. MassGIS Data: 2021 Aerial Imagery. ArcGIS Online Views of Boston. Accessed March 2024. Available at: https://www.mass.gov/info-details/massgis-data-2021-aerial-imagery (accessed 08 May 2024).

Michaelis, A. C., J. Willison, G. M. Lackmann, and W. A. Robinson. 2017. Changes in winter North Atlantic extratropical cyclones in high-resolution regional pseudo–global warming simulations. Journal of Climate 30(17):6905–6925.

Northeast Regional Association of Coastal and Ocean Observing Systems (NERACOOS). 2022.ERDAP – Tabledap data sets NDBC 44029(A01), NDBC 44032 (E01), NDBC 44033(F01), NDBC 44034(I01), https://www.neracoos.org/erddap/tabledap/index.html?page=1&itemsPerPage=1000/ (accessed July 2022).

National Aeronautics and Space Administration (NASA). 2022. Interagency Sea Level Rise Scenario Tool Available at: https://sealevel.nasa.gov/task-force-scenario-tool/ (accessed July 2022).

National Oceanographic and Atmospheric Association (NOAA). 2021. NOAA Tides and Currents Website. Available at: https://tidesandcurrents.noaa.gov/ (accessed January 2021).

National Oceanographic and Atmospheric Association (NOAA). 2021. National Buoy Data Center (NDBC). Available at: https://vdatum.noaa.gov/welcome.html/ (accessed January 2021).

National Oceanographic and Atmospheric Association (NOAA). 2022a. Vertical Datum Transformation. Available at: https://tidesandcurrents.noaa.gov/ (accessed December 2022).

National Oceanographic and Atmospheric Association (NOAA) National Center for Environmental Information (NCEI). 2022b. Global Hourly-Integrated Surface Data. Available at: https://www.ncei.noaa.gov/products/land-based-station/integrated-surface-database/ (accessed December 2022).

National Oceanographic and Atmospheric Association (NOAA) National Weather Service. Surge Wave Grid Development. Available at: https://www.weather.gov/sti/coastalact_surgewg (accessed 18 March 2024).

Shearman, R. J., and A. A. Zelenko. 1989.Wind measurements reduction to a standard level. World Meteorological Organization.

Stempel, P., E. Nasr-Azadani, A. Grilli, S. Grilli, E. Shuh, F. Groetsch, I. Ginis, D. Crowley, J. P. Walsh, I. Whaling, and C. Damon. 2023. 3D morphodynamic visualizations of storm impacts for decision support. Journal of Digital Landscape Architecture 2023(8):554–563.

Stempel, P., I. Ginis, D. Ullman, A. Becker, and R. Witkop. 2018. Real-time chronological hazard impact modeling. Journal of Marine Science and Engineering 6(4):134.

Simulating Waves in the Nearshore Team. 2006. SWAN User Manual. Delft University of Technology, the Netherlands.

Sweet, W. V., B. D Hamlington, R. E. Kopp, C. P. Weaver, P. L. Barnard, D. Bekaert, and C. Zuzak, C. 2022. Global and regional sea level rise scenarios for the United States: Updated mean projections and extreme water level probabilities along US coastlines (No.01). NOAA Technical Report.

Tebaldi, C., B. H. Strauss, and C. E. Zervas. 2012. Modelling sea level rise impacts on storm surges along US coasts. Environmental Research Letters 7(1):014032.

Thompson, P. R., G. T. Mitchum, C. Vonesch, and J. Li, J. 2013. Variability of winter storminess in the eastern United States during the twentieth century from tide gauges. Journal of Climate 26(23):9713–9726.

United States Geological Survey (USGS). 2021. USGS Water Data for the Nation. Available at: https://waterdata.usgs.gov/nwis/ (accessed January 2021).

United States Geological Survey (USGS). 2024 Data Available from Land Processes Distributed Active Archive Center (LP DAAC). Available at: https://landsatlook.usgs.gov/ (accessed March 2024).

Office for Coastal Management (OCM) Partners. 2023. 2021–2022 USGS Lidar: Midcoast Maine. Available at: https://www.fisheries.noaa.gov/inport/item/69360 (accessed 18 March 2024).

Zhang, K., B. C. Douglas, and S. P. Leatherman. 2000. Twentieth-century storm activity along the US east coast. Journal of Climate 13(10):1748–1761.

National Park Service
U.S. Department of the Interior

Science Report NPS/SR—2024/133
https://doi.org/10.36967/2304306



Natural Resource Stewardship and Science
1201 Oakridge Drive, Suite 150
Fort Collins, CO 80525

NPS 962/193736, June 2024